Dissertação submetida para a obtenção do Grau de Mestre em Física Nuclear e de Partículas

Thermal history of the universe with dark energy component induced by conformal fluctuations of the metric

Natacha Violante Gomes Leite

Orientador: Professor Doutor Alex Heinz Ladislaus Blin

Departamento de Física
Faculdade de Ciências e Tecnologia

Coimbra, 2013

Ao meu Avô

Resumo

Estuda-se o comportamento de um universo como fluido perfeito, onde a energia negra é associada ao efeito macroscópico de variações conformais do tensor da métrica. Modela-se a evolução do factor de escala, da temperatura e da densidade com o tempo, num universo composto por radiação, energia negra, matéria negra e matéria bariónica, usando *Maple*. Analisam-se os principais eventos da história térmica e a transição entre eras dominadas por diferentes entidades.

Abstract

The behaviour of a perfect fluid universe is studied, where dark energy is associated to the macroscopic effect of conformal variations of the metric tensor. The evolution of the scale factor, temperature and density over time in a universe comprised of radiation, dark energy, dark matter and baryonic matter is modelled using *Maple*. The main events of the thermal history and the transition between different entity-dominated eras are analysed.

Acknowledgements

First, I want to thank my supervisor, Alex Blin, for his exceptional guidance, dedication, availability and good humour along the project. I am very grateful for the opportunity of being advised by him.

I thank my parents and Luís for all their care and support in the academic journey. I am grateful to my aunt, Palmira, for the financial support which made my stay in Coimbra possible.

I want to thank Melo, Borlido and Tiago for their patience and valuable suggestions. I also thank Afonso, Andoni, Araújo and Marco for providing me with good quality breaks and boosting my motivation to work.

I am grateful to everybody that crossed my path in the University, to the people who enriched my life by voluntarily or involuntarily being part of it, making me grow as an individual.

x

Contents

List of Figures

List of Tables

Chapter 1

Introduction

Not too long ago, we lived with no clue that our birthplace was an evolving 14 billion years old process. We now call its beginning the Big Bang and we send machines to space to grasp what our eyes can not see but our intellect demands to know: how did it unfold in the fascinating scenery we witness today?

In the attempt to embrace all the complexity we can appreciate, many individuals disclosed fundamental keys that helped to understand how the universe works, where it came from and where it is going to. Our present estimation is that approximately 95% of the universe is constituted by dark energy and dark matter, entities we do not have much certainties about.

From the ground constructed by so many researchers over the years and from the speculations of other many on the unsolved mysteries of the cosmos, we can approximate our universe with various models that reproduce with more or less precision the observational data we were able to collect so far.

In the last century, modern cosmology became a subject on its own. It began with the formulation of general relativity by Albert Einstein in 1915. This theory allowed gravity to be seen as a geometrical modification of the space-time continuum according on its matter and energy content. In 1929, the law of Edwin Hubble, connecting the redshift of galaxies with the expansion of the universe, made us realize the cosmos is not static. This gives sense to Alexander Friedmann's solution to Einstein's equations for a homogeneous and isotropic universe, which was time-dependent. The term that Einstein introduced in order for his field equations to yield a static solution, the cosmological constant, had no more reason to be and was then dropped.

Georges Lemaître proposed the hypothesis that later turned into the Big Bang theory for the origin of the universe and which is widely accepted today. The technological resources particle physics enjoys presently make it possible to probe energies that mimic the ones present in the early stages of the universe, enabling our study of this subject.

Jan Oort in 1932 and Fritz Zwicky in 1933 postulated a new type of matter, dark mat-

ter, to explain the orbital velocities of stars in galaxies, which could not be reached only accounting the visible, or baryonic, matter. The particles that may comprise it are being sought after, believed to interact weakly with normal matter. Among the many candidates proposed [1–4], one of the most popular approaches considers them to be non-relativistic, the so-called cold dark matter, while other works prefer to focus on lighter and faster possibilities.

Near the end of the twentieth century, the astronomical observations on the redshift of supernovae [5, 6] showed that the universe was expanding at an accelerated rate, which justified the introduction of an entity with negative pressure to account for it, the dark energy. This revived the cosmological constant in a different context, now bearing responsibility for the accelerated expansion of the universe by acting as a repulsive gravity. Astrophysics is trying to figure out the origin and nature of the cosmological constant [7], for example, as a result of vacuum fluctuations or of quantum fluctuations of the metric [8, 9]. There are also Quintessence models of dark energy, which use a scalar field instead of a cosmological constant [10].

The standard cosmological picture is then based on the observational evidence that the universe is highly homogeneous, isotropic and flat, composed by approximately 72% of dark energy, 23% of dark matter and 5% of baryonic matter [11], which is known as the ΛCDM model. Other hypotheses consider the dark components as a missing part of gravitation and thus base themselves on modified gravity models.

Joining the cosmological model with the Big Bang, the pertinent question of how the universe evolved can be studied. We can still not fully trace the universe back to its beginning, but it is possible to write its history in detail in some epochs and extrapolate it in others [12]. On the other hand, this means there is still plenty of room to imaginatively speculate about major events of the cosmic history and on the nature of its dark components [13].

In this work we approximate the universe with a perfect fluid comprised of radiation, baryonic matter, dark energy and dark matter as the ΛCDM model claims. We consider it particularly important to take quantum effects on gravity into account, which provide an explanation for dark energy [9]. We will study the thermal evolution of this kind of universe over time, as outlined next.

In the second chapter, we shortly introduce the basics of general relativity that will be useful to our analysis.

In chapter 3, we present the standard cosmological model. In the first part we derive the relevant expressions to write the thermal history of the universe as we know it. In order to understand what components our model of the universe will include, the last section of this chapter is devoted to state the theoretical foundations of the hot Big Bang theory, its limitations and the necessity of including dark matter and dark energy in the standard

model.

Next, we go beyond standard cosmology in chapter 4 and, by using a scalar field to introduce conformal variations of the metric in the classical metric tensor, we consider quantum fluctuations, significant at the Planck scale. We then derive the mathematical expressions that enable us to comprehend the consequences that this modification represents in Einstein's equations, showing that it can be translated into a term of the form of a cosmological constant. This term will be our source of dark energy.

In chapter 5, with the help of thermodynamics, we present the main features of the thermal history of the universe after inflation. While processes like baryogenesis and nucleosynthesis are only quickly reviewed, we spend more time with the events that we will be able to observe in our simulation, such as the transitions during which different particle species and entities decouple from the equilibrium with radiation.

Chapter 6 is dedicated to explain how the simulation of temperature and density of the universe was performed, as can be seen in appendix A in more detail, and to show the results of this analysis.

The last chapter is dedicated to the conclusions and comments about the results.

Chapter 2

General Relativity

The foundation of general relativity is the **Principle of equivalence**, stated by Albert Einstein as the impossibility to distinguish between a (non-rotating) free falling system subject to a gravitational field and a linearly accelerated system in an inertial frame [14]. This guarantees that it is always possible to find a coordinate system where gravitation can be locally eliminated – all observers are equivalent.

To cope with the equivalence principle, the equations of physics should be formulated in such a way that they remain invariant under a coordinate transformation. This is achieved in a tensorial theory – **Principle of general covariance** [15].

The generalization of the special theory of relativity to include gravitation, in order to describe the geodesic equations by a metric connection, leads to a curved metric. The metric takes now the role of the potentials in the former theory and second partial differential equations in the form of tensors are sought to describe the new theory. When the variation of the gravitational field is substantial, in a non-local regime, a vector V^λ parallel transported along a geodesics on a closed infinitesimal path will be subject to a change δV^λ, which depends on the metric and can be represented by the Riemann curvature tensor [16].

To write the curvature tensor, let us begin by distinguishing between covariant and contravariant vectors (tensors of order 1).

A contravariant vector transforms as follows under a change of coordinates [15]

$$V'^\alpha = \frac{\partial x'^\alpha}{\partial x^\beta} V^\beta \qquad (2.1)$$

and a covariant vector transforms according to

$$V'_\alpha = \frac{\partial x^\beta}{\partial x'^\alpha} V_\beta. \qquad (2.2)$$

The covariant derivative of a vector V^λ can be written as

$$\nabla_\nu V^\lambda = \partial_\nu V^\lambda + \Gamma^\lambda_{\mu\nu} V^\mu, \qquad (2.3)$$

5

where $\Gamma^\lambda_{\mu\nu}$ represents the **Christoffel symbol**. For notational simplicity, we introduce

$$\nabla_\nu V^\lambda \equiv V^\lambda_{;\nu}. \tag{2.4}$$

The Christoffel symbol is a scalar object, also called affine connection and can be written in terms of the metric as follows [15]

$$\Gamma^\lambda_{\mu\nu} = \frac{1}{2} g^{\lambda\tau} \left(\frac{\partial g_{\tau\mu}}{\partial x^\nu} + \frac{\partial g_{\tau\nu}}{\partial x^\mu} - \frac{\partial g_{\mu\nu}}{\partial x^\tau} \right) \tag{2.5}$$

where, for the sake of notational simplicity we introduce

$$\frac{\partial g_{\alpha\beta}}{\partial x^\delta} \equiv g_{\alpha\beta,\delta}. \tag{2.6}$$

It is important to refer that in any coordinate system the following identity holds, [16]

$$\Gamma^\lambda_{\mu\nu} \equiv \Gamma^\lambda_{\nu\mu}. \tag{2.7}$$

The **Riemann curvature tensor** can then be written in the following form [15]

$$R^\lambda_{\mu\nu\rho} = \Gamma^\lambda_{\mu\rho,\nu} - \Gamma^\lambda_{\mu\nu,\rho} + \Gamma^\lambda_{\sigma\nu}\Gamma^\sigma_{\rho\mu} - \Gamma^\lambda_{\sigma\rho}\Gamma^\sigma_{\mu\nu}. \tag{2.8}$$

The Riemann tensor becomes covariant with the following transformation

$$R_{\sigma\mu\nu\rho} = g_{\sigma\lambda} R^\lambda_{\mu\nu\rho} \tag{2.9}$$

and it possesses some very interesting properties [17]:

- Symmetry

$$R_{\sigma\mu\nu\rho} = R_{\nu\rho\sigma\mu} \tag{2.10}$$

- Antisymmetry

$$R_{\sigma\mu\nu\rho} = -R_{\mu\sigma\nu\rho} = -R_{\sigma\mu\rho\nu} = R_{\mu\sigma\rho\nu} \tag{2.11}$$

- Cyclicity

$$R_{\sigma\mu\nu\rho} + R_{\sigma\rho\mu\nu} + R_{\sigma\nu\rho\mu} = 0 \tag{2.12}$$

- Bianchi identities

$$R_{\sigma\mu\nu\rho;\lambda} + R_{\sigma\mu\lambda\rho;\nu} + R_{\sigma\mu\rho\lambda;\nu} = 0 \tag{2.13}$$

Being $R^\lambda_{\mu\nu\rho}$ the curvature tensor, when it vanishes, the space is flat.

Realizing $R^\lambda_{\mu\nu\rho}$ is a tensor and involves second order partial differentiation of the metric tensor, it is a suitable candidate to appear in the equations we are seeking to describe gravity. Even more suitable would be a contraction of this tensor into a second-order one, which we can do as follows

$$R_{\mu\rho} = g^{\sigma\nu} R_{\sigma\mu\nu\rho} = R^\nu_{\mu\nu\rho}, \tag{2.14}$$

where $R_{\mu\rho}$ is the **Ricci tensor**, which is symmetric.

The Ricci tensor can be further contracted to originate the **Ricci scalar** or curvature scalar

$$R = g^{\mu\rho}R_{\mu\rho}. \tag{2.15}$$

Using the Ricci tensor and the curvature scalar, we can define the **Einstein tensor** [15]

$$G_{\mu\nu} \equiv R_{\mu\nu} - \frac{1}{2}g_{\mu\nu}R, \tag{2.16}$$

which is also symmetric and whose covariant derivative vanishes from the Bianchi identities

$$\nabla_\nu G^{\mu\nu} \equiv 0. \tag{2.17}$$

This tensor is appropriate to describe the curvature of space-time.

We seek now a way to describe the source of the gravitational field, which is found by turning our attention to special relativity, where a continuous distribution of matter is represented by an **energy-momentum tensor** $T^{\mu\nu}$. It expresses the flux of the four-momentum p^μ across a surface of constant x^ν. Its form changes according to the matter distribution considered and its components have different physical meanings [16]:

- T^{00} – energy density

- T^{i0} – p^i momentum density

- T^{0i} – energy flux across x^i surface

If we consider a dust distribution, the energy-momentum tensor will take the form

$$T^{\mu\nu} = \rho u^\mu u^\nu, \tag{2.18}$$

where ρ represents the mass-energy density and $u^\alpha = dx^\alpha/d\tau$ a unit timelike vector field that represents the 4-velocity [18].

If we consider a perfect fluid, the energy-momentum tensor will take the form [19]

$$T^{\mu\nu} = \left(\rho + \frac{P}{c^2}\right)u^\mu u^\nu - Pg^{\mu\nu}, \tag{2.19}$$

where P represents the pressure of the fluid. It is worth mentioning that (2.19) is a diagonal tensor.

The conservation laws of energy and momentum make the divergence of this tensor vanish in special relativity

$$\partial_\nu T^{\mu\nu} = 0. \tag{2.20}$$

The following generalization allows to adapt the conservation of $T^{\mu\nu}$ to general relativity [15]

$$\nabla_\nu T^{\mu\nu} = 0. \tag{2.21}$$

(2.17) and (2.21) suggest the Einstein tensor and the energy-momentum tensor to be proportional

$$G_{\mu\nu} = \kappa T_{\mu\nu}, \tag{2.22}$$

where κ is a constant called the coupling constant given by

$$\kappa = \frac{8\pi G}{c^4}. \tag{2.23}$$

In this way we just obtained the **Einstein field equations** [15–17]

$$G_{\mu\nu} = \frac{8\pi G}{c^4} T_{\mu\nu}. \tag{2.24}$$

The implications of this law of gravitation pertain to consider gravitation as a modification – a bending – of the space-time continuum described on the left hand side of the equation, caused by a matter field source, present on the right hand side of the equation.

At the time when Einstein's equations were formulated, the universe was pictured as a static and homogeneous entity, which lead Einstein to find closed static solutions to his field equations. In order to achieve this, an extra term, consistent with the field equations, was needed. Taking into account

$$\nabla_\nu g^{\mu\nu} = 0, \tag{2.25}$$

a linear term in $g^{\mu\nu}$ can be added to (2.24), yielding

$$G_{\mu\nu} = \frac{8\pi G}{c^4} T_{\mu\nu} + \Lambda g_{\mu\nu}, \tag{2.26}$$

where $\Lambda g_{\mu\nu}$ is the cosmological term that enables the equations to describe a static universe and Λ is a constant, called the cosmological constant.

At the present moment, there is enough evidence to state that the universe is not static but subject to (accelerated) expansion. It is still useful to introduce the cosmological term in the field equations because it can be interpreted as the energy density of the vacuum, an entity which might have played an important role in the early universe. It can be also related with the presence of dark energy in the universe, a hypothesis we shall discuss in further chapters. [13]

Henceforward, we will work with $c = 1$ units.

Chapter 3

Standard Cosmology Model

The standard model for cosmology stipulates that the universe originated from a hot dense state 13.7×10^9 years ago; at this time expansion and cooling down started. This model is based on the observational evidence that galaxies are moving away from each other, that the cosmic microwave background radiation (CMBR), as well as the largest known structures of the Universe, are homogeneous and isotropic.

The **Cosmological principle** tells us all positions in the universe are essentially equivalent. The assumption that the universe presents the same aspect from every point at each epoch, except for local irregularities, is a cornerstone of cosmology. If the universe is, in average and not in detail, homogeneous and isotropic, it can be considered spherically symmetric about us, as well as about any other point, since it is assumed we do not occupy a privileged position [15, 17].

3.1 Robertson-Walker Metric

From the cosmological principle, we can define a time coordinate that decreases monotonically as the universe evolves as a clock. Considering such a time coordinate and the isotropy of the universe, the metric must take a form of the kind [19]

$$d\tau^2 = dt^2 - Q^2(t)[f^2(r)dr^2 + g^2(r)d\psi^2], \tag{3.1}$$

where $f(r)$ and $g(r)$ are arbitrary and $Q(t)$ is the scale factor. Due to spherical symmetry, we can decompose $d\psi^2 = d\theta^2 + sin^2\theta d\phi$.

The most general metric it is possible to build in spherical coordinates for this space considers $f^2 = \frac{1}{1-kr^2}$ and $g^2 = r^2$. It is called the Friedmann-Lemaître-Robertson-Walker (FLRW) metric

$$ds^2 = dt^2 - Q(t)^2 \left[\frac{dr^2}{1 - kr^2} + r^2(d\theta^2 + \sin^2\theta d\phi^2) \right], \tag{3.2}$$

where k represents the curvature of the space.

The space curvature constant k is responsible for the geometry of the space:

- $k < 0$, a negative curvature describes an open universe (hyperbolic);

- $k = 0$, a zero curvature describes a flat universe;

- $k > 0$, a positive curvature describes a closed universe (spherical).

The metric tensor will be, in this case

$$g_{\mu\nu} = \begin{pmatrix} 1 & 0 & 0 & 0 \\ 0 & -\frac{Q(t)^2}{1-kr^2} & 0 & 0 \\ 0 & 0 & -Q(t)^2 r^2 & 0 \\ 0 & 0 & 0 & -Q(t)^2 r^2 \sin^2\theta \end{pmatrix}. \tag{3.3}$$

3.2 Friedmann's Equation

The field equations (2.24), when conjugated with the Robertson-Walker metric and the energy-momentum tensor for a perfect fluid (2.19), yield two independent equations

$$R_{00} - \frac{1}{2} g_{00} R - \Lambda g_{00} = 8\pi G T_{00}, \tag{3.4}$$

$$R_{ii} - \frac{1}{2} g_{ii} R - \Lambda g_{ii} = 8\pi G T_{ii}. \tag{3.5}$$

The energy-momentum tensor, in co-moving coordinates in which $u_i = (1, 0, 0, 0)$, will be

$$T_{00} = \rho \tag{3.6}$$

$$T_{ii} = -g_{ii} P. \tag{3.7}$$

For our metric, the non-vanishing Christoffel symbols will yield the following Ricci tensors

$$R_{00} = -3\frac{\ddot{Q}}{Q}, \tag{3.8}$$

$$R_{ii} = -g_{ii}\left(\frac{\ddot{Q}}{Q} + 2\frac{\dot{Q}^2 + k}{Q^2}\right). \tag{3.9}$$

This allows us to write the curvature scalar

$$R = g^{tt} R_{tt} + g^{rr} R_{rr} + g^{\phi\phi} R_{\phi\phi} + g^{\theta\theta} R_{\theta\theta} \tag{3.10}$$

$$= -3\frac{\ddot{Q}}{Q} - 3\left(\frac{\ddot{Q}}{Q} + 2\frac{\dot{Q}^2 + k}{Q^2}\right) \tag{3.11}$$

$$= -6\left(\frac{\ddot{Q}}{Q} + \frac{\dot{Q}^2 + k}{Q^2}\right). \tag{3.12}$$

Then, the time component of the field equation yields

$$3\frac{\dot{Q}^2 + k}{Q^2} - \Lambda = 8\pi G\rho, \tag{3.13}$$

which is called the Friedmann equation and describes how the density and curvature of the universe are connected to its velocity of expansion.

And the ii-th component yields

$$2\frac{\ddot{Q}}{Q} + \frac{\dot{Q}^2 + k}{Q^2} - \Lambda = -8\pi GP. \tag{3.14}$$

Inserting (3.13) in (3.14) and rearranging, results in

$$\frac{\ddot{Q}}{Q} = \frac{\Lambda}{3} - \frac{4\pi G}{3}(\rho + 3P), \tag{3.15}$$

which is called the equation of acceleration. Together with (3.13), it forms the Friedmann-Lemaître equations.

Rearranging (3.13) into

$$\dot{Q}^2 + k = \frac{Q^2}{3}(8\pi G\rho + \Lambda), \tag{3.16}$$

taking its time derivative

$$2\ddot{Q}\dot{Q} = \frac{2\dot{Q}Q}{3}(8\pi G\rho + \Lambda) + Q^2\frac{8\pi G\dot{\rho}}{3}, \tag{3.17}$$

simplifying and inserting (3.15) in it, yields

$$-\frac{4\pi G(\rho + 3P)}{3} + \frac{\Lambda}{3} = \left(\frac{8\pi G\rho}{3} + \frac{\Lambda}{3}\right) + \frac{4\pi G\dot{\rho}}{3}\frac{Q}{\dot{Q}}$$

$$\dot{\rho} = -3\frac{\dot{Q}}{Q}(\rho + P), \tag{3.18}$$

which describes the energy-mass conservation. If we computed $T^{\mu\nu}_{;\nu} = 0$, we would achieve this same conservation equation [15]. This equation can be written independently for each component of the universe as long as there is no significant conversion between the various components, as

$$\dot{\rho}_i = -3\frac{\dot{Q}}{Q}(\rho_i + P_i). \tag{3.19}$$

3.3 Parameters of an Expanding Universe

3.3.1 Hubble's Law

To determine the expansion rate of the universe, we begin by defining the Hubble parameter [12, 19]

$$H \equiv \frac{\dot{Q}(t)}{Q(t)}. \tag{3.20}$$

Its present value ($t = t_0$) is called the Hubble constant, H_0, and is 70.4 ± 2.5 km s^{-1} Mpc^{-1} [11]. It is used in Hubble's law

$$\vec{v} = H_0 \vec{r}, \tag{3.21}$$

which expresses the observational evidence, discovered by Edwin Hubble, that the recession velocity of a galaxy is proportional to the distance from that galaxy to Earth – an object moves the faster away from Earth the more distant it is. In this moment it was realized the universe is expanding!

3.3.2 Critical Density

In the Friedmann equation (3.13), we can absorb the cosmological constant writing it as a component of the energy density

$$\rho_\Lambda = \frac{\Lambda}{8\pi G}. \tag{3.22}$$

If the Hubble parameter and (3.22) is inserted in (3.13), this yields

$$3 \left(H^2 + \frac{k}{Q(t)^2} \right) = 8\pi G \tilde{\rho}, \tag{3.23}$$

where

$$\tilde{\rho} = \rho + \rho_\Lambda. \tag{3.24}$$

(3.23) can be rearranged into [12]

$$\frac{k}{Q(t)^2 H^2} = \frac{\tilde{\rho}}{\frac{3H^2}{8\pi G}} - 1 \equiv \Omega - 1, \tag{3.25}$$

where we define the density parameter Ω as the ratio

$$\Omega = \frac{\tilde{\rho}}{\rho_c}. \tag{3.26}$$

Here, ρ_c denotes the critical density

$$\rho_c = \frac{3H^2}{8\pi G}, \tag{3.27}$$

which, for a given expansion rate, represents the density that will result in $k = 0$ (making the comoving part of the metric look Euclidean) [19]. If a universe presents a density above this critical value, $\Omega > 1 \implies k > 0$, it will be spatially closed, while a universe with a lower critical value will have $\Omega < 1 \implies k < 0$ and be spatially open, as seen in §3.1.

3.3.3 Density Parameter

We can define different density parameters for different universe entities, namely

$$\Omega_{mat} = \frac{\rho_{mat}}{\rho_c} \tag{3.28}$$

$$\Omega_r = \frac{\rho_r}{\rho_c} \tag{3.29}$$

$$\Omega_\Lambda = \frac{\rho_\Lambda}{\rho_c} \tag{3.30}$$

the density parameter for matter, radiation and cosmological constant, respectively. We can further distinguish between the density of baryonic matter and cold dark matter writing $\Omega_{mat} = \Omega_b + \Omega_c$ and absorb the curvature term of the Friedmann equation into the energy density as we did for the cosmological constant

$$\Omega_k = \frac{\rho_k}{\rho_c}, \qquad \rho_k = -\frac{k}{(QH)^2}. \tag{3.31}$$

3.3.4 Equations of State

In the following treatment, it is useful to introduce an equation of state to describe the way energy density changes with pressure [12]

$$\omega = \frac{P}{\rho}, \tag{3.32}$$

which will have a different value according to the type of entity considered. Introducing H, Ω and ω in the energy conservation equation (3.19), we can rewrite it as

$$\dot{\Omega} = -3H\Omega(1 + \omega). \tag{3.33}$$

When ω is independent of time, an assumption we will make throughout this work, the density will evolve with the expansion rate by (3.19). Integrating this equation, results in

$$\rho_i \propto Q^{-3(1+\omega_i)}, \tag{3.34}$$

where the constant of proportionality can be found by assuming this equation is valid at any epoch. Then, it is also valid in the present moment (t_0). If we choose the following conditions to apply

$$\begin{cases} Q(t_0) = Q_0 = 1 \\ \dot{Q}(t_0) = \dot{Q}_0 = 1 \end{cases} \tag{3.35}$$

then (3.34) will yield

$$\rho_0 = AQ_0^{-3(1+\omega)} \implies A = \rho_0. \tag{3.36}$$

Let us now write the equations of state for each of the components present in the universe.

Non-relativistic matter interacts only gravitationally, behaving as dust, which means pressure does not give any contribution in this case

$$P_{mat} = 0. \tag{3.37}$$

This makes it possible to write for a matter-dominated universe (a universe where the energy density of matter is so high in comparison with the energy density of other components that we can neglect them)

$$\omega_{mat} = 0. \tag{3.38}$$

On the other hand, for radiation we know

$$P_r = \frac{1}{3}\rho_r, \tag{3.39}$$

from black-body radiation considerations. This yields

$$\omega_r = \frac{1}{3}. \tag{3.40}$$

Another contribution to the universe is the cosmological constant, accounting for the accelerated expansion of the universe. It can be interpreted as the energy-density of the vacuum or dark energy. From the Friedmann equations and the energy-momentum tensor, Λ is characterized by

$$P_\Lambda = -\rho_\Lambda, \tag{3.41}$$

which results in

$$\omega_\Lambda = -1. \tag{3.42}$$

This allows us to write

$$\rho_{mat} = \frac{\rho_{mat}(t_0)}{Q(t)^3} \tag{3.43}$$

$$\rho_r = \frac{\rho_r(t_0)}{Q(t)^4} \tag{3.44}$$

$$\rho_\Lambda = \rho_\Lambda(t_0) = \frac{\Lambda}{8\pi G} \tag{3.45}$$

for the energy density of matter, radiation and dark energy, respectively.

3.4   Cosmological Dynamics

3.4.1   Equations of Motion

We shall now derive the equations of motion of the universe from the Friedmann equation, which can be written in a more convenient form for now

$$\dot{Q}(t) = \sqrt{\frac{8\pi G\tilde{\rho}}{3}Q(t)^2 - k}, \tag{3.46}$$

where Λ is once again included as part of the total energy density $\tilde{\rho}$.

In the first part of this section let us consider a flat universe, $k = 0$. This assumption is consistent with the latest measurements of the curvature of the universe [11, 20] and with the fact that it corresponds to a negligible term in the early universe [12]. By this means, it is possible to analytically find the evolution of the scale factor with time, considering different entities of the universe.

For a (non-relativistic) matter-dominated universe, (3.43) holds, yielding

$$\dot{Q}(t) = \sqrt{\frac{8\pi G\rho_{mat}(t_0)}{3Q(t)}}. \tag{3.47}$$

For a radiation-dominated universe, with the help of (3.44), we write

$$\dot{Q}(t) = \sqrt{\frac{8\pi G\rho_r(t_0)}{3Q(t)^2}}. \tag{3.48}$$

For a dark energy-dominated universe, using (3.45), results

$$\dot{Q}(t) = \sqrt{\frac{8\pi G\rho_\Lambda(t_0)Q(t)^2}{3}}. \tag{3.49}$$

Integrating the previous expressions in time, we obtain the equations of motion

$$Q(t) = \begin{cases} [6\pi G\rho_{mat}(t_0)]^{\frac{1}{3}} t^{\frac{2}{3}} & \text{for matter-dominated} \tag{3.50} \\[2mm] \left(\dfrac{32\pi G\rho_r(t_0)}{3}\right)^{\frac{1}{4}} t^{\frac{1}{2}} & \text{for radiation-dominated} \tag{3.51} \\[2mm] Q_0 e^{\sqrt{\frac{\Lambda}{3}}t} & \text{for dark energy-dominated} \tag{3.52} \end{cases}$$

The case of a flat, matter-dominated universe governed by (3.50) is known as Einstein-DeSitter model.

For a "general" universe – a universe in a regime where none of the entities is dominant – the only simplification of the Friedmann equation consists in inserting relations (3.43), (3.44), (3.45) and dividing them by ρ_c

$$\dot{Q}(t) = \sqrt{(\Omega_b + \Omega_c + \Omega_r + \Omega_\Lambda)\,Q(t)^2 + \Omega_k} \tag{3.53}$$

$$= \sqrt{\frac{\Omega_r(t_0)}{Q(t)^2} + \frac{\Omega_b(t_0) + \Omega_c(t_0)}{Q(t)} + \Omega_k(t_0) + \Omega_\Lambda Q(t)^2}. \tag{3.54}$$

3.4.2 Density Parameter

The Friedmann equation expressing the conservation of mass (3.19) allows us to write for each component of a general universe, taking into account (3.43), (3.44) and (3.45),

$$
\begin{cases}
\dot{\Omega}_b + \dot{\Omega}_c = -3\dfrac{\Omega_b(t_0) + \Omega_c(t_0)}{Q(t)^3}\sqrt{\dfrac{\Omega_r(t_0)}{Q(t)^4} + \dfrac{\Omega_b(t_0) + \Omega_c(t_0)}{Q(t)^3} + \dfrac{\Omega_k(t_0)}{Q(t)^2} + \Omega_\Lambda} & \text{for matter} \\[3ex]
\dot{\Omega}_r = -4\dfrac{\Omega_r(t_0)}{Q(t)^4}\sqrt{\dfrac{\Omega_r(t_0)}{Q(t)^4} + \dfrac{\Omega_b(t_0) + \Omega_c(t_0)}{Q(t)^3} + \dfrac{\Omega_k(t_0)}{Q(t)^2} + \Omega_\Lambda} & \text{for radiation} \\[3ex]
\Omega_\Lambda = \Omega_\Lambda(t_0) & \text{for dark-energy}
\end{cases}
$$

3.4.3 Temperature

From the energy density of the black-body radiation,

$$\rho_{rad} \propto T^4, \tag{3.55}$$

where T represents the temperature of the body. For the case of radiation, (3.44) holds, meaning

$$T \propto Q^{-1}. \tag{3.56}$$

The proportionality factor of this relation can be calculated as in (3.36), resulting in

$$T_r = \frac{T_r(t_0)}{Q(t)}, \tag{3.57}$$

where $T_r(t_0)$ represents the present temperature of radiation.

3.5 Foundations and Overview

3.5.1 Big Bang Theory

To enable nucleosynthesis, the hypothesis of a dense, hot universe in early times is needed. It cooled down as it expanded and as a direct consequence, a relic background radiation of approximately 2.7 K is measurable [21]. Extrapolating the present expansion backward in time, the universe would have began in an infinitely dense and hot singularity, which is known as the Big Bang [22]. A hot Big Bang is inferred from our previous analysis by realizing that in (3.57), as $Q(t) \to 0$, $T \to \infty$. General relativity breaks down at this point and only after the Planck time can we track what happened in the universe, from particle physics and thermodynamics considerations. Prior to it, quantum fluctuations assume a paramount importance and, presently, no theory combines quantum mechanics consistently with general relativity.

Although suitable to predict the observed abundance of light elements and the CMBR, the Big Bang model poses a number of pertinent problems, which justify the need of a complementary theory. The best one to date is inflationary cosmology.

3.5.2 The Inflationary Model

As pointed out, the universe is highly homogeneous and isotropic and no matter how distant from each other photons are today, they share a uniform temperature depicted by the CMBR. This is even so in parts of the universe that did not have causal contact with each other and the Big Bang model offers no explanation on why this is possible. This is called the horizon problem. At the same time, the anisotropies in the background radiation which give rise to the large scale structures are also not explained. Another unanswered question is why the universe is flat – referred to as the flatness problem. In the list of unsolved questions figure also gravitinos and monopoles – topological defects arising from symmetry breaking in particle theories – predicted by the hot Big Bang, but not observed until now [22, 23].

Inflation proposes a brief period of exponential (or quasi-exponential) growth for early times, instead of the power expansion, described in (3.50) and (3.51), that we observe afterwards. It resorts to a scalar field that has a large energy density and decreases very slowly at early times, making expansion obey an exponential law. Past a certain point in the expansion, this field decreases faster, becoming small and letting the universe enter a power law expansion. This hypothesis does not imply a large energy density of the field had to appear throughout the whole universe at the same time, but only in a small region, which after inflating would easily comprise almost all the volume of the universe [24].

The consequence is a huge expansion in a short period of time, which allows a small causal region in thermal contact in the past to be blown up and account for the homogeneity of everything we see so far. It transforms the particles existing before inflation in such an insignificant fraction of the universe that its density essentially reaches zero. An exponential expansion decreases curvature, solving the flatness problem and the inhomogeneities observed in today's universe can be a product of microscopic quantum fluctuations that were stretched out by inflation. Only fluctuations at the end of the inflation era can be seen today, since at early inflationary stages quantum fluctuations were stretched to such large distances that we can not observe them [24].

3.5.3 ΛCDM Model

The ΛCDM model is the incorporation of dark energy, as a cosmological constant Λ, and dark matter in our theory in order for standard cosmology to match astrophysical observational evidence. The term "dark" refers to a non-absorbing and non-luminous entity. Galaxies, stars, globular clusters and other luminous objects move faster than it is gravitationally predicted accounting for all visible objects. In the Milky Way, as well as in other galaxies studied, instead of a velocity law decreasing with $r^{-1/2}$, the velocity re-

mains approximately constant with the change of the radius. The existence of a dark halo of matter can solve this paradox and this is where dark matter, which can also explain gravitational lensing effects, can lend us a hand. It is not yet known what dark matter is formed of, but there are several particle candidates, as well as experiments to detect them directly or indirectly. Since dark matter needs to fill certain requirements that can be inferred from observation, e.g. through galaxy clusters velocity dispersion and X-ray measurement, it was possible to get many constraints on its nature [25]. We shall discuss more about it later, in §5.9.

A requirement of dark matter is that it must interact weakly with typical matter, i. e. baryons, in order to explain why we never did observe it. CDM stands for Cold Dark Matter and refers to non-relativistic matter, since evidence points to a particle which is heavy enough to clump together and to explain the discrepancy between the total mass which exerts gravitational influence and the observed mass of baryonic matter in the universe.

Measurements of type Ia Supernovae redshift tell us the universe is undergoing accelerated expansion and that the presence of a positive cosmological constant can be the key to explain how [5,6]. It can also help finding the missing energy component in the composition of the universe. If the universe is flat, we see from (3.25) the energy density needs to equal the critical density, which measurements show does not happen. The missing component, although accounting for 2/3 of the critical density, must not have interfered with structure formation, which constrains it to be distributed smoothly over the universe and have an energy density evolution with Q slower than that of matter. From (3.34) we see this last condition implies $\omega < 0$ which is equivalent to a negative pressure.

In quantum field theory, the covariant form for the vacuum energy can only take the form of a cosmological constant

$$T_{\mu\nu}^{vac} = \rho^{vac} g_{\mu\nu}, \tag{3.58}$$

where ρ^{vac} describes the energy density of a perfect fluid with isotropic pressure $p^{vac} = -\rho^{vac}$ [26]. Then, vacuum energy would be the perfect candidate to dark energy, yielded it not a contribution up to 120 orders of magnitude more than the present critical density [27,28]. This unavoidable discrepancy is known as the cosmological constant problem. There are other candidates, namely the quintessence field [10].

The proposal in this work is to identify dark energy with a cosmological constant arising from conformal variations of the metric tensor. We will spend the next chapter understanding how fluctuations of the metric can turn out in the form of a cosmological constant and chapter 6 modelling a universe where these fluctuations are present in the dark energy component.

Chapter 4

Beyond the Standard Cosmological Model

4.1 Fluctuations of the Metric

At the Planck scale, gravity and quantum mechanics can not be seen as independent. The space-time is coarse grained at this scale, requiring a quantum metric tensor. If a scalar field φ is introduced to account for the quantum fluctuations of the metric tensor around its classical value, the resulting metric will be a quantum variable.

The simplest way of generalizing the metric to include quantum effects is through conformal variations of the metric. The advantage of using conformal variations is that causality is obeyed, since the light cone structure remains intact. These fluctuations can be written as follows [8, 9]

$$g_{\mu\nu} = (1 + \varphi)^2 \bar{g}_{\mu\nu} \tag{4.1}$$

$$= \Phi^2 \bar{g}_{\mu\nu}, \tag{4.2}$$

where $\bar{g}_{\mu\nu}$ represents the usual metric tensor, here called classical, about which the fluctuations occur. The fluctuation average of this background metric is $< \varphi > = < \varphi_{,\mu} > = 0$, centering the generalized metric around its classical value and yielding no drift of φ in space-time.

The derivative of the generalized metric is now

$$g_{\mu\nu,\rho} = 2\Phi\varphi_{,\rho}\bar{g}_{\mu\nu} + \Phi^2 \bar{g}_{\mu\nu,\rho}. \tag{4.3}$$

In the same fashion, the inverse of the metric tensor is

$$g^{\mu\nu} = \Phi^{-2} \bar{g}^{\mu\nu}. \tag{4.4}$$

4.2 Modified Einstein Equations

As we have seen in (2.26), Einstein's equation with a cosmological constant $\bar{\Lambda}$ has the following form

$$\bar{G}_{\mu\nu} - \bar{\Lambda}g_{\mu\nu} = 8\pi G T_{\mu\nu} \Leftrightarrow \bar{R}_{\mu\nu} - \frac{1}{2}g_{\mu\nu}\bar{R} - \bar{\Lambda}g_{\mu\nu} = 8\pi G T_{\mu\nu}. \tag{4.5}$$

How will variations about the metric tensor influence it?

4.2.1 Curvature Tensor with Fluctuations

A new Ricci tensor arises if it is considered that fluctuations around the metric do exist. Let us begin with the usual Ricci tensor

$$R_{\mu\nu} = R^{\rho}_{\mu\rho\nu} = -R^{\rho}_{\mu\nu\rho}, \tag{4.6}$$

which can be written in terms of affine connections as

$$R^{\lambda}_{\mu\nu\rho} = \Gamma^{\lambda}_{\mu\rho,\nu} - \Gamma^{\lambda}_{\mu\nu,\rho} + \Gamma^{\lambda}_{\sigma\nu}\Gamma^{\sigma}_{\rho\mu} - \Gamma^{\lambda}_{\sigma\rho}\Gamma^{\sigma}_{\mu\nu}. \tag{4.7}$$

Using (2.5) and (4.3), this can be written in terms of the classical metric tensor

$$\Gamma^{\lambda}_{\mu\nu} = \frac{1}{2}\bar{g}^{\lambda\tau}\left(\bar{g}_{\tau\mu,\nu} + \bar{g}_{\tau\nu,\mu} - \bar{g}_{\mu\nu,\tau}\right)$$
$$+ \frac{1}{2}\Phi^{-2}\bar{g}^{\lambda\tau}\left(2\Phi\varphi_{,\nu}\bar{g}_{\tau\mu} + 2\Phi\varphi_{,\mu}\bar{g}_{\tau\nu} - 2\Phi\varphi_{,\tau}\bar{g}_{\mu\nu}\right). \tag{4.8}$$

The first term of (4.8) can immediately be identified as the classical affine connection. Knowing $\bar{g}^{\rho\sigma}\varphi_{,\sigma}\bar{g}_{\mu\nu} = \varphi^{,\rho}\bar{g}_{\mu\nu}$ and provided $\bar{g}_{\mu\nu}$ is diagonal

$$\Gamma^{\lambda}_{\mu\nu} = \bar{\Gamma}^{\lambda}_{\mu\nu} + \Phi^{-1}\left(\varphi_{,\nu}\delta^{\lambda}_{\mu} + \varphi_{,\mu}\delta^{\lambda}_{\nu} - \varphi^{,\lambda}\bar{g}_{\mu\nu}\right). \tag{4.9}$$

The derivative of the affine connection yields

$$\Gamma^{\lambda}_{\mu\nu,\rho} = \bar{\Gamma}^{\lambda}_{\mu\nu,\rho} + \Phi^{-2}(-\varphi_{,\rho}\varphi_{,\nu}\delta^{\lambda}_{\mu} - \varphi_{,\rho}\varphi_{,\mu}\delta^{\lambda}_{\nu} + \varphi_{,\rho}\varphi^{,\lambda}\bar{g}_{\mu\nu})$$
$$+ \Phi^{-1}(\varphi_{,\nu,\rho}\delta^{\lambda}_{\mu} + \varphi_{,\mu,\rho}\delta^{\lambda}_{\nu} - \varphi^{,\lambda}\bar{g}_{\mu\nu,\rho}). \tag{4.10}$$

Now the first two terms of the Riemann tensor can be computed

$$\Gamma^{\rho}_{\mu\rho,\nu} - \Gamma^{\rho}_{\mu\nu,\rho} = \bar{\Gamma}^{\rho}_{\mu\rho,\nu} - \bar{\Gamma}^{\rho}_{\mu\nu,\rho} + \Phi^{-2}\left(-\delta^{\rho}_{\rho}\varphi_{,\nu}\varphi_{,\mu} + \varphi_{,\nu}\varphi^{,\rho}\bar{g}_{\mu\rho} + \delta^{\rho}_{\nu}\varphi_{,\rho}\varphi_{,\mu} - \varphi_{,\rho}\varphi^{,\rho}\bar{g}_{\mu\nu}\right)$$
$$+ \Phi^{-1}\left(\delta^{\rho}_{\rho}\varphi_{,\mu,\nu} - \varphi^{,\rho}_{,\nu}\bar{g}_{\mu\rho} - \varphi^{,\rho}\bar{g}_{\mu\rho,\nu} - \delta^{\rho}_{\nu}\varphi_{,\mu,\rho} + \varphi^{,\rho}_{,\rho}\bar{g}_{\mu\nu} + \varphi^{,\rho}\bar{g}_{\mu\nu,\rho}\right) \tag{4.11}$$
$$= \bar{\Gamma}^{\rho}_{\mu\rho,\nu} - \bar{\Gamma}^{\rho}_{\mu\nu,\rho} - \Phi^{-2}\left(2\varphi_{,\nu}\varphi_{,\mu} + \varphi_{,\rho}\varphi^{,\rho}\bar{g}_{\mu\nu}\right)$$
$$+ \Phi^{-1}\left(3\varphi_{,\mu,\nu} + \varphi^{,\rho}_{,\rho}\bar{g}_{\mu\nu} - \varphi^{,\rho}\bar{g}_{\mu\rho,\nu} + \varphi^{,\rho}\bar{g}_{\mu\nu,\rho} - \varphi^{,\rho}_{,\nu}\bar{g}_{\mu\rho}\right), \tag{4.12}$$

where the properties $g_{\alpha\beta} = g_{\beta\alpha}$ and $g_{\alpha\beta,\delta}g^{\beta\gamma} = -g_{\alpha\beta}g^{\beta\gamma}_{,\delta}$ were used.

Multiplying this expression by $\Phi^{-2}\bar{g}^{\mu\nu}$ to simplify the fluctuation-dependent part, the last two terms yield

$$
\begin{aligned}
&-\Phi^{-2}\left(2\varphi_{,\nu}\varphi_{,\mu} + \varphi_{,\rho}\varphi^{,\rho}\bar{g}_{\mu\nu}\right) + \Phi^{-1}\left(3\varphi_{,\mu,\nu} + \varphi^{,\rho}_{,\rho}\bar{g}_{\mu\nu} - \varphi^{,\rho}\bar{g}_{\mu\rho,\nu} + \varphi^{,\rho}\bar{g}_{\mu\nu,\rho} - \varphi^{,\rho}_{,\nu}\bar{g}_{\mu\rho}\right) \\
&= -2\Phi^{-4}\varphi^{,\mu}\varphi_{,\mu} + 3\Phi^{-3}\varphi_{,\mu,\nu}\bar{g}^{\mu\nu} - 4\Phi^{-4}\varphi_{,\mu}\varphi^{,\mu} + 4\Phi^{-3}\varphi^{,\mu}_{,\mu} - \Phi^{-3}\varphi^{,\rho}\bar{g}^{\mu\nu}\bar{g}_{\mu\nu,\rho} \\
&\quad -\Phi^{-3}\varphi^{,\mu}_{,\mu}
\end{aligned}
\tag{4.13}
$$

It is now useful to derive the following relation

$$
\left(\bar{g}^{\mu\nu}\varphi_{,\mu}\right)_{,\nu} = \bar{g}^{\mu\nu}_{,\nu}\varphi_{,\mu} + \bar{g}^{\mu\nu}\varphi_{,\mu,\nu}
\tag{4.14}
$$

$$
= \bar{g}_{\mu\rho}\bar{g}^{\mu\nu}_{,\nu}\varphi^{,\rho} + \bar{g}^{\mu\nu}\varphi_{,\mu,\nu}
\tag{4.15}
$$

$$
= -\bar{g}_{\mu\rho,\nu}\bar{g}^{\mu\nu}\varphi^{,\rho} + \bar{g}^{\mu\nu}\varphi_{,\mu,\nu}.
\tag{4.16}
$$

Using (4.16), (4.13) results in

$$
\begin{aligned}
&-2\Phi^{-4}\varphi^{,\mu}\varphi_{,\mu} + 3\Phi^{-3}\varphi_{,\mu,\nu}\bar{g}^{\mu\nu} - 4\Phi^{-4}\varphi_{,\mu}\varphi^{,\mu} + 4\Phi^{-3}\varphi^{,\mu}_{,\mu} - \Phi^{-3}\varphi^{,\rho}\bar{g}^{\mu\nu}\bar{g}_{\mu\nu,\rho} - \Phi^{-3}\varphi^{,\mu}_{,\mu} \\
&= -6\Phi^{-4}\varphi^{,\mu}\varphi_{,\mu} + 6\Phi^{-3}\varphi^{,\mu}_{,\mu} + 2\Phi^{-3}\bar{g}^{\mu\nu}\bar{g}_{\mu\rho,\nu}\varphi^{,\rho} + \Phi^{-3}\bar{g}^{\mu\nu}\bar{g}_{\mu\nu,\rho}\varphi^{,\rho}.
\end{aligned}
\tag{4.17}
$$

The next step is to compute the last two terms of the Riemann curvature tensor

$$
\begin{aligned}
\Gamma^{\rho}_{\sigma\nu}\Gamma^{\sigma}_{\rho\mu} - \Gamma^{\rho}_{\sigma\rho}\Gamma^{\sigma}_{\mu\nu} &= \bar{\Gamma}^{\rho}_{\sigma\nu}\bar{\Gamma}^{\sigma}_{\rho\mu} - \bar{\Gamma}^{\rho}_{\sigma\rho}\bar{\Gamma}^{\sigma}_{\mu\nu} \\
&+\bar{\Gamma}^{\rho}_{\sigma\nu}\Phi^{-1}\left(\delta^{\sigma}_{\rho}\varphi_{,\mu} + \delta^{\sigma}_{\mu}\varphi_{,\rho} - \varphi_{,\sigma}\bar{g}_{\rho\mu}\right) + \Phi^{-1}\left(\delta^{\rho}_{\sigma}\varphi_{,\nu} + \delta^{\rho}_{\nu}\varphi_{,\sigma} - \varphi^{,\rho}\bar{g}_{\sigma\nu}\right)\bar{\Gamma}^{\sigma}_{\rho\mu} \\
&-\bar{\Gamma}^{\rho}_{\sigma\rho}\Phi^{-1}\left(\delta^{\sigma}_{\nu}\varphi_{,\mu} + \delta^{\sigma}_{\mu}\varphi_{,\nu} - \varphi^{,\sigma}\bar{g}_{\nu\mu}\right) - \Phi^{-1}\left(\delta^{\rho}_{\sigma}\varphi_{,\rho} + \delta^{\rho}_{\rho}\varphi_{,\sigma} - \varphi^{,\rho}\bar{g}_{\sigma\rho}\right)\bar{\Gamma}^{\sigma}_{\mu\nu} \\
&+\Phi^{-2}\left(\delta^{\rho}_{\sigma}\varphi_{,\nu} + \delta^{\rho}_{\nu}\varphi_{,\sigma} - \varphi^{,\rho}\bar{g}_{\sigma\nu}\right)\left(\delta^{\rho}_{\sigma}\varphi_{,\rho} + \delta^{\rho}_{\rho}\varphi_{,\sigma} - \varphi^{,\rho}\bar{g}_{\sigma\rho}\right) \\
&-\Phi^{-2}\left(\delta^{\sigma}_{\rho}\varphi_{,\mu} + \delta^{\sigma}_{\mu}\varphi_{,\rho} - \varphi_{,\sigma}\bar{g}_{\rho\mu}\right)\left(\delta^{\sigma}_{\nu}\varphi_{,\mu} + \delta^{\sigma}_{\mu}\varphi_{,\nu} - \varphi^{,\sigma}\bar{g}_{\nu\mu}\right),
\end{aligned}
\tag{4.18}
$$

which after some computation, playing with the fact that $\delta^{\alpha}_{\alpha} = 4$ in our metric and $\varphi^{,\beta}\bar{g}_{\alpha\beta} = \varphi_{,\alpha}$, results in

$$
\begin{aligned}
\Gamma^{\rho}_{\sigma\nu}\Gamma^{\sigma}_{\rho\mu} - \Gamma^{\rho}_{\sigma\rho}\Gamma^{\sigma}_{\mu\nu} &= \bar{\Gamma}^{\rho}_{\sigma\nu}\bar{\Gamma}^{\sigma}_{\rho\mu} - \bar{\Gamma}^{\rho}_{\sigma\rho}\bar{\Gamma}^{\sigma}_{\mu\nu} + \Phi^{-1}\left(-2\bar{\Gamma}^{\sigma}_{\mu\nu}\varphi_{,\sigma} - \bar{\Gamma}^{\rho}_{\sigma\nu}\varphi^{,\sigma}\bar{g}_{\rho\mu}\right. \\
&\left.-\bar{\Gamma}^{\rho}_{\sigma\mu}\varphi^{,\sigma}\bar{g}_{\rho\nu} + \bar{\Gamma}^{\rho}_{\sigma\rho}\varphi^{,\sigma}\bar{g}_{\nu\mu}\right) + \Phi^{-2}\left(-2\varphi_{,\mu}\varphi_{,\nu} + 2\varphi_{,\sigma}\varphi^{,\sigma}\bar{g}_{\mu\nu}\right)
\end{aligned}
\tag{4.19}
$$

As before, multiplying it by $\Phi^{-2}\bar{g}^{\mu\nu}$ for the sake of simplicity, one gets

$$
\begin{aligned}
\Phi^{-2}\bar{g}^{\mu\nu}\left(\Gamma^{\rho}_{\sigma\nu}\Gamma^{\sigma}_{\rho\mu} - \Gamma^{\rho}_{\sigma\rho}\Gamma^{\sigma}_{\mu\nu}\right) &= \Phi^{-2}\bar{g}^{\mu\nu}\left(\bar{\Gamma}^{\rho}_{\sigma\nu}\bar{\Gamma}^{\sigma}_{\rho\mu} - \bar{\Gamma}^{\rho}_{\sigma\rho}\bar{\Gamma}^{\sigma}_{\mu\nu}\right) \\
&-2\Phi^{-3}\bar{g}^{\mu\nu}\bar{\Gamma}^{\sigma}_{\mu\nu}\varphi_{,\sigma} \\
&+2\Phi^{-3}\bar{\Gamma}^{\rho}_{\sigma\rho}\varphi^{,\sigma} + 6\Phi^{-4}\varphi^{,\nu}\varphi_{,\nu}
\end{aligned}
\tag{4.20}
$$

Writing the affine connections not purely classical in terms of the metric

$$
\begin{aligned}
\Phi^{-2}\bar{g}^{\mu\nu}\left(\Gamma^{\rho}_{\sigma\nu}\Gamma^{\sigma}_{\rho\mu} - \Gamma^{\rho}_{\sigma\rho}\Gamma^{\sigma}_{\mu\nu}\right) &= \Phi^{-2}\bar{g}^{\mu\nu}\left(\bar{\Gamma}^{\rho}_{\sigma\nu}\bar{\Gamma}^{\sigma}_{\rho\mu} - \bar{\Gamma}^{\rho}_{\sigma\rho}\bar{\Gamma}^{\sigma}_{\mu\nu}\right) \\
&\quad -2\Phi^{-3}\bar{g}^{\mu\nu}\bar{g}^{\sigma\tau}\left(\bar{g}_{\tau\mu,\nu} + \bar{g}_{\tau\nu,\mu} - \bar{g}_{\mu\nu,\tau}\right)\varphi_{,\sigma} \\
&\quad +2\Phi^{-3}\bar{g}^{\rho\tau}\left(\bar{g}_{\tau\sigma,\rho} + \bar{g}_{\tau\rho,\sigma} - \bar{g}_{\rho\sigma,\tau}\right)\varphi^{,\sigma} + 6\Phi^{-4}\varphi^{,\nu}\varphi_{,\nu} \\
&= \Phi^{-2}\bar{g}^{\mu\nu}\left(\bar{\Gamma}^{\rho}_{\sigma\nu}\bar{\Gamma}^{\sigma}_{\rho\mu} - \bar{\Gamma}^{\rho}_{\sigma\rho}\bar{\Gamma}^{\sigma}_{\mu\nu}\right) \\
&\quad -2\Phi^{-3}\bar{g}^{\mu\nu}\bar{g}_{\mu\rho,\nu}\varphi^{,\rho} + 2\Phi^{-3}\bar{g}^{\mu\nu}\bar{g}_{\mu\nu,\rho}\varphi^{,\rho} \\
&\quad +6\Phi^{-4}\varphi^{,\nu}\varphi_{,\nu}.
\end{aligned}
\tag{4.21}
$$

Finally, Ricci's tensor becomes

$$
\begin{aligned}
R_{\mu\nu} &= -\left(\bar{\Gamma}^{\rho}_{\mu\rho,\nu} - \bar{\Gamma}^{\rho}_{\mu\nu,\rho} + \bar{\Gamma}^{\rho}_{\sigma\nu}\bar{\Gamma}^{\sigma}_{\rho\sigma} - \bar{\Gamma}^{\rho}_{\sigma\rho}\bar{\Gamma}^{\sigma}_{\mu\rho}\right) \\
&\quad -\left(-6\Phi^{-4}\varphi^{,\mu}\varphi_{,\mu} + 6\Phi^{-3}\varphi^{,\mu}_{,\mu} + 2\Phi^{-3}\bar{g}^{\mu\nu}\bar{g}_{\mu\rho,\nu}\varphi^{,\rho} + \Phi^{-3}\bar{g}^{\mu\nu}\bar{g}_{\mu\nu,\rho}\varphi^{,\rho}\right) \\
&\quad -\left(-2\Phi^{-3}\bar{g}^{\mu\nu}\bar{g}_{\mu\rho,\nu}\varphi^{,\rho} + 2\Phi^{-3}\bar{g}^{\mu\nu}\bar{g}_{\mu\nu,\rho}\varphi^{,\rho} + 6\Phi^{-4}\varphi^{,\nu}\varphi_{,\nu}\right)
\end{aligned}
\tag{4.22}
$$

$$
= \bar{R}_{\mu\nu} - \left(6\Phi^{-3}\varphi^{,\mu}_{,\mu} + 3\Phi^{-3}\bar{g}^{\mu\nu}\bar{g}_{\mu\nu,\rho}\varphi^{,\rho}\right).
\tag{4.23}
$$

In this fashion, we obtain for the curvature scalar

$$
R = g^{\mu\nu}R_{\mu\nu} = \Phi^{-2}\bar{R} - \Phi^{-3}\left(3\bar{g}^{\mu\nu}\bar{g}_{\mu\nu,\rho}\varphi^{,\rho} + 6\varphi^{,\mu}_{,\mu}\right).
\tag{4.24}
$$

From

$$
\varphi^{;\mu}_{;\mu} = \varphi^{,\mu}_{,\mu} + \bar{\Gamma}^{\mu}_{\nu\mu}\varphi^{,\nu},
\tag{4.25}
$$

adding and subtracting $3\Phi^{-3}\bar{g}^{\mu\tau}\bar{g}_{\tau\mu,\nu}\varphi^{,\nu}$ to (4.24), we can rearrange it into

$$
R = \Phi^{-2}\bar{R} - \Phi^{-3}\left[3\bar{g}^{\mu\tau}\left(\bar{g}_{\tau\nu,\mu} + \bar{g}_{\tau\mu,\nu} - \bar{g}_{\nu\mu,\tau}\right)\varphi^{,\nu} + 6\varphi^{,\mu}_{,\mu}\right]
\tag{4.26}
$$

$$
= \Phi^{-2}\bar{R} - 6\Phi^{-3}\left(\varphi^{,\mu}_{,\mu} + \bar{\Gamma}^{\mu}_{\nu\mu}\varphi^{,\nu}\right)
\tag{4.27}
$$

$$
= \Phi^{-2}\bar{R} - 6\Phi^{-3}\varphi^{;\mu}_{;\mu}
\tag{4.28}
$$

$$
= \frac{\bar{R}}{\Phi^2} - \frac{6\Box\varphi}{\Phi^3},
\tag{4.29}
$$

where $\Box$ represents the D'Alembert operator.

4.2.2 Einstein Equations with Fluctuations from a Variational Principle

One way of deducing Einstein's equations is from the principle of least action. The action principle is based on the assumption that the action remains stationary for small variations of some dynamical variable. We are interested in a stationary action with respect to arbitrary variations of the metric tensor

$$
\delta S = 0.
\tag{4.30}
$$

This is the starting point to deduce Einstein's equations with fluctuations from a variational principle. The action can be found integrating the Lagrangian density over space

and time.

In this regard, the following relations are worth mentioning

$$\sqrt{-g} = \sqrt{-det(g_{\lambda\mu})} = \Phi^4\sqrt{-\bar{g}}, \tag{4.31}$$

$$\delta\sqrt{-g} = \frac{\delta g}{2\sqrt{-g}} = -\frac{1}{2}\sqrt{-g}g_{\lambda\mu}\delta g^{\lambda\mu}. \tag{4.32}$$

The action due to the gravitational field can be expressed as follows [15, 17]

$$S_g = \frac{1}{16\pi G}\int d^4x\sqrt{-g}(R + 2\bar{\Lambda}), \tag{4.33}$$

where G is the gravitational constant, R the Ricci scalar and $\bar{\Lambda}$ the cosmological constant. It can be divided into a R-dependent and a $\bar{\Lambda}$-dependent part

$$S_g = S_R + S_{\bar{\Lambda}}. \tag{4.34}$$

The action due to the cosmological constant is

$$S_{\bar{\Lambda}} = \frac{2\bar{\Lambda}}{16\pi G}\int d^4x\Phi^4\sqrt{-\bar{g}}. \tag{4.35}$$

The variation of the action for this term yields

$$\delta S_{\bar{\Lambda}} = \frac{2\bar{\Lambda}}{16\pi G}\left(\int d^4x\Phi^4\delta\sqrt{-\bar{g}} + \int d^4x 4\Phi^3\delta\varphi\sqrt{-\bar{g}}\right) \tag{4.36}$$

$$= \frac{2\bar{\Lambda}}{16\pi G}\int d^4x\sqrt{-\bar{g}}\left(-\frac{\Phi^4}{2}\bar{g}_{\lambda\mu}\delta\bar{g}^{\lambda\mu} + 4\Phi^3\delta\varphi\right), \tag{4.37}$$

which can be simplified into

$$\delta S_{\bar{\Lambda}} = \frac{1}{16\pi G}\int d^4x\sqrt{-\bar{g}}\left(-\bar{\Lambda}\Phi^4\bar{g}_{\lambda\mu}\delta\bar{g}^{\lambda\mu} + 8\bar{\Lambda}\Phi^3\delta\varphi\right). \tag{4.38}$$

From (4.31) and (4.28), we can write

$$S_R = \frac{1}{16\pi G}\int d^4x\sqrt{-\bar{g}}\left(\Phi^2\bar{R}_{\lambda\mu}\bar{g}^{\lambda\mu} - 6\Phi\bar{g}^{\lambda\mu}\varphi_{;\lambda\mu}\right) \tag{4.39}$$

$$= \frac{1}{16\pi G}\int d^4x\sqrt{-\bar{g}}\left(\Phi^2\bar{R} + 6\bar{g}^{\lambda\mu}\varphi_{,\lambda}\varphi_{,\mu}\right) \tag{4.40}$$

We can proceed computing its variation

$$\delta S_R = \frac{1}{16\pi G}\int d^4x\sqrt{-\bar{g}}\Big[-\frac{\Phi^2}{2}\bar{g}_{\lambda\mu}\delta\bar{g}^{\lambda\mu}\bar{R}_{\nu\rho}\bar{g}^{\nu\rho} + 2\Phi\delta\varphi\bar{R}_{\lambda\mu}\bar{g}^{\lambda\mu} + \Phi^2\delta\bar{R}_{\lambda\mu}\bar{g}^{\lambda\mu} + \Phi^2\bar{R}_{\lambda\mu}\delta\bar{g}^{\lambda\mu}$$
$$- \left(3\bar{g}_{\lambda\mu}\delta\bar{g}^{\lambda\mu}\bar{g}^{\nu\rho}\varphi_{,\nu}\varphi_{,\rho} - 6\delta\bar{g}^{\lambda\mu}\varphi_{,\lambda}\varphi_{,\mu} - 6\bar{g}^{\lambda\mu}\delta\varphi_{,\lambda}\varphi_{,\mu} - 6\bar{g}^{\lambda\mu}\varphi_{,\lambda}\delta\varphi_{,\mu}\right)\Big] \tag{4.41}$$

Analysing the terms of (4.41):

- Palatini's identity [15] states that

$$\delta\bar{R}_{\lambda\mu} = \left(\delta\bar{\Gamma}^{\nu}_{\lambda\mu}\right)_{;\mu} - \left(\delta\bar{\Gamma}^{\nu}_{\lambda\mu}\right)_{;\nu} \tag{4.42}$$

- $\Phi^2 \bar{g}^{\lambda\mu} = g^{\lambda\mu}$, which implies

$$\sqrt{-g}g^{\lambda\mu}\delta\bar{R}_{\lambda\mu} = \left(\sqrt{-g}g^{\lambda\mu}\delta\bar{\Gamma}^{\nu}_{\lambda\mu}\right)_{;\mu} - \left(\sqrt{-g}g^{\lambda\mu}\delta\bar{\Gamma}^{\nu}_{\lambda\mu}\right)_{;\nu} \tag{4.43}$$

These are surface terms, meaning their integral will vanish.

- Collecting the terms with $\delta\bar{g}^{\lambda\mu}$ dependency

$$\frac{1}{16\pi G}\int d^4x\sqrt{-\bar{g}}\delta\bar{g}^{\lambda\mu}\left[\Phi^2\left(\bar{R}_{\lambda\mu} - \frac{1}{2}\bar{g}_{\lambda\mu}\bar{R}\right) - 3\bar{g}_{\lambda\mu}\varphi^{,\rho}\varphi_{,\rho} + 6\varphi_{,\lambda}\varphi_{,\mu}\right] \tag{4.44}$$

- Collecting the $\delta\varphi$-dependent terms

$$\frac{1}{16\pi G}\int d^4x\sqrt{-\bar{g}}\left[6\bar{g}^{\lambda\mu}\left(\delta\varphi_{,\mu}\varphi_{,\lambda} + \varphi_{,\mu}\delta\varphi_{,\lambda}\right) + \bar{g}^{\lambda\mu}2\Phi\delta\varphi\bar{R}_{\lambda\mu}\right] \tag{4.45}$$

Using $\bar{g}^{\lambda\mu}\varphi_{,\lambda} = \varphi^{,\mu} = \varphi^{;\mu}$ we can write

$$\int d^4x\sqrt{-\bar{g}}\varphi^{,\mu}\delta\varphi_{,\mu} = -\int d^4x\left(\sqrt{-\bar{g}}\varphi^{;\mu}\right)_{,\mu}\delta\varphi \tag{4.46}$$

$$= -\int d^4x\delta\varphi\sqrt{-\bar{g}}\varphi^{;\mu}_{;\mu}. \tag{4.47}$$

Which allows us to rewrite the terms in $\delta\varphi$ as follows

$$\frac{1}{16\pi G}\int d^4x\sqrt{-\bar{g}}\delta\varphi\left[2\Phi\bar{R} - 12\varphi^{;\mu}_{;\mu}\right]. \tag{4.48}$$

The last two terms of (4.44) can also be rewritten as

$$\frac{1}{16\pi G}\int d^4x\sqrt{-\bar{g}}\delta\bar{g}^{\lambda\mu}\left(3\Phi\bar{g}_{\lambda\mu}\varphi^{;\rho}_{;\rho} - 6\Phi\varphi_{;\lambda\mu}\right). \tag{4.49}$$

Let us now write the variation of the action corresponding to the matter part [15, 17]

$$\delta S_m = \frac{1}{2}\int d^4x\sqrt{-g}\delta g_{\rho\sigma}T^{\rho\sigma}. \tag{4.50}$$

Since $\delta g_{\rho\sigma} = -g_{\lambda\rho}g_{\mu\sigma}\delta g^{\lambda\mu}$,

$$\delta S_m = -\frac{1}{2}\int d^4x\sqrt{-g}\delta g^{\lambda\mu}T_{\lambda\mu}. \tag{4.51}$$

From (4.31) and $\delta g^{\lambda\mu} = \Phi^{-2}\delta\bar{g}^{\lambda\mu} - 2\Phi^{-3}\delta\varphi\bar{g}^{\lambda\mu}$, the variation of S_m is

$$\delta S_m = -\int d^4x\sqrt{-\bar{g}}\left(\frac{\Phi^2}{2}\delta\bar{g}^{\lambda\mu}T_{\lambda\mu} - \Phi\bar{g}^{\lambda\mu}T_{\lambda\mu}\right). \tag{4.52}$$

Remembering (4.30)

$$\delta S_g + \delta S_m = 0 \implies \delta S_g = -\delta S_m \tag{4.53}$$

This way, we can write two equations, gathering in one the δg-dependency of S_g and S_m and in another the $\delta\varphi$-dependency, respectively, as

$$\begin{cases} \Phi^2\left(\bar{R}_{\lambda\mu} - \frac{1}{2}\bar{g}_{\lambda\mu}\bar{R}\right) - \bar{\Lambda}\Phi^4\bar{g}_{\lambda\mu} + \frac{3}{2}\Phi\varphi^{;\rho}_{;\rho}\bar{g}_{\lambda\mu} = 8\pi G\Phi^2 T_{\lambda\mu} \\ 2\Phi\bar{R} - 12\varphi^{;\mu}_{;\mu} + 8\bar{\Lambda}\Phi^3 = -16\pi G\Phi\bar{g}^{\lambda\mu}T_{\lambda\mu} \end{cases} \tag{4.54}$$

Then, the second equation can be written as

$$\varphi^{;\mu}_{;\mu} = \frac{\Phi}{6}\bar{R} + \frac{2}{3}\bar{\Lambda}\Phi^3 + \frac{4}{3}\pi G\Phi\bar{g}^{\lambda\mu}T_{\lambda\mu}. \tag{4.55}$$

Inserting (4.55) in the $\delta\bar{g}^{\lambda\mu}$-part *of the system 4.54*

$$\Phi^2\left(\bar{R}_{\lambda\mu} - \frac{1}{2}\bar{g}^{\lambda\mu}\bar{R}\right) - \bar{\Lambda}\Phi^4\bar{g}_{\lambda\mu}$$

$$+ \frac{3}{2}\Phi\left(\frac{\Phi}{6}\bar{R} + \frac{2}{3}\bar{\Lambda}\Phi^3 + \frac{4}{3}\pi G\Phi T_{\lambda\mu}\bar{g}^{\lambda\mu}\right)\bar{g}_{\lambda\mu} = 8\pi G\Phi^2 T_{\lambda\mu}, \tag{4.56}$$

will yield

$$\bar{R}_{\lambda\mu} - \frac{1}{2}\bar{g}^{\lambda\mu}\bar{R} - \bar{g}_{\lambda\mu}\left(-\frac{1}{4}\bar{R} - 2\pi G T_{\lambda\mu}\bar{g}^{\lambda\mu}\right) = 8\pi G T_{\lambda\mu}. \tag{4.57}$$

If we identify the term in brackets with a new cosmological constant, which has its origin from considering quantum fluctuations around the metric tensor, Einstein's equations takes the following form

$$\bar{R}_{\lambda\mu} - \frac{1}{2}\bar{g}^{\lambda\mu}\bar{R} - \bar{g}_{\lambda\mu}\Lambda = 8\pi G T_{\lambda\mu}, \tag{4.58}$$

with

$$\Lambda = -\frac{1}{4}\left(\bar{R} + 8\pi G T_{\lambda\mu}\bar{g}^{\lambda\mu}\right). \tag{4.59}$$

This means (4.58) give us back Einstein's equation with a cosmological constant, as in (2.26). Note, however, that the cosmological constant $\bar{\Lambda}$ which was initially put into the action by hand disappears from the result [29], but is replaced by a cosmological constant which stems from the fluctuations.

It is possible to show [9] that the magnitude of Λ is consistent with the observational values attributed to dark energy. Thus, the accelerated expansion that dark energy accounts for in standard cosmology can be seen as a consequence of considering quantum fluctuations present at Planck scale.

4.3 Λ in Perfect Fluid Model

How constant is indeed the cosmological constant we derived for the universe modelled as a perfect fluid?

From §3.2 we can rewrite (4.59), inserting on it (3.12) and using (3.3), (3.6) and (3.7). We then obtain

$$\Lambda = \frac{3}{2}\left(\frac{\ddot{Q}}{Q} + \frac{\dot{Q}^2 + k}{Q^2}\right) - 2\pi G(\rho - 3P). \tag{4.60}$$

The equation of motion that results from (4.58) with the cosmological constant (4.59) is

$$\frac{\ddot{Q}}{Q} = \frac{\dot{Q}^2 + k}{Q^2} - 4\pi G(\rho + P). \tag{4.61}$$

Hence we can compute Λ by inserting (4.61) in (4.60)

$$\Lambda = \frac{3}{2}\left(\frac{\dot{Q}^2 + k}{Q^2} - 4\pi G(\rho + P) + \frac{\dot{Q}^2 + k}{Q^2}\right) - 2\pi G(\rho - 3P) \tag{4.62}$$

$$= 3\frac{\dot{Q}^2 + k}{Q^2} - 8\pi G\rho. \tag{4.63}$$

Let us now take its time derivative

$$\dot{\Lambda} = 6\frac{\ddot{Q}\dot{Q}Q^2 - \dot{Q}Q(\dot{Q}^2 + k)}{Q^4} - 8\pi G\dot{\rho} \tag{4.64}$$

Inserting (3.19) and (4.61) in (4.64)

$$\dot{\Lambda} = 6\frac{\dot{Q}}{Q}\left(\frac{\dot{Q}^2 + k}{Q^2} - 4\pi G(\rho + P) - \frac{\dot{Q}^2 + k}{Q^2}\right) - 8\pi G\dot{\rho} \tag{4.65}$$

$$= -24\pi G\frac{\dot{Q}}{Q}(\rho + P) + 24\pi G\frac{\dot{Q}}{Q}(\rho + P) \tag{4.66}$$

$$= 0, \tag{4.67}$$

being clear the cosmological constant remains a constant in our model.

Chapter 5

Thermal History of the Universe

In this chapter we will present the most relevant features of the thermal evolution of the universe to understand its history in terms of the cosmological model discussed before.

5.1 Very Early Universe

From the previous chapters, we suspect that $Q(t)$ reached zero at some finite time $t = 0$ in the past. Letting t_0 be the present moment, it also denotes the age of universe. Until the Planck time, at $t \sim 10^{-43}$ seconds, gravity can not be considered as a classical background. Since the physical processes involved at such early time (attempted to be accounted for by quantum gravity, supersymmetry and grand unification theories – GUTs – among others) are yet to be understood, we are going to jump forward to the end of inflation.

The inflationary period, mentioned in §3.5.2, will leave us with a universe that is highly flat, homogeneous and wiped clean from particles. Then, all the particles we observe today must have been created afterwards. The inflaton, the particle associated with the field that gave birth to inflation, becomes highly unstable when its energy density decreases enough for the exponential expansion to stop, decaying into other particles and fields successively [22, 23]. This decay will compensate the sudden drop in temperature that the universe experienced during inflation due to the sudden increase in volume, in a process called **reheating**.

Is it estimated that inflation ended at $t \sim 10^{-34}$ s, with $T \sim 10^{27}$ K [12]. Several phase transitions take place as the universe begins to cool down again. The **GUT transition**, happening around the end of inflation, consists of a symmetry breaking via Higgs mechanism that causes the gauge group of particle physics to degenerate from the grand-unified gauge group G to the standard model $SU(3) \otimes SU(2) \otimes U(1)$ [19]. At $T \approx 300$ GeV $\approx 10^{15}$ K, the $SU(2) \otimes U(1)$ is broken by the Higgs mechanism and the **electroweak transition** takes place, yielding two different interactions – the electromagnetic and the

weak interaction [19].

Due to the high temperature of this early universe, particles moved at speeds close to the speed of light, which means that the contribution to the energy of a particle from its momentum plays a major role and relativistic effects must be considered. Relativistic particles can be approximately treated as radiation and in this case they will contribute to the energy density of radiation, thus evolving as (3.44). When the temperature falls below the rest mass of a given particle species, it becomes non-relativistic and the energy available is not enough to create pairs of particle-antiparticle of this type. The particles then annihilate with their antiparticles without further production of pairs.

The early universe can be pictured as a plasma of relativistic particles interacting – let us say, colliding – with each other. We can quantify these interactions defining the **interaction rate** per particle as [12]

$$\Gamma \equiv n\sigma v, \tag{5.1}$$

where n represents the number density of target particles, σ the cross section of the interaction and v the relative velocity.

The thermal plasma is expected to follow (3.57) and to decrease its temperature with the scale factor. Then, the rate change of the temperature will be

$$\frac{\dot{T}}{T} = -\frac{\dot{Q}}{Q} = H. \tag{5.2}$$

If the interaction rate of a particle is sufficient to accompany the change in temperature of the universe, i.e.

$$\Gamma \geqslant H, \tag{5.3}$$

the particle will remain in thermal equilibrium. For temperatures as high as at the end of inflation, all particles were indeed in thermal equilibrium. The universe was therefore **radiation-dominated**.

However, $\Gamma < H$ is not sufficient to determine whether a species is out of equilibrium or not. A non-interacting massless species which was once in equilibrium will continue being relativistic and follow (3.57).

To understand the behaviour of the different particles, we need to have a look at the thermodynamics at stake.

5.2 Particles in Thermal Equilibrium

A relativistic perfect gas of particles (in units of $\hbar = c = k_B = 1$) has the following number density [12]

$$n = \frac{g}{(2\pi)^3} \int f(\overrightarrow{p}) d^3p, \tag{5.4}$$

where g denotes the number of internal degrees of freedom, $\overrightarrow{p}$ the momentum and $f(\overrightarrow{p})$ is the phase space distribution function of a species in kinetic equilibrium given by

$$f(\overrightarrow{p}) = \left(e^{\frac{E-\mu}{T}} \pm 1\right)^{-1}, \tag{5.5}$$

with μ representing the chemical potential of the species. $+1$ is used in the case of a Fermi-Dirac distribution and -1 is used for Bose-Einstein distributions.

To get the energy density of this gas, the integrand of (5.4) must simply be multiplied by the energy $E(\overrightarrow{p})$,

$$\rho = \frac{g}{(2\pi)^3} \int E(\overrightarrow{p}) f(\overrightarrow{p}) d^3 p. \tag{5.6}$$

From the kinetic theory, the pressure of the gas can be obtained from $P = npv/3$ [19]. The particle velocity is related to its momentum by $v = \frac{p}{E} \implies P = n\frac{p^2}{3E}$. Thus,

$$P = \frac{g}{(2\pi)^3} \int \frac{p^2}{3E(\overrightarrow{p})} f(\overrightarrow{p}) d^3 p. \tag{5.7}$$

A gas with these characteristics is consistent with the perfect fluid considered in the previous chapters.

5.2.1 On the Chemical Potential

For the purpose of this work, simplifying the chemical potential μ that appears in the distribution function (5.5) is important to evaluate the thermodynamic integrals presented above. Based on conservations laws, we can make the following considerations [17]:

- $\mu_\gamma = 0$, since photons can be emitted or absorbed in any number in a given reaction;

- $\mu_a = \mu_{\bar{a}}$, because particle-antiparticle pairs annihilate into photons;

- $\mu_{e^-} - \mu_{\nu_e} = \mu_{\mu^-} - \mu_{\nu_\mu} = \mu_{\tau^-} - \mu_{\nu_\tau} = \mu_n - \mu_p$, considering the conversion of electrons and muons into their associated neutrinos by colliding with each other and with nucleons.

This leaves us with *five* independent chemical potentials, which can be determined by the density of charge, the baryon density number, the electron-lepton density number, the muon-lepton density number and the τ-lepton density number N_Q, N_B, N_E, N_M and N_τ (all $\propto Q^{-3}$), respectively.

We know that $\langle N_Q \rangle \approx 0$, since the universe must be electrically neutral.

Considering that $N_B \simeq n_p + n_n - n_{\bar{p}} - n_{\bar{n}}$ is more than 9 orders less than n_γ [25], we can also approximate it to zero.

For $N_E \simeq n_{e^-} + n_{\nu_e} - n_{e^+} - n_{\bar{\nu}_e}$, $N_M \simeq n_{\mu^-} + n_{\nu_\mu} - n_{\mu^+} - n_{\bar{\nu}_\mu}$ and $N_\tau \simeq n_{\tau^-} + n_{\nu_\tau} - n_{\tau^+} - n_{\bar{\nu}_\tau}$, it is a reasonable guess that the magnitude of of these density numbers will also be much less than n_γ, since $N_B \ll n_\gamma$ [17]. In this way, $N_Q = N_B = N_E = N_M = N_\tau = 0$ and $\mu_i = 0$ is a good approximation.

5.2.2   On the Energy Density

Let us single out the energy density. Using the fact that $p = \sqrt{E^2 - m^2}$, we can write (5.6) as

$$\rho = \frac{g}{2\pi^2} \int_m^\infty \frac{\sqrt{E^2 - m^2}}{e^{\frac{E-\mu}{T}} \pm 1} E^2 dE. \tag{5.8}$$

Taking the relativistic limit of $T \gg m$ for negligible chemical potentials ($T \gg \mu$), the energy density results in

$$\rho = \begin{cases} \dfrac{\pi^2}{30} g T^4 & \text{for bosons} \\[2ex] \dfrac{7}{8} \dfrac{\pi^2}{30} g T^4 & \text{for fermions} \end{cases} \tag{5.9}$$

We can rewrite it as

$$\rho = \frac{\pi^2}{30} \left(\sum_B g_B + \frac{7}{8} \sum_F g_F \right) T^4, \tag{5.10}$$

where g_B and g_F are the number of degrees of freedom of each species of bosons and fermions, respectively. Defining $N(T)$ as the effective number of degrees of freedom present at a given temperature T, the relativistic energy density assumes the form of [21]

$$\rho = \frac{\pi^2}{30} N(T) T^4. \tag{5.11}$$

For the particles of the standard model, we can count the degrees of freedom of each species to obtain $N(T)$ for the initial relativistic soup and for subsequent times. This is done by taking into account that a species decouples from equilibrium when its rest mass is higher than the temperature, the point at which it stops contributing to $N(T)$. Presently ($T_r(t_0) = 2.725$ K [30]), only photons remain thermalized. We can then compute $N(T(t_0))$ as the sum of their degrees of freedom, $g_\gamma = 2$ (2 transverse polarizations).

As the temperature drops when time passes, different particles drop out of equilibrium and annihilate with their antiparticles when their mass threshold is reached by the temperature of the universe, reducing the number of degrees of freedom present. Table 5.1 gives the values of $N(T)$ as standard model particles are annihilated, dropping from the thermal equilibrium. Alternatively, we can visualise the inverse process: as the temperature rises when we travel backwards in time, new particles are created when their mass threshold is reached by the temperature of the universe, unfolding new degrees of freedom.

Among these particles and their respective antiparticles, we find quarks (up, down, charm, strange, bottom and top), leptons (electrons, muons, τ and neutrinos) and bosons (pions, gluons, $W^\pm$, Z^0, photons and Higgs).

For temperatures above the electron mass, photons, neutrinos, electrons and positrons are thermalized. Electrons posses $g_{e^\pm} = 4$ (2 spin states, particle+antiparticle), as well as muons and τ particles.

Table 5.1: Effective degrees of freedom values as the temperature rises above the rest mass of standard model particles and other transitions that change $N(T)$ (adapted from [21] [1]).

T	New particles	$4N^{Maj}(T)$		$4N^{Dir}(T)$	
		$4N_r(T)$	$4N_\nu(T)$	$4N_r(T)$	$4N_\nu(T)$
$T < m_e$	γ's	8	21	8	42
$m_e < T < T_{D_\nu}$	$e^\pm$	22		22	
$T_{D_\nu} < T < m_\mu$	ν's	43		64	
$m_\mu < T < m_\pi$	$\mu^\pm$	57		78	
$m_\pi < T < T_c$	π's	69		90	
$T_c < T < m_s$	$u, \bar{u}, d, \bar{d} +$ gluons $-\pi$'s	205		226	
$m_s < T < m_c$	s and $\bar{s}$	247		268	
$m_c < T < m_\tau$	c and $\bar{c}$	289		310	
$m_\tau < T < m_b$	$\tau^\pm$	303		324	
$m_b < T < m_{W,Z}$	b and $\bar{b}$	345		366	
$m_{W,Z} < T < m_H$	$W^\pm$ and Z^0	381		402	
$m_H < T < m_t$	H^0	385		406	
$T < m_t$	t and $\bar{t}$	427		448	

Neutrinos may have $g_\nu^{Maj} = 6$ (2 spin states, 3 families) if we consider them Majorana fermions or $g_\nu^{Dir} = 12$ (2 spin states, 3 families, particle+antiparticle) if they are considered Dirac fermions. The first hypothesis suggests that the neutrino is its own antiparticle. Provided that the data on massive neutrinos is not enough to determine whether this happens or not, several particle physics treatments (such as [25]) take neutrinos to be Majorana particles. But since neutrinos might as well be Dirac particles, and have antiparticles in their own right as any other known fermion, we will not discard this possibility.

Neutrinos drop from equilibrium in a different way than the other particle species. Instead of reaching a mass threshold, neutrinos decouple at a temperature T_{D_ν} because their interaction rate with radiation is too low for equilibrium to be maintained, as we will see in §5.4. This means that no annihilation occurs when T_{D_ν} is reached and consequently the extra heat that the universe gains when particle species decouple and annihilate will not be available this time [31]. The degrees of freedom of neutrinos, as the ones of other particle species, become separated from the degrees of freedom of radiation when they

---

[1]The difference between [21] and our analysis is that in [21] neutrinos are considered to be Majorana particles and to remain in thermal equilibrium with photons even after $e^\pm$ decouple from radiation. In our approach both Majorana and Dirac neutrinos are accounted and we explicitly separate the number of degrees of freedom of neutrinos into $N_\nu(T)$ after they decouple from radiation.

decouple, but neutrinos remain sharing the temperature of radiation until the next anni-
hilation occurs, which will happen between electrons and positrons. In this way, between
T_{D_ν} and m_e, we consider $N_r(T) + N_\nu(T)$. After the temperature crosses m_e, radiation
and neutrinos will have different temperatures and if before we could consider the degrees
of freedom of neutrinos in the total $N(T)$ of (5.11) when writing the density of radiation,
afterwards they will no more be comprised in the radiation density. Their degrees of free-
dom will enter the density of neutrinos, a component which is now separated from the
radiation density.

Until pions decouple, their degrees of freedom $g_\pi = 3$ (3 charges) also contribute to $N(T)$.
T_c is the temperature below which quarks lose their asymptotic freedom, becoming con-
fined. This is called the **quantum chromodynamics** (QCD) **phase transition**, when
the interaction between quarks and gluons becomes important. Quarks then form hadrons,
which can be divided into mesons and baryons. Each quark species has $g_q = 12$ (2 spins,
3 colors, particle+antiparticle) and the gluons render $g_g = 16$ (8 types, 2 helicities).

The electroweak gauge bosons $W^\pm$ and Z^0 have $g = 3$ (2 transverse polarizations, 1 lon-
gitudinal polarization) and the Higgs boson adds one more degree of freedom $g_H = 1$ to
the initial soup.

In this way, the relativistic energy density will decrease with time not only in the fashion
of (3.44), but also due to the decrease of the effective number of degrees of freedom in
(5.11). When a particle species goes out of equilibrium, the heat released from the an-
nihilation with its antiparticle slightly reheats the universe. The leftover particles that
become non-relativistic will enter the matter energy density contribution.

From (5.11) and (3.27), we can compute the present density parameter of radiation,
using

$$\Omega_\gamma(t_0) = \frac{\rho_\gamma(t_0)}{\rho_c(t_0)} = \frac{\pi^2}{30} N(T_r(t_0)) T_r(t_0)^4 \frac{8\pi G}{3H_0^2}. \tag{5.12}$$

Knowing that $T_r(t_0) = 2.725$ K and $N(T_r(t_0)) = 2$, inserting the value of the other
constants in this last expression, we obtain

$$\Omega_\gamma(t_0) \simeq 4.986 \times 10^{-5}. \tag{5.13}$$

5.2.3   On the Entropy

The second law of thermodynamics for a system of volume $V = Q^3$ in equilibrium, where
the chemical potential is negligible, is [32]

$$dE = TdS - PdV. \tag{5.14}$$

Considering that $\rho = E/V$, (5.14) can be written as

$$TdS = d(\rho V) + PdV. \tag{5.15}$$

The conservation of energy (3.19) can be expressed as

$$\dot{\rho} = -\frac{\dot{V}}{V}(\rho + P).$$ (5.16)

If we substitute it in (5.15) dividing by dt, it yields

$$T\frac{dS}{dt} = \frac{d\rho}{dt}V + \frac{dV}{dt}\rho + P\frac{dV}{dt}$$
$$= -\frac{dV}{dt}(\rho + P) + (\rho + P)\frac{dV}{dt} \implies \frac{dS}{dt} = 0.$$ (5.17)

This shows us that, when there is no change in the particle number, the total entropy in a comoving volume is conserved ($sQ^3 = \text{constant}$).

The entropy density can be defined as

$$s = \frac{S}{V},$$ (5.18)

which inserted in (5.15) will yield

$$T(sdV + Vds) = d\rho V + (\rho + P)dV,$$ (5.19)

that in turn can be rearranged into

$$d\rho - Tds = (Ts - \rho - P)\frac{dV}{V}.$$ (5.20)

In this expression ρ, P and s are intensive quantities (they are independent of the size of the system), which allows them to be written as functions of the temperature. This means that the first term will be proportional to dT. On the other hand, the second term is proportional to dV, an extensive quantity, which implies that the coefficients of dT and of dV must vanish separately. In the case of a volume change at constant temperature ($dT = 0$), the coefficient of dV should yield zero. Thus, the following relation for the entropy density holds

$$s = \frac{\rho + P}{T}.$$ (5.21)

Since the universe possesses many orders of magnitude more photons than baryons, ρ and P in this expression can be approximated to the case of a system of relativistic particles using (5.10) and (3.39), then yielding

$$s = \frac{2\pi^2}{45}g_{*s}T^3,$$ (5.22)

where [12]

$$g_{*s} = \sum_B g_B \left(\frac{T_B}{T}\right)^3 + \frac{7}{8}\sum_F g_F \left(\frac{T_F}{T}\right)^3.$$ (5.23)

5.3 Baryogenesis

In order for the observable universe to be as we know it, matter was privileged over antimatter. From our planet and solar system to the data collected on galaxy clusters, there is an observed asymmetry between particles and antiparticles and this asymmetry is almost absolute. Cosmic rays show that the ratio between antiprotons and protons is about 10^{-4} and it is estimated that these antiprotons are secondary, caused by collisions between the cosmic rays and the intergalactic medium [12]. How is the present absence of antimatter explained?

Nucleons (and antinucleons) were produced when quarks lost their asymptotic freedom, becoming confined after the QCD phase transition. At this temperature, baryons can already be considered nonrelativistic. The nucleons began annihilating with antinucleons immediately, however there was an excess of particles over antiparticles that remained after annihilation. This fact implies that some mechanism generated this excess between the end of inflation (any previous asymmetry would have been diluted at the end inflation due to the large entropy production associated with reheating) and the epoch of baryon-antibaryon annihilation. Presently we observe almost no antimatter, but in the early universe, when the density number of quarks and antiquarks was of the order of the density number of photons, the asymmetry was [12]

$$\frac{n_q - n_{\bar{q}}}{n_q} \simeq 3 \times 10^{-8}, \tag{5.24}$$

very tiny. Hence, the mechanism at play at that point caused only a slight deviation between the number of quarks and antiquarks.

The ingredients necessary for the creation of the asymmetry are called Sakharov conditions for baryogenesis and comprise [33]:

- B (baryon number) violation;

- C (charge conjugation) and CP (charge conjugation and parity) violation;

- Loss of thermal equilibrium.

B violation produces an excess of both baryons and antibaryons, while C and CP violation change the net baryon number. GUTs and non-perturbative sectors of the Standard Model may accommodate both ingredients. The process that generates the baryon asymmetry is required to occur away from equilibrium, because this way the inverse reaction of producing baryons in excess cannot take place, allowing the excess of baryons to remain non compensated. Non-equilibrium conditions are found in an expanding universe.

It is not certain how these conditions contribute to the observed asymmetry, but the most relevant baryogenesis theories are [13]:

- A $B - L$(lepton number) $\neq 0$ GUT-scale process;

- Electroweak violation during the phase transition;

- Lepton asymmetry that by electroweak violation $(B + L)$ is converted to baryon asymmetry.

The first hypothesis includes the scenario of a massive particle (such as a superheavy GUT gauge of Higgs boson) decaying. It has the advantage of preventing the asymmetry to be washed away by $B + L$ violation, but implies a reheating temperature higher than most inflation models reach ($T \gg 10^5$ GeV). There is also a mechanism that involves the decay of flat directions in supersymmetric models, known as the Affleck-Dine mechanism [25]. The second hypothesis states the possibility of generating the asymmetry at the electroweak scale (e.g. by using the non-perturbative interactions of sphalerons). This could be probed in an accelerator, but would require new CP violation methods at TeV energies along with a phase transition disfavoured by the actual Higgs boson mass [25]. In the third hypothesis, the Majorana neutrino mass would provide the lepton number violation needed (for example by the decay of a superheavy right-handed neutrino) to generate a lepton asymmetry, which is transmuted into a baryon asymmetry at the electroweak scale. This mechanism is called lepto-baryogenesis and would imply the annihilation catastrophe did not take place thanks to neutrinos having mass! [13] After baryogenesis and the decoupling of electrons from equilibrium, nucleons began to form light atoms in a much better understood process that we will shortly overview afterwards. In table 5.1, the degrees of freedom of baryons are not contemplated. The moment when quarks become confined corresponds to the emergence of a new component in the energy density – the baryonic energy density – that behaves according to (3.43). These particles will continue to share the temperature law of radiation (until the universe stops being radiation-dominated), provided the number of baryons is so small compared to the species in equilibrium that the collisions with them thermalize the baryons. The asymmetry between the masses of the proton and the neutron will originate more protons than neutrons as the temperature drops. The neutron to proton ratio will freeze at roughly 1/6 [25].

5.4   Neutrino Decoupling

As we can see from table 5.1, neutrinos separate from radiation after most of the other species do. The interactions that maintained neutrinos in equilibrium in the early universe were weak interactions of the kind of $\bar{\nu}\nu \leftrightarrow e^+e^-$ and $\nu e \leftrightarrow \nu e$. Its cross section may be written as $\sigma \simeq G_F^2 T^2$, where G_F corresponds to the Fermi coupling constant. Due to the very small mass of neutrinos ($m_\nu < 2$ eV [25]), they can be taken as massless in our

analysis, and then it is possible to use the relation $n \simeq T^3$ for a massless species [12]. From (5.1), we have an estimate of the interaction rate. While the universe was radiation-dominated, interactions mediated by a massless gauge boson would yield $H \sim T^2/m_{Pl}$, where m_{Pl} corresponds to the Planck mass. We already saw that a species needs its interaction rate to be larger than the expansion rate to remain in equilibrium, thus [12]

$$\frac{\Gamma}{H} \simeq \frac{G_F^2 T^5 m_{Pl}}{T^2} \simeq \left(\frac{T}{1\mathrm{MeV}}\right)^3 . \qquad (5.25)$$

This means that, for temperatures below 1 MeV $\sim 10^{10}$ K, the interaction rate is less than the expansion rate and neutrinos will decouple around this point. Before decoupling, neutrinos shared the radiation temperature law (3.57); after decoupling, they follow their own temperature law that will be no different from (3.57), since they are an almost massless species just like photons and neutrinos were sharing their temperature with radiation until they dropped from equilibrium. Neutrinos before and after decoupling have exactly the same phase space distribution function (5.5).

When the temperature drops below the equivalent mass of the electron ($m_e = 511$ keV), there occurs $e^\pm$-pair annihilation, which produces radiation that will contribute to the radiation temperature at that time. The entropy of the $e^\pm$-pairs (with $g_{e^\pm} = 4$) is transferred to the photons (with $g_\gamma = 2$) and, by looking at (5.23), the total internal degrees of freedom for $T > m_e$ will be $g_{*s} = 11/2$. For $T < m_e$, only the internal degrees of freedom of photons contribute to (5.23), yielding now $g_{*s} = 2$.

$g_{*s}(QT)^3$ is a constant for particles in thermal equilibrium, as described in section §5.2.3. This implies that, after the $e^\pm$-pair annihilation, $(QT)^3$ must be larger than before to compensate the decrease in degrees of freedom. We then have

$$g_{*s}^{before}(QT)^3_{before} = g_{*s}^{after}(QT)^3_{after} \qquad (5.26)$$

$$\Leftrightarrow \frac{11}{2}(QT_\nu)^3 = 2(QT_\gamma)^3 \qquad (5.27)$$

$$\Leftrightarrow \frac{T_\gamma}{T_\nu} = \left(\frac{11}{4}\right)^{\frac{1}{3}} . \qquad (5.28)$$

By this expression, we can see that neutrinos render a different cosmic radiation background than photons due to the entropy transfer that occurred at the $e^\pm$-pair annihilation, shortly after neutrino decoupled. The temperature of the neutrinos from this point on, given by (3.57), has to consider (5.28), yielding

$$T_\nu = \left(\frac{4}{11}\right)^{\frac{1}{3}} \frac{T_r(t_0)}{Q(t)} . \qquad (5.29)$$

Similarly to what we did in §5.2.2 for photons, we can now compute the present energy density of neutrinos using

$$\Omega_\nu(t_0) = \frac{\rho_\nu(t_0)}{\rho_c(t_0)} = \frac{\pi^2}{30} N(T_\nu(t_0)) T_\nu(t_0)^4 \frac{8\pi G}{3H_0^2} , \qquad (5.30)$$

where

$$T_\nu(t_0) = \left(\frac{4}{11}\right)^{\frac{1}{3}} \frac{T_r(t_0)}{Q(t_0)} \simeq 1.945 \text{ K}. \tag{5.31}$$

From table 5.1, neutrinos see their own number of degrees of freedom for times subsequent to $e^\pm$-pair annihilation. Then, for Majorana neutrinos we have $N(T_\nu(t_0)) = 21/4$ and for Dirac neutrinos we have $N(T_\nu(t_0)) = 42/4$. Inserting it, and the remaining constants, in (5.30), we obtain

$$\Omega_\nu(t_0) \simeq \begin{cases} 3.40 \times 10^{-5}, & \text{Majorana} \\ 6.79 \times 10^{-5}, & \text{Dirac} \end{cases} \tag{5.32}$$

5.5 Radiation Density

After understanding that the radiation component of our universe underwent several decouplings for the different particle species, we can study what happened to the density of radiation over time. We know how it relates to the scale factor by (3.44) and to the radiation temperature by (5.11), which in its turn relates to the scale factor by (3.57). This makes us identify

$$\rho_{r,N}(t_0) = \frac{\pi^2}{30} N(T) T_{r,N}(t_0)^4, \tag{5.33}$$

where $\rho_{r,N}(t_0)$ and $T_{r,N}(t_0)$ are not constant over time. The value of $\rho_{r,N}(t_0)$ changes every time the degrees of freedom decrease. The parameter $T_{r,N}(t_0)$ is also not constant over time as the photons created in the annihilation of a decoupled species increase its value, due to conservation of entropy, every time the effective number of degrees of freedom decreases from N_b to N_a.

Let us see how the change occurs. In the last section we saw how the entropy transfer works at neutrino decoupling. For any decoupling (5.26) holds, allowing us to write

$$N_b(QT_b)^3 = N_a(QT_a)^3 \implies T_a = \left(\frac{N_b}{N_a}\right)^{\frac{1}{3}} T_b. \tag{5.34}$$

Thus, for the relation between the density before and after the decoupling of a species, in terms of the density parameter, we have

$$\frac{\Omega_a}{\Omega_b} = \frac{N_a}{N_b} \left(\frac{T_a}{T_b}\right)^4 \implies \Omega_a = \left(\frac{N_b}{N_a}\right)^{\frac{1}{3}} \Omega_b. \tag{5.35}$$

This enables us to write the proportionality constant between the density parameter of radiation and the temperature

$$\Omega_r(t) = \Omega_r(t_x)T(t)^4, \quad \Omega_r(t_x) = \left(\frac{N_b}{N_a}\frac{4}{11}\right)^{\frac{1}{3}} \Omega_\gamma(t_0) + \left(\frac{N_b}{N_a}\right)^{\frac{1}{3}} \Omega_\nu(t_0), \tag{5.36}$$

that holds between a certain particle threshold and the next threshold at t_x. By knowing the present density parameter of photons (5.12) and neutrinos (5.30) and using the effective number of degrees of freedom of table 5.1, we can bring these constants together in table 5.2.

Table 5.2: Proportionality constant between the density parameter of radiation and the temperature for each interval where the effective degrees of freedom remain constant, computed using (5.36).

$\Omega_r(t_x)$	T	New particles	Ω_r^{Maj} ($\times 10^{-5}$)	Ω_r^{Dir} ($\times 10^{-5}$)
$\Omega_r(t_0)$	$T < m_e$	γ's	8.38	11.78
$\Omega_r(t_e)$	$m_e < T < T_{D_\nu}$	$e^\pm$	6.96	10.35
$\Omega_r(t_e)$	$T_{D_\nu} < T < m_\mu$	ν's	6.96	10.35
$\Omega_r(t_\mu)$	$m_\mu < T < m_\pi$	$\mu^\pm$	6.33	9.69
$\Omega_r(t_\pi)$	$m_\pi < T < T_c$	π's	5.94	9.24
$\Omega_r(t_{T_c})$	$T_c < T < m_s$	$u, \bar{u}, d, \bar{d}$ + gluons $-\pi$'s	4.13	6.80
$\Omega_r(t_s)$	$m_s < T < m_c$	s and $\bar{s}$	3.88	6.42
$\Omega_r(t_c)$	$m_c < T < m_\tau$	c and $\bar{c}$	3.69	6.12
$\Omega_r(t_\tau)$	$m_\tau < T < m_b$	$\tau^\pm$	3.63	6.03
$\Omega_r(t_b)$	$m_b < T < m_{W,Z}$	b and $\bar{b}$	3.47	5.79
$\Omega_r(t_{W,Z})$	$m_{W,Z} < T < m_H$	$W^\pm$ and Z^0	3.36	5.61
$\Omega_r(t_H)$	$m_H < T < m_t$	H^0	3.35	5.59
$\Omega_r(t_t)$	$T < m_t$	t and $\bar{t}$	3.24	5.41

5.6   Matter-Radiation Equality

The matter energy density, whose baryonic component originated at baryogenesis, has a dependence $\rho_{mat} \propto Q^{-3}$, as in (3.43), while the radiation energy density, comprised of photons and neutrinos, follows (3.44), with $\rho_r \propto Q^{-4}$. It is easy to see that at some point in time both energy densities intersect and this phenomenon is called matter-radiation equality. It marks the entrance in the **matter-dominated** era of the universe.

5.7   Recombination and Nucleosynthesis

After the temperature drops below $T \sim 10^9$ K (corresponding to an age $t \sim 1$ s), nucleons begin to merge into heavier nuclei and form an ionized gas of hydrogen and helium. The temperature continues to drop until electrons cool enough for the ionized plasma to be able to capture them, forming atoms. The density of free electrons then becomes less and less and radiation decouples from matter when the interaction rate is not enough to

maintain the thermal contact

$$\Gamma_\gamma \simeq H \tag{5.37}$$

$$n_e \sigma_T \simeq H, \tag{5.38}$$

where n_e is the number density of free electrons and σ_T is the Thomson cross-section [12]. The universe becomes transparent, with photons travelling freely in all directions. The last scattering of photons with electrons is the origin of the CMBR, that today yields a temperature of $T = 2.725$ K [30] in all directions. This value is recovered from the relation (3.57) knowing the temperature and the scale factor at the recombination time.

As we did in section §3.4.3 for the radiation temperature, we can obtain the temperature law for matter, now that its history is separated from radiation. Let us call the temperature at which matter decouples from radiation T_D at a time t_D, with the respective scale factor Q_D.

In the nonrelativistic limit ($m \gg T$), the particle number is given by [12]

$$n = g \left(\frac{mT}{2\pi} \right)^{\frac{3}{2}} e^{-\frac{m-\mu}{T}}, \tag{5.39}$$

where m represents the mass of the particles that form matter. We know that the particle number must scale with $Q(t)$ as

$$n = \frac{N}{Q(t)^3}. \tag{5.40}$$

For this condition to be met, we need to have a μ behaving as [12]

$$\mu(t) = m + (\mu_D - m)\frac{T(t)}{T_D}, \tag{5.41}$$

in order for the exponent of (5.39) to be constant and $T(t)$ behaving as

$$T(t) \propto \frac{1}{Q(t)^2}. \tag{5.42}$$

Another way to understand why the temperature law of matter has this form without requirements on the particle number is to picture that, after the decoupling, the universe continues to expand, which causes the momentum of the particles to redshift as

$$p(t)Q(t) = p_D Q_D \Leftrightarrow p(t) = p_D \frac{Q_D}{Q(t)}. \tag{5.43}$$

Squaring this expression and dividing by twice the mass of the particles considered, we obtain the kinetic energy

$$\frac{p(t)^2}{2m} = \frac{p_D^2}{2m}\left(\frac{Q_D}{Q(t)}\right)^2 \implies E_K(t) = E_K(t_D)\left(\frac{Q_D}{Q(t)}\right)^2. \tag{5.44}$$

The distribution function at p_D will be

$$f = \frac{d^3 n}{dp^3} = f\left(p\frac{Q}{Q_D}, t_D\right) = \left[\exp\left(\frac{E_K(t_D)}{T_D}\right) \pm 1\right]^{-1}. \tag{5.45}$$

Inserting (5.44) in it, results

$$f = \left[\exp \left(\frac{E_K(t)Q(t)^2}{Q_D^2 T_D} \right) \pm 1 \right]^{-1}. \tag{5.46}$$

We know f needs to correspond to $\left(e^{\frac{E}{T}} \pm 1 \right)^{-1}$, thus the temperature T will have the following form

$$T(t) = T_D \left(\frac{Q_D}{Q(t)} \right)^2, \tag{5.47}$$

which can be written as

$$T(t) = \frac{T_{mat}(t_0)}{Q(t)^2}, \tag{5.48}$$

where $T_{mat}(t_0) = T_D Q_D^2$ can be easily determined.

As pointed out in §5.3, the ratio of neutrons to protons will freeze-out. This ratio is given by $n/p = e^{-Q/T}$, where Q represents the difference between the mass of neutrons and protons (1.293 MeV/c^2). When the conversion rate between these two species

$$\Gamma_{n \leftrightarrow p} \sim G_F^2 T^5, \tag{5.49}$$

mediated by weak interactions, falls faster than the Hubble expansion rate $H \sim \sqrt{N(T)G}T^2$, they stop being in equilibrium. The neutron-proton fraction becomes fixed at that time, corresponding to a temperature $T_{fr} \sim 10^9$ K and thus to $e^{-Q/T_{fr}} \simeq 1/6$. After the freeze-out, neutrons are free to decay via β^-, causing the neutron fraction to drop to $n/p \simeq 1/7$ by the time nuclear reactions begin [25].

The nucleosynthesis chain begins with the formation of deuterium, whose production is delayed due to the high number density of photons. This means we need to wait for n_γ to decrease and only when the temperature of the universe is well below the binding energy of D can nuclei begin to form without being immediately dissociated by photons. At the end of the three first minutes of the universe, the lightest elements, namely D, ^{3}He, ^{4}He and ^{7}Li, were already synthesized. Nucleosynthesis successfully explains the observed abundances of these light elements in the universe. The element production in stars is not sufficient to explain the amount of deuterium and ^{4}He observed, but the nucleosynthesis produces them in the primordial abundance that is necessary [12]. This process further allows us to impose important constraints on the baryon density parameter. The density of nucleons at nucleosynthesis is lower than required for heavier nuclei to form, meaning that all the other elements are products of star fusion. It is the nucleosynthesis that allows the structure formation that will take place after this point in the thermal history. The physics involved in the Big Bang nucleosynthesis is well understood in terms of the Standard Model, thus consisting in the oldest well established feature of the early universe [25].

5.8 Dark Energy-Dominated Era

The present values of the different density parameters are depicted in table 5.3. We notice

Table 5.3: Density parameters obtained for a ΛCDM model ($\Omega_{cdm}(t_0)$, $\Omega_b(t_0)$, Ω_Λ and Ω_k from [11]; $\Omega_\gamma(t_0)$ from (5.13); $\Omega_\nu^{Maj}(t_0)$ and $\Omega_\nu^{Dir}(t_0)$ from (5.32)).

Parameter	Symbol	Value
Cold dark matter density	$\Omega_{cdm}(t_0)$	0.229 ± 0.0015
Baryon density	$\Omega_b(t_0)$	0.0458 ± 0.0016
Cosmological constant	Ω_Λ	0.725 ± 0.0016
Curvature parameter	Ω_k	-1.10 ± 0.14
Photon density	$\Omega_\gamma(t_0)$	4.986×10^{-5}
Majorana neutrino density	$\Omega_\nu^{Maj}(t_0)$	3.40×10^{-5}
Dirac neutrino density	$\Omega_\nu^{Dir}(t_0)$	6.79×10^{-5}

that dark energy comprises 72.5% of the total density, which means that at some point in the matter-dominated era, the dark energy component became more important than the matter contribution and the universe shifted to a dark energy-dominated era. This is the era we are currently experiencing and provided that the dark energy density is a constant, as we saw in §3.3.4 , and that the other density components will only decrease with expansion, the fate of the universe is to remain dominated by dark energy in the future.

5.9 Dark Matter

Dark matter, as summarized before, has many candidate particles that may form it. They can be mainly divided into WIMPs (Weakly Interacting Massive Particles) – non-baryonic subatomic particles – and MACHOs (Massive Astrophysical Compact Halo Objects) – large dark matter objects, made of baryonic matter, such as brown dwarf stars or black holes [34].
It is believed that MACHOs can not be the main constituent of dark matter as they account only for a small percentage of the mass of our galaxy [35]. We shall thus focus on non-baryonic matter candidates in this work.

5.9.1 WIMPs

WIMPs have a small mass compared to MACHOs, which requires a large amount of particles to account for the missing matter, implying that a large number of these particles is

passing through baryonic matter without being noticed by us. The gravitational attraction between WIMPs and ordinary matter can be the key to explain why matter clumped into galaxies if it was evenly distributed before [34]. This requires their mass to be large in comparison to other subatomic particles.

Light WIMPs, the hot dark matter, would be close to relativistic particles, which do not present the necessary free-streaming for clumping to occur, thus making the warm and cold dark matter hypothesis more appealing. Interacting weakly with matter is a characteristic of both WIMPs and neutrinos, but the first ones need to be considerably heavier. We find particles just like that in supersymmetric theories (SUSY). Supersymmetric extensions of the standard model of particle physics predict WIMPs with mass range 10-1000 GeV [36], which led the sensitivity of detection experiments to be optimized to these scales. However, light WIMPs (1-10 GeV) are also pertinent as signals reported from some experiments are localized in this range [33, 37]. To complete the picture, there are also model independent analyses that point to CDM particles with masses in the keV range [1] and quantum warm dark matter (WDM) fermionic models obtain masses at the same scale [2]. Fermionic WDM treated quantum mechanically gives physical galactic properties totally compatible with observations [38].

There are plenty of experiments that try to detect dark matter particles and that until now were able to pose some upper and lower constraints on its mass, for example by observing the annihilation of dark matter in dwarf spheroidal galaxies and taking into account its present relic abundance [39, 40], by using detectors such as cryogenic germanium detectors [41] or by observing the momentum distribution of dark matter in the galactic halo [42].

5.9.2 Dark Matter Candidates

Possible WDM candidates are the sterile neutrinos, right-handed heavy neutrinos that interact through mixing with neutrinos from the Standard Model (and gravitationally) [3]. Their existence is searched for in Ly-α forests and its mass is estimated to be in the keV range [43].

Axions, light bosons with masses between 100-1000 keV proposed to explain the strong interaction CP violation [44], could also behave as CDM if their existence is proved. One way to detect them would be through weak coupling with electromagnetism [45].

The minimal supersymmetric standard model (MSSM) predicts CDM in a natural way, where the lightest supersymmetric particle (LSP) may be the most suited candidate for dark matter and would be observable as a relic density. The lightest neutralino, probably the LSP, has a parameter space compatible with the density parameter of CDM. Lower and upper bounds on its mass give $m_{\tilde{\chi}} > 43$ GeV [46] and $m_{\tilde{\chi}} < 1.8$ TeV [47], respectively. The next-to-lightest supersymmetric particle is the gravitino, an also prominent candidate

given its parameter space [4].

5.9.3 Neutralino

By now we must be ready to agree that there is a lot of speculation about the nature of dark matter and many plausible hypotheses. In order to approach the thermal evolution of this component, we need to focus on some candidate and we will choose the neutralino hypothesis.

The lightest neutralino $\tilde{\chi}_1^0$ results from linear combinations of the neutral bino, Wino and Higgsinos states [48]

$$\tilde{\chi}_1^0 = Z_{11}\tilde{B}^0 + Z_{12}\tilde{W}_3^0 + Z_{13}\tilde{H}_1^0 + Z_{14}\tilde{H}_2^0, \tag{5.50}$$

where Z_{1j} are the elements of a real orthogonal matrix that diagonalizes the neutralino mass matrix. It will be a stable particle if R-parity is conserved. The LSP is a pure bino in most of the parameter space constrained by MSSM and we will assume so here too.

5.9.4 Thermal Decoupling

For our WIMPs, the neutralinos, the process of going out of thermal equilibrium hypothetically occurs as follows. When the temperature drops below the mass of the neutralino $M_{\tilde{\chi}}$, it interacts with fermions trough $\tilde{\chi} + \tilde{\chi} \leftrightarrow F + \bar{F}$ and the number density of neutralinos rapidly decreases. When the interaction rate of this reaction becomes comparable to the expansion rate of the universe, it becomes difficult for a neutralino to find another neutralino to annihilate with. It can be written as [48]

$$\Gamma_{ann}(T) = \langle v\sigma_{ann}\rangle(T)n_{\tilde{\chi}}(T) \tag{5.51}$$

$$= \frac{2}{\pi}\sum_F \left(\frac{G_F M_W^2}{M_{\tilde{F}}^2 + M_{\tilde{\chi}}^2}\right)^2 \Big[(b_F^2 + c_F^2)^2 m_F^2 +$$

$$4(b_F^4 + c_F^4)\frac{M_{\tilde{F}}^4 + M_{\tilde{\chi}}^4}{(M_{\tilde{F}}^2 + M_{\tilde{\chi}}^2)^2}M_{\tilde{\chi}}T\Big]n_{\tilde{\chi}}(T). \tag{5.52}$$

In this expression $v\sigma_{ann}$ is expanded for small values of $m_F/M_{\tilde{\chi}}$ and of the velocity up to second order. M_W is the mass of the W boson, b_F and c_F are the left and right chiral vertices and $M_{\tilde{F}}$ is the mass of the sfermions (in this approach we assume that all sfermions have the same mass). Defining $x_{cd} \equiv M_{\tilde{\chi}}/T$, (5.52) can be solved iteratively yielding [48]

$$x_{cd}^{(0)} = \ln\left(1.6\times10^{-4}\frac{m_{Pl}(M_{\tilde{F}}^4 + M_{\tilde{\chi}}^4)M_{\tilde{\chi}}^3}{(M_{\tilde{F}}^2 + M_{\tilde{\chi}}^2)^2}\right), \tag{5.53}$$

$$x_{cd}^{(1)} \approx x_{cd}^{(0)} - \frac{1}{2}\ln\left(x_{cd}^{(0)}\right). \tag{5.54}$$

The parameter space of the MSSM typically gives a value around $x_{cd} \approx 25$. Thus, neutralinos decouple chemically from the thermal plasma at a temperature

$$T_{cd} \approx \frac{M_{\tilde{\chi}}}{25}, \tag{5.55}$$

when their number becomes frozen and its relic abundance must correspond to the observed value of Ω_{cdm}.

Although dark matter is now a separate species, elastic scattering processes allow neutralinos to remain in local thermal equilibrium (in the same way baryonic matter did until the universe became matter-dominated). This local thermal equilibrium is expected to be broken when this interaction does not accompany the expansion, $\Gamma_{el} < H$. But even before WIMPs scatter for the last time, they fall out of equilibrium because the expansion rate weakens their relaxation processes [49]. This is called the kinetic decoupling, which can be determined from $\tau_r(T_{kd}) = H^{-1}(T_{kd})$, where the relaxation time τ_r corresponds to the time one needs to wait until a neutralino that deviated from local equilibrium returns to it. The relaxation time is related to the collision time $\tau_{coll} = 1/\Gamma_{el}$ by the number of elastic scatterings happening at thermal equilibrium

$$N(T) = \frac{p_{\tilde{\chi}}}{\Delta p_{\tilde{\chi}}}, \tag{5.56}$$

with $p_{\tilde{\chi}}$ the momentum of the neutralino for a given temperature and $\Delta p_{\tilde{\chi}}$ the momentum transfer occurring in an elastic scattering. The momentum transfer must be tiny in comparison to the momentum of the particle, hence $N(T)$ is expected to be very large. The Mandelstam variable t gives us $(\Delta p_{\tilde{\chi}})^2 = 2E^2$ [48] and by the equipartition theorem of energy, $E = \frac{3}{2}T$. Thus,

$$\tau_r(T) \approx \sqrt{\frac{2}{3}} \frac{M_{\tilde{\chi}}}{T} \tau_{coll}. \tag{5.57}$$

Between the chemical and kinetic decoupling, the scattering processes keeping WIMPs in equilibrium are $\tilde{\chi} + F \rightarrow \tilde{\chi} + F$. After the QCD transition, the neutralino has only leptons left to scatter (pions are neglected for the sake of simplicity and because usually $T_{kd} \ll m_\pi$) and the interactions are now $\tilde{\chi} + L \rightarrow \tilde{\chi} + L$. Knowing the elastic scattering interaction rate, it is possible to obtain an expression to estimate the temperature of the kinetic decoupling. According to [48], it is given by

$$T_{kd} = \left(1.2 \times 10^{-2} \frac{m_{Pl}}{M_{\tilde{\chi}}(M_L^2 - M_{\tilde{\chi}}^2)^2} \right)^{-\frac{1}{4}}. \tag{5.58}$$

The difference between the two decoupling temperatures is caused by the target density difference that enters the interaction rate – at the chemical decoupling neutralinos stopped annihilating with each other, while at kinetic decoupling neutralinos stopped scattering with relativistic leptons, which had a much larger target density.

Chapter 6

Simulation and Results

In this chapter we will model the universe, considering it a perfect fluid, in terms of the scale factor Q, the density parameter Ω and the temperature T, including dark energy and dark matter, to understand its evolution in time.

6.1 Simulation Process

The expansion of a universe with the characteristics discussed in the previous chapters can be described by the scale factor and both Ω and T can also be written in terms of $Q(t)$, computing (3.54). Since there is no analytical solution to this equation, we need to recur to numerical methods. In order to do so, most of this work consisted in finding the most appropriate way to simulate the variables we are interested in.

6.1.1 Parameters

As known conditions, we have the density parameters of each component of the universe and the background radiation value, given by the observations of the 7-year Wilkinson Microwave Anisotropy Probe (WMAP) [11] and $T_r(t_0) = 2.725$ K [11, 30], respectively. We have calculated the present density parameters of photons and neutrinos and we use these values to obtain the present density parameter of radiation

$$\Omega_r(t_0) = \Omega_\gamma(t_0) + \Omega_\nu(t_0), \tag{6.1}$$

which yields two values, as seen in (5.32), depending on whether we consider Majorana or Dirac neutrinos. When the density parameter constant (5.36) needs to account for different points in time than t_0, we use the values of table 5.2. When we are comparing Majorana and Dirac neutrinos, we refer to $\Omega_r^{Maj}(t_x)$ and $\Omega_r^{Dir}(t_x)$, respectively. For other purposes, we assume $\Omega_r(t_x) = \Omega_r^{Maj}(t_x)$, because, as will be shown later, the difference between both neutrino types is small and, since the available data does not allow us

to determine whether antineutrinos and neutrinos are the same or not, this is the most common assumption. For the present density parameter of matter, we use

$$\Omega_{mat}(t_0) = \Omega_b(t_0) + \Omega_{cdm}(t_0). \tag{6.2}$$

All these values can be found in table 5.3. We choose the present scale factor to be $Q_0 = 1$ and then the time t will be given in units of the Hubble time H_0^{-1}.

6.1.2 Method

The numerical treatment was performed in *Maple 15* and is presented in appendix A. The first approach was to solve the differential equation of $\dot{Q}(t)$ with respect to t, from the present initial conditions to the past, provided we are more confident in the present values than in values predicted for the past. The fact that errors accumulate significantly for the early universe made us perform a variable change into a logarithmic approach, where orders of magnitude changes, happening as we go back in time, were expected to render softer errors. As this was not successful, a simulation from the past to the present was attempted, as well as treating analytically the universe as radiation-dominated in the past and change to a general universe near present times.

For the sake of coherence, after many trials and refinements, we preferred the numerical solutions of the differential equation (3.54), from the past to the moment when electrons drop from equilibrium with radiation and from that point until the present time (which we will call $Q_2(t)$ in virtue of being separated into two parts). As we shall see in picture (6.8), the particle annihilation thresholds do not present a very significant deviation from the law $T \propto Q^{-1}$ except in the $e^{\pm}$ case, which makes it plausible to consider the only point where the density parameter of radiation entering the differential equation should be changed, according to table 5.2.

The other thresholds are probably small enough for the difference between $Q(t)$ computed with Ω_b or with Ω_a to be negligible. Nevertheless, we are interested in studying how small this difference actually is, because we see that at T_c there is an important decrease in degrees of freedom and that the cumulative effect may be important, as the difference between $\Omega_r(t_e)$ and $\Omega_r(t_t)$ is actually larger than the one between $\Omega_r(t_0)$ and $\Omega_r(t_e)$ (the scale factor computed this way will be called $Q_{12}(t)$, in virtue of combining the solutions of twelve differential equations).

As initial conditions, extrapolations of the conditions at the end of inflation were considered.

The Fehlberg fourth-fifth order Runge-Kutta method was the numerical procedure used. In this method, the step size h is automatically adjusted by comparing the solutions of the Runge-Kutta method of order 4 and of order 5. If they match to a certain accuracy, the step size is accepted and the procedure continues. If not, the step size is reduced until

both solutions agree.

We will primarily obtain the temperature corresponding to a $Q(t)$ computed with $\Omega_r(t_e)$, which is valid between the rest-mass thresholds of $\mu^\pm$ and $e^\pm$, but is also a good approximation from the end of inflation until $e^\pm$-pair annihilation. We call it $T_r^1(t)$, because it is computed considering only one region with the same scale factor and density constant. From this we can determine at which time $e^\pm$ decoupled (as well as at which time $\mu^\pm$ decoupled) and obtain the initial conditions (on t and $Q(t)$) to integrate the differential equation that will give us $Q(t)$ from the $e^\pm$ decoupling until the present. For the temperature we can write $T_r^2(t)$, that is identical to $T_r^1(t)$ until electrons drop from the equilibrium and has a different value – a different scale factor and another density constant afterwards.

In the same way, we can obtain the time at which $\mu^\pm$ and the other particles decoupled by the thresholds at $T(t)$ and then integrate multiple differential equations to account for the scale factor from one threshold to the other, where the corresponding constant for the density parameter of radiation is inserted. This is how we write $Q_{12}(t)$, enabling us to obtain $T_r^{12}(t)$.

6.1.3   Temperature Treatment

As we noted in the last chapter, the temperature of the universe decreases with the expansion but decreases slightly less every time a relativistic species goes out of equilibrium and annihilates with its antiparticle. The temperature of the relativistic plasma follows (3.57), and it needs to account as well for the decrease in the effective number of degrees of freedom of table 5.1. The particle masses used, necessary to compute $N(T)$, are shown in table 6.1.

Radiation Temperature

The process of a species leaving equilibrium takes a certain time to occur – for every particle to stop scattering with the species that remain thermalized, over the whole universe. However, if we consider this process instantaneous, that is, when the temperature drops below the rest mass of a certain species, its particles lose thermal contact with the other relativistic species, then we are able to use a step function to mathematically model it. This is the assumption we will make in order to describe the radiation temperature evolution. Joining (3.44) and (5.10), we can write

$$\frac{\rho_r(t_0)}{Q(t)^4} = \frac{\pi^2}{30}N(T)T_r^4, \tag{6.3}$$

Table 6.1: Masses of standard model particles (from [21]).

Particle	Symbol	Mass (eV/c^2)
Electron	m_e	0.510998928×10^6
Muon	m_μ	105.65837×10^6
Pion	m_π	139.5701×10^6
QCD phase transition	T_c	200×10^6
Strange quark	m_s	483×10^6
Charm quark	m_c	1.275×10^9
τ	m_τ	1.77682×10^9
Bottom quark	m_b	4.65×10^9
$W^\pm$ and Z^0	$m_{W,Z}$	91.1876×10^9
Higgs	m_H	126×10^9
Top quark	m_t	173.5×10^9

which can be rearranged into

$$T_r(t) = \left(\frac{30\rho_r(t_0)}{\pi^2 N(T)} \right)^{\frac{1}{4}} \frac{1}{Q(t)}. \tag{6.4}$$

Using (3.29) and shifting the dependence of N from T to t through (3.57), it results in

$$T_r(t) = \left(\frac{90 H_0^2 \Omega_r^T(t_x)}{8\pi^3 G N(t)} \right)^{\frac{1}{4}} \frac{1}{Q(t)}. \tag{6.5}$$

To write $N(t)$ we need to analyse the situation. For values of T_r between two threshold masses (in table 5.1), we require that it yield a specific number of effective degrees of freedom, but since T_r already includes $N(t)$ in its definition, we need to adapt it differently according to each step that will be performed.

After the temperature drops below the rest mass of electrons, we need to account for the effect of neutrino decoupling. Until that point we consider $\Omega_r^T(t_x)$ as the density parameter of radiation, with both the photon and neutrino contributions, but for subsequent times the photon contribution will be the only one entering (6.5), since the density of neutrinos is now part of the separate temperature law of neutrinos. Then, we need to change the constant of the density parameter that enters (6.5), from $\Omega_\gamma(t_0) + \Omega_\nu(t_0)$, as in the $\Omega_r(t_x)$ of table 5.2, to only $\Omega_\gamma(t_0)$ after the $e^\pm$-pair annihilation. To distinguish the constant density that enters the temperature law from the total radiation density parameter constant $\Omega_r(t_x)$, that includes neutrinos, we use the superscript "T". We would like to begin by considering

t_e to be the only point where $\Omega_r^T(t_x)$ changes significantly

$$\Omega_r^T(t_x) = \begin{cases} \Omega_r(t_e), & t < t_e \\ \Omega_\gamma(t_0), & t \geq t_e \end{cases}, \tag{6.6}$$

while we have

$$\Omega_r(t_x) = \begin{cases} \Omega_r(t_e), & t < t_e \\ \Omega_r(t_0), & t \geq t_e \end{cases}. \tag{6.7}$$

However, we still do not know the time t_e that corresponds to it, so firstly we consider $\Omega_r^T(t_x) = \Omega_r(t_x) = \Omega_r(t_e)$ for all times, until we determine the value of t_e.

We need as well to account for the degrees of freedom of neutrinos separately from that moment on, such that $N = N_\gamma$.

Let us begin by taking neutrinos to be Majorana particles. For example, from the present time until the temperature reaches the rest mass of the electron, for the effective number of degrees of freedom we use the value of table 5.1 $4N = 8$ and for the density parameter we use (5.13). Then, we have

$$T_r^e(t) = \left(\frac{90 H_0^2 \Omega_r^T(t_x)}{8\pi^3 G \frac{8}{4}} \right)^{\frac{1}{4}} \frac{1}{Q(t)} = 8^{-\frac{1}{4}}\xi, \tag{6.8}$$

where we define

$$\xi \equiv \left(\frac{90 H_0^2 \Omega_r^T(t_x) 4}{8\pi^3 G} \right)^{\frac{1}{4}} \frac{1}{Q(t)}. \tag{6.9}$$

In the temperature range between the mass of the electron and the mass of the muon $\Omega_r(t_x)$ changes, as do the total number of effective degrees of freedom of radiation, that included only photons until the temperature reaches m_e. From that point on, neutrinos, electrons and positrons are in equilibrium with photons and we account for them by taking $4N = 4(N_\gamma + N_{e^\pm} + N_\nu) = 43$. N_ν is already part of N between m_e and T_{D_ν} despite it being a decoupled species, because it shares the radiation temperature.

In this case, the temperature of radiation will yield

$$T_r^\mu(t) = 43^{-\frac{1}{4}}\xi. \tag{6.10}$$

However, giving the steps a careful look (in the direction of decreasing temperatures), we will find that when $T_r^\mu = m_e$, T_r^e is still higher than m_e, which originates a region where no value of N_r is specified. This situation is shown in figure 6.1 to help visualize it.

 The physical process behind each step is the annihilation of particle-antiparticle pairs into photons, which slightly reheats the universe that is cooling down as it expands. Instead of picturing the reheating as occurring suddenly when the degrees of freedom of the thermal plasma decrease, it seems more accurate to understand it as a slowing down of the cooling process. Then, we will choose to reflect it in our model by letting the temperature of
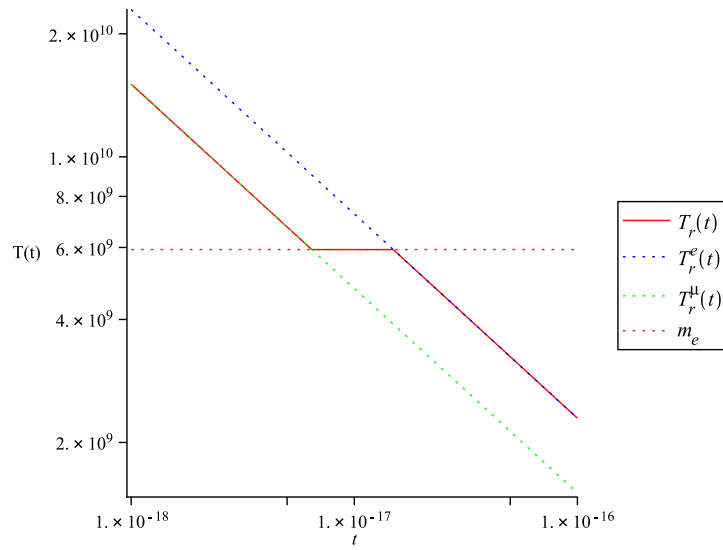
Figure 6.1: Radiation temperature around the decoupling of $e^{\pm}$, in logarithmic scale, with t in H_0^{-1} units and T in K, to illustrate what happens in the transition region where $T_r^{\mu}(t) < m_e$ and $T_r^e(t) > m_e$ at the same time, in $k_B = c = 1$ units.

the universe remain constant while it expands in the transition region. The length of this region depends on the difference between the effective number of degrees of freedom that were present before the transition and the ones that were made available afterwards.

In other words, when the temperature drops to the annihilation threshold $T = T_x$ of a certain species x (given by (6.4) with the value $N = N_b$ before the threshold), the effective number of degrees of freedom $N(t)$ starts do decrease due to the disappearance of that species, until it reaches the new value $N = N_a$ after the threshold. Meanwhile, $Q(t)$ increases from the initial value Q_b at threshold until $N(t)$ reaches the new value N_a, which defines the exit point $Q = Q_a$. We assume the temperature to stay constant $(T = T_x)$ during this process, where the increase in the scale factor with time, from Q_b to Q_a, compensates for the change of $N(t)$. The value of Q_a is obtained from (6.4) with the new value $N = N_a$ and the requirement to still yield the same temperature $T = T_x$. From this point on the temperature starts to drop again. Note that the energy necessary to temporarily halt the decrease of the temperature due to expansion is supplied by the annihilation processes.

In order to translate this mechanism to our program, the value of $N(t)$ in these regions

needs to be such that T_r will correspond to the rest-mass of the particles. We define it as

$$S(t) = \xi^4 \begin{cases} m_e^{-4}, & 43^{-\frac{1}{4}}\xi < m_e \\ m_\mu^{-4}, & 57^{-\frac{1}{4}}\xi < m_\mu \\ m_\pi^{-4}, & 69^{-\frac{1}{4}}\xi < m_\pi \\ T_c^{-4}, & 205^{-\frac{1}{4}}\xi < T_c \\ m_s^{-4}, & 247^{-\frac{1}{4}}\xi < m_s \\ m_c^{-4}, & 289^{-\frac{1}{4}}\xi < m_c \\ m_\tau^{-4}, & 303^{-\frac{1}{4}}\xi < m_\tau \\ m_b^{-4}, & 345^{-\frac{1}{4}}\xi < m_b \\ m_{W,Z}^{-4}, & 381^{-\frac{1}{4}}\xi < m_{W,Z} \\ m_H^{-4}, & 385^{-\frac{1}{4}}\xi < m_H \\ m_t^{-4}, & 427^{-\frac{1}{4}}\xi < m_t \end{cases} \quad . \tag{6.11}$$

Let us write the explicit form of $N(t)$,

$$4N(t) = \begin{cases} 8, & 8^{-\frac{1}{4}}\xi \leq m_e \\ 43, & m_e < 43^{-\frac{1}{4}}\xi \leq m_\mu \\ 57, & m_\mu < 57^{-\frac{1}{4}}\xi \leq m_\pi \\ 69, & m_\pi < 69^{-\frac{1}{4}}\xi \leq T_c \\ 205, & T_c < 205^{-\frac{1}{4}}\xi \leq m_s \\ 247, & m_s < 247^{-\frac{1}{4}}\xi \leq m_c \\ 289, & m_c < 289^{-\frac{1}{4}}\xi \leq m_\tau \\ 303, & m_\tau < 303^{-\frac{1}{4}}\xi \leq m_b \\ 345, & m_b < 345^{-\frac{1}{4}}\xi \leq m_{W,Z} \\ 381, & m_{W,Z} < 381^{-\frac{1}{4}}\xi \leq m_H \\ 385, & m_H < 385^{-\frac{1}{4}}\xi \leq m_t \\ 427, & m_t < 427^{-\frac{1}{4}}\xi \\ S(t), & \text{otherwise} \end{cases} \quad . \tag{6.12}$$

6.2   Scale Factor $Q(t)$

Knowing the constant density parameter we considered ($\Omega_r(t_e)$) is valid in the region where temperature is higher than m_e, we are now in conditions to obtain the time at which electrons drop from equilibrium, yielding $t_e = 6.45 \times 10^{-18} \, H_0^{-1}$. This enables us

to use (6.7) and thus, write (3.54) in the form

$$\dot{Q}(t) = \sqrt{\frac{\Omega_r(t_x)}{Q(t)^2} + \frac{\Omega_{mat}(t_0)}{Q(t)} + \Omega_k(t_0) + \Omega_\Lambda Q(t)^2},$$

(6.13)

where $\Omega_r(t_x)$ is given by (6.7).

At the end of inflation (and of reheating), it is estimated that the temperature of the universe was of the order $T \sim 10^{27}$ K [12] and since at this point radiation-dominated considerations hold, (3.57) will give us an estimation of $Q(t) \sim 10^{-27}$. From (3.51), we obtain the corresponding time $t \sim 10^{-54} H_0^{-1} \sim 10^{-37}$ s. These are the ingredients necessary to numerically integrate (3.54) until t_e. From that point to the present, we use as initial condition $Q(t_e)$. An overview of the behaviour of $Q(t)$, whose integration is performed separately in the two regions previously mentioned, is depicted in figure 6.2.

We can observe that for recent times the behaviour of $Q(t)$ in logarithmic scale deviates
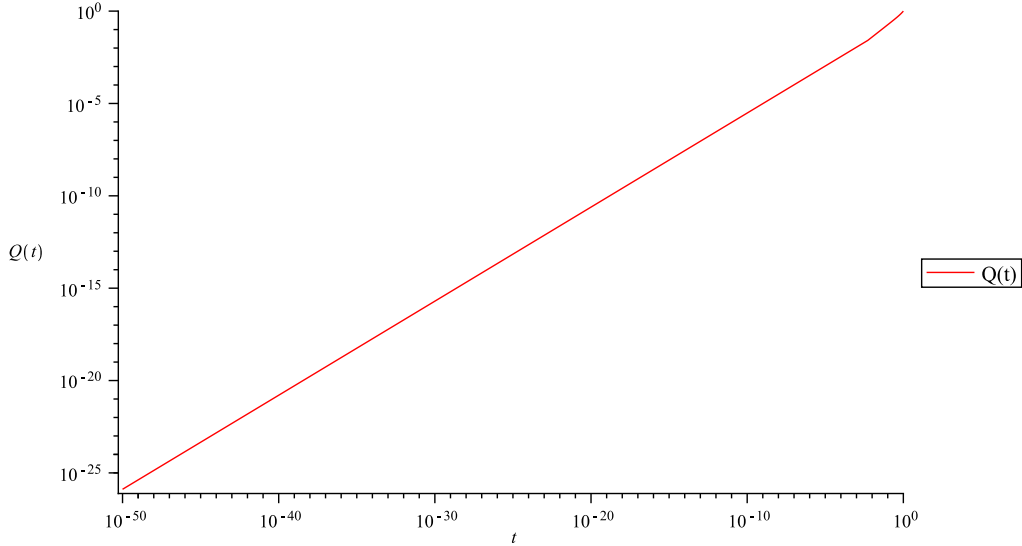
Figure 6.2: Scale factor over time for a general universe, integrated in two parts, $Q_2(t)$, in logarithmic scale, with t in H_0^{-1} units.

from the apparently linear in the past. As we know, for the early universe $Q(t) \propto \sqrt{t}$ and this feature shows us that for later times it is important to consider that the universe is composed of more than radiation. We will see later that the time when the universe becomes matter-dominated corresponds to the point where the behaviour of the scale factor curve changes. We can also see that at the value of the present epoch scale parameter $Q_0 = 1$, the age of the universe (in units H_0^{-1}) is close to unity.

When $\Omega_r(t_x)$ changes, around $t \sim 10^{-17}$, the curve continues following the behaviour it had in previous times. In the large range of times of figure 6.2, we would not observe any divergence between integrating the differential equation with the same constant density

Figure 6.3: Scale factor over time, where $Q_1(t)$ represents the scale factor integrated with $\Omega_r(t_x) = \Omega_r(t_e)$ and $Q_2(t)$ represents the scale factor integrating the two seperate parts of 6.7, in logarithmic scale, with t in H_0^{-1} units.

parameter of radiation for the whole universe (obtaining $Q_1(t)$) or dividing it into two parts as in (6.13) (obtaining $Q_2(t)$), but if we zoom into the region around which electrons decouple from radiation, we can see there is a small deviation between both approaches. We depict it in figure 6.3.

6.2.1 From a Set of Two to a Set of Twelve Differential Equations

Our estimate is that the previous approach is approximately valid from the end of inflation until t_e, making it possible to determine the points t_x when $T_r(t)$ reaches the rest-mass of the species x, as it is done in table 6.2. The goal is now to numerically integrate a differential equation $\dot{Q}(t)$ with the adequate value of $\Omega_r(t_x)$ for each interval.

We define the initial condition for the integration of each equation that holds from t_x until the next species decouples as the scale factor the previous integration yields at t_x. This means that, for instance, to obtain the scale factor between the decoupling of muons and electrons, we use as initial condition that $Q(t_\mu)$ in this case must correspond to the value of the scale factor at time t_μ integrated between the decoupling of pions and muons. This way, we obtain a set of solutions for $Q(t)$, where each integration uses a different

Table 6.2: Times when the temperature of the universe reaches rest-mass of the particle species, computed from (6.5) with (6.6) and (6.13) with (6.7).

Particle	t_x	Time (H_0^{-1})
Electron	t_e	6.45×10^{-18}
Muon	t_μ	1.32×10^{-22}
Pion	t_π	7.50×10^{-23}
QCD phase transition	t_{T_c}	1.99×10^{-23}
Strange quark	t_s	3.305×10^{-24}
Charm quark	t_c	4.32×10^{-25}
τ	t_τ	2.00×10^{-25}
Bottom quark	t_b	2.93×10^{-26}
$W^\pm$ and Z^0	$t_{W,Z}$	7.15×10^{-29}
Higgs	t_H	3.55×10^{-29}
Top quark	t_t	1.869×10^{-29}

$\Omega_r(t_x)$ value

$$
\Omega_r(t_x) = \begin{cases}
\Omega_r(t_t), & t < t_t \\
\Omega_r(t_H), & t_t \leq t < t_H \\
\Omega_r(t_{W,Z}), & t_H \leq t < t_{W,Z} \\
\Omega_r(t_b), & t_{W,Z} \leq t < t_b \\
\Omega_r(t_\tau), & t_b \leq t < t_\tau \\
\Omega_r(t_c), & t_\tau \leq t < t_c \\
\Omega_r(t_s), & t_c \leq t < t_s \\
\Omega_r(t_{T_c}), & t_s \leq t < t_{T_c} \\
\Omega_r(t_\pi), & t_{T_c} \leq t < t_\pi \\
\Omega_r(t_\mu), & t_\pi \leq t < t_\mu \\
\Omega_r(t_e), & t_\mu \leq t < t_e \\
\Omega_r(t_0), & t \geq t_e
\end{cases}
\tag{6.14}
$$

according to the time interval.

We can plot the scale factor over the range of particle annihilation, obtained from inserting (6.14) on (6.13), as is shown in figure 6.4 and compare it with the scale factor obtained by integrating (6.13) with (6.7). We observe only a very small deviation between both curves for the earliest times, which tells us the approximation of $Q_2(t)$ is actually very good considering we use only a set of two differential equations to obtain it, opposed to
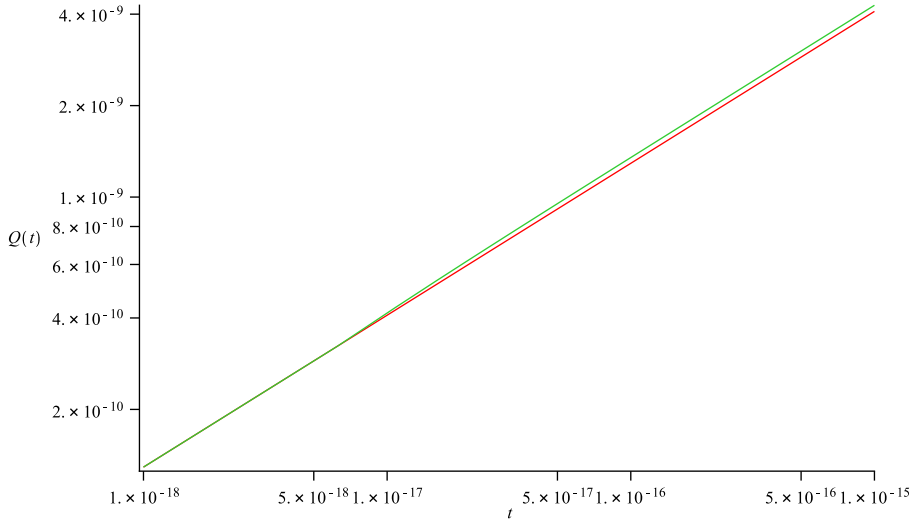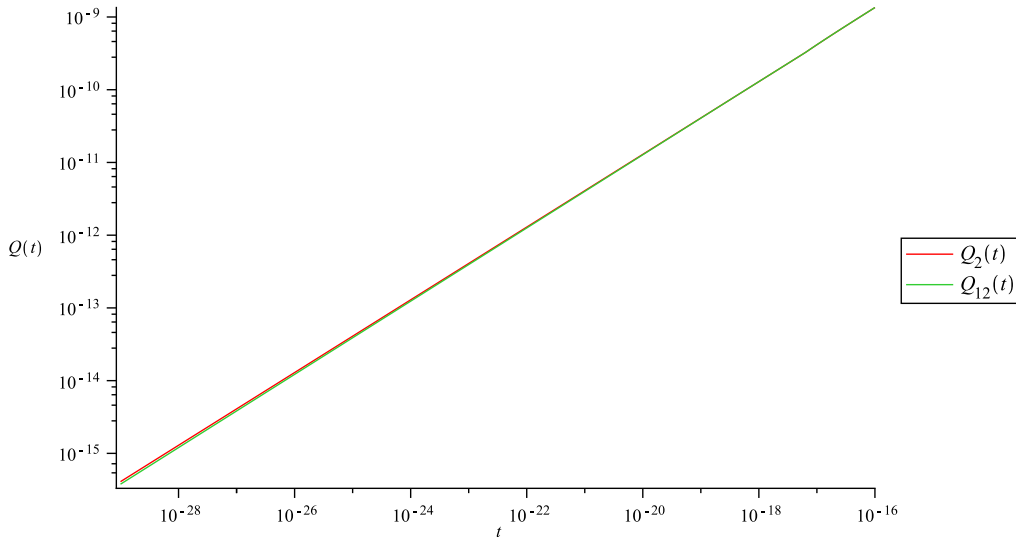
Figure 6.4: Scale factor over time, where $Q_2(t)$ represents the scale factor integrated with $\Omega_r(t_x)$ given by (6.7) and $Q_{12}(t)$ represents the scale factor integrated with $\Omega_r(t_x)$ given by 6.14, in logarithmic scale, with t in H_0^{-1} units.

the twelve differential equations needed to compute $Q_{12}(t)$.

6.2.2   Majorana versus Dirac Neutrinos

One last feature we want to investigate about the scale factor is how it modifies if we take neutrinos as Dirac particles instead of Majorana, as we did until now. What happens is we need to alter $\Omega_r(t_x)$, as we have seen in table 5.2, to its Dirac values. Doing it for $Q_2(t)$, we obtain a different curve, that in figure 6.5 is plotted along with the Majorana curve. In the range of the figure, we observe $Q_2^{Maj}(t)$ and $Q_2^{Dir}(t)$ have a small deviation and are parallel.

6.3   Temperature History $T(t)$

6.3.1   Radiation Temperature

The change in the constant of the density parameter of radiation affects both the scale factor and the density constant entering (6.5). Let us see the difference, relative to figure 6.1, that the use of a different constant density after the $e^{\pm}$-pair annihilation has on the temperature of radiation. In figure 6.6 we can see how relevant it is to use $\Omega_\gamma(t_0)$ (and $\Omega_r(t_0)$ in (6.13)) after the annihilation between electrons and positrons, accounting for the change in $N(t)$ that happens at this event.

We can also see, in the range of particle annihilation, what the difference between
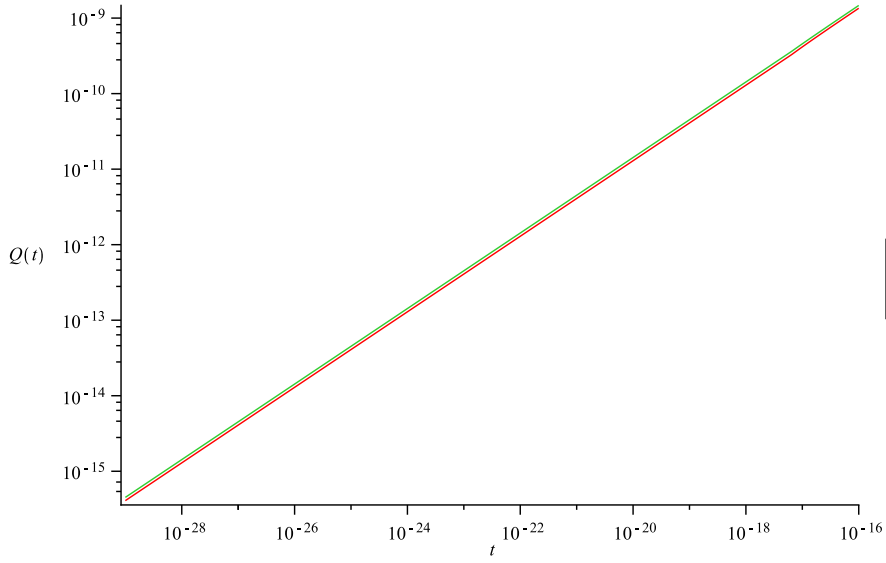
Figure 6.5: Scale factor over the range of particle annihilation, where $Q_2^{Maj}(t)$ represents the scale factor integrated taking the values of (6.7) as Majorana values and $Q_2^{Dir}(t)$ represents the scale factor integrated taking the values of (6.7) as Dirac values, in logarithmic scale, with t in H_0^{-1} units.
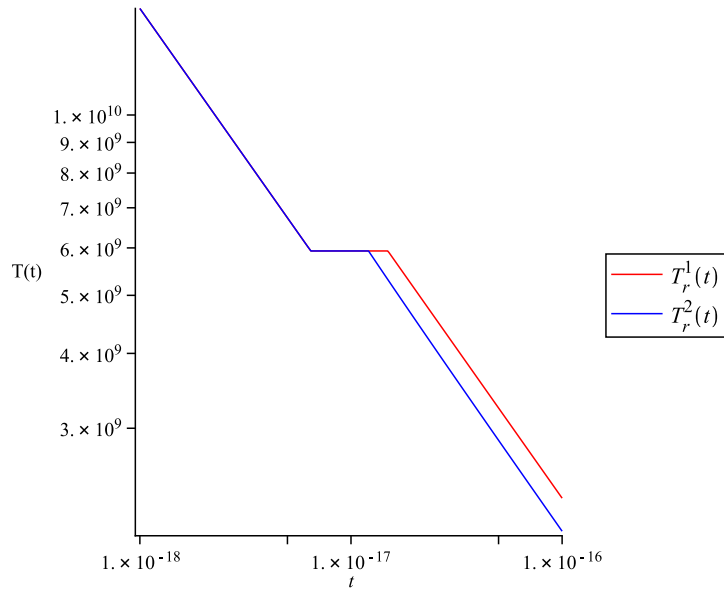
Figure 6.6: Radiation temperature around the decoupling of $e^{\pm}$, where $T_r^1(t)$ represents the temperature calculated with $\Omega_r^T(t_x) = \Omega_r(t_e)$ and $T_r^2(t)$ represents the temperature calculated with (6.6), in logarithmic scale, with t in H_0^{-1} units and T in K.

computing the radiation temperature is with $\Omega_r^T(t_x)$ according to (6.7), and indirectly with (6.13) according to (6.6), or computing it with

$$
\Omega_r^T(t_x) = \begin{cases}
\Omega_r(t_t), & t < t_t \\
\Omega_r(t_H), & t_t \leq t < t_H \\
\Omega_r(t_{W,Z}), & t_H \leq t < t_{W,Z} \\
\Omega_r(t_b), & t_{W,Z} \leq t < t_b \\
\Omega_r(t_\tau), & t_b \leq t < t_\tau \\
\Omega_r(t_c), & t_\tau \leq t < t_c \\
\Omega_r(t_s), & t_c \leq t < t_s \\
\Omega_r(t_{T_c}), & t_s \leq t < t_{T_c} \\
\Omega_r(t_\pi), & t_{T_c} \leq t < t_\pi \\
\Omega_r(t_\mu), & t_\pi \leq t < t_\mu \\
\Omega_r(t_e), & t_\mu \leq t < t_e \\
\Omega_\gamma(t_0), & t \geq t_e
\end{cases}
\tag{6.15}
$$

and indirectly according to (6.14). This is depicted in figure 6.7, where we observe no difference between both curves. This is another indication that $T_r^2(t)$ is accurate enough for our purposes.
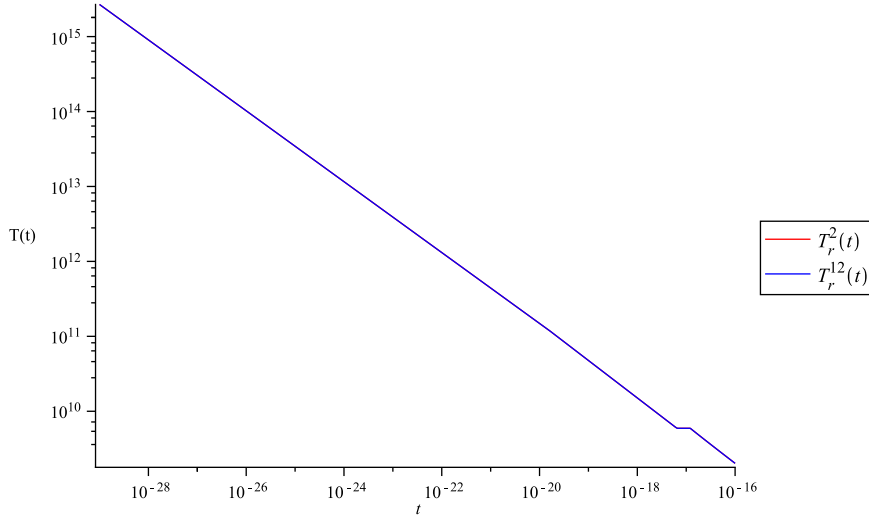
Figure 6.7: Radiation temperature over the particle annihilation, where $T_r^2(t)$ represents the temperature calculated with $\Omega_r^T(t_x)$ given by (6.6) and $Q_2(t)$, and $T_r^{12}(t)$ represents the temperature calculated with $\Omega_r^T(t_x)$ given by (6.15) and $Q_{12}(t)$, in logarithmic scale, with t in H_0^{-1} units and T in K.

Plotting the temperature over time, as it is done in figure 6.8, in the range where particles are dropping from equilibrium with radiation, the steps performed by the temperature due to the inclusion of (6.12) in (6.5) are almost all too tiny in comparison with the electron drop, around $t \sim 10^{-17} H_0^{-1}$, to be perceived at this scale. But if we zoom into the regions where the temperature equals the rest-mass of the other particle species, the steps become noticeable, as is emphasized by figures 6.9, 6.10 and 6.11.
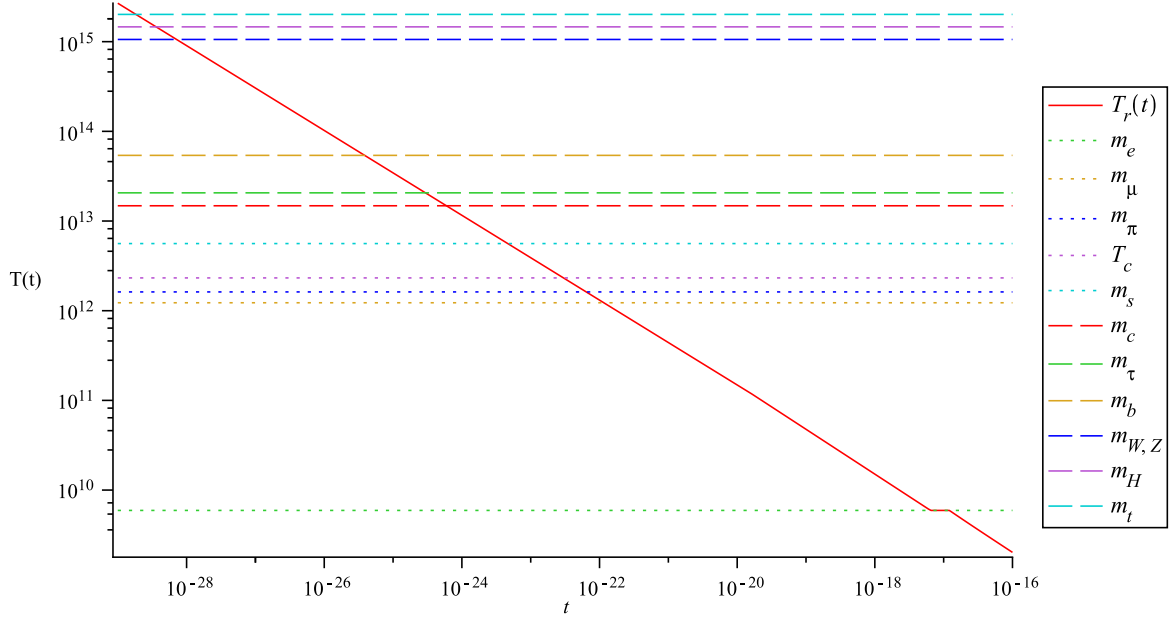
Figure 6.8: Radiation temperature in the range of particle annihilation for a general universe, in logarithmic scale, with t in H_0^{-1} units and T in K.

Majorana versus Dirac Neutrinos

When we discussed the degrees of freedom of the different particles in §5.2.2, we saw that neutrinos could be described as Majorana or Dirac fermions. The above temperature expressions considered them Majorana particles.

We shall now see the implications of having Dirac neutrinos, which represent an increase of $(7/8)6 = 21/4$ units in each $N(t)$ step and a change from $\Omega_r^T(t_x)$ and $\Omega_r(t_x)$ to its Dirac
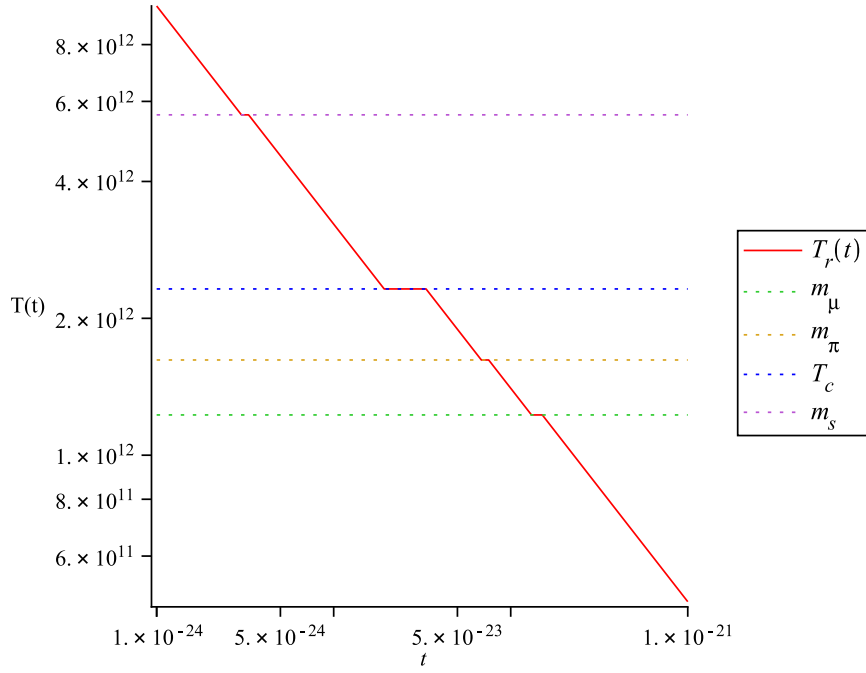
Figure 6.9: Radiation temperature, in logarithmic scale, with t in H_0^{-1} units and T in K, showing the threshold of annihilation of μ, π, hadrons and strange quark.

values. This results in

$$
4N^{Dir}(t) = \begin{cases}
8, & 8^{-\frac{1}{4}}\xi \leq m_e \\
64, & m_e < 64^{-\frac{1}{4}}\xi \leq m_\mu \\
78, & m_\mu < 78^{-\frac{1}{4}}\xi \leq m_\pi \\
90, & m_\pi < 90^{-\frac{1}{4}}\xi \leq T_c \\
226, & T_c < 226^{-\frac{1}{4}}\xi \leq m_s \\
268, & m_s < 268^{-\frac{1}{4}}\xi \leq m_c \\
310, & m_c < 310^{-\frac{1}{4}}\xi \leq m_\tau \\
324, & m_\tau < 324^{-\frac{1}{4}}\xi \leq m_b \\
366, & m_b < 366^{-\frac{1}{4}}\xi \leq m_{W,Z} \\
402, & m_{W,Z} < 402^{-\frac{1}{4}}\xi \leq m_H \\
406, & m_H < 406^{-\frac{1}{4}}\xi \leq m_t \\
448, & m_t < 448^{-\frac{1}{4}}\xi \\
S^{Dir}(t), & \text{otherwise}
\end{cases} , \tag{6.16}
$$
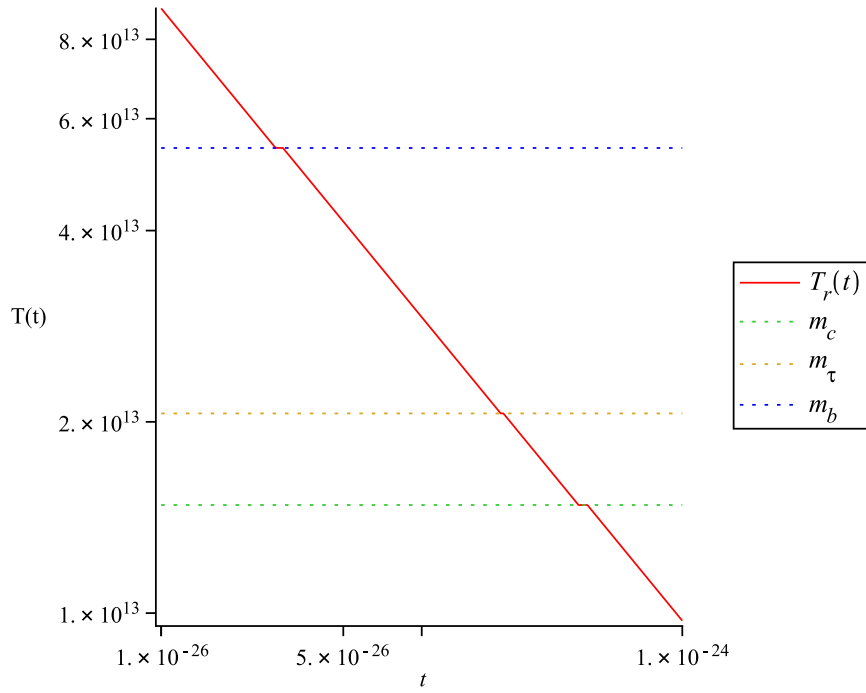
Figure 6.10: Radiation temperature, in logarithmic scale, with t in H_0^{-1} units and T in K, showing the threshold of annihilation of charm quark, τ particle and bottom quark.

with

$$
S^{Dir}(t) = \xi^4
\begin{cases}
m_e^{-4}, & 64^{-\frac{1}{4}}\xi < m_e \\
m_\mu^{-4}, & 78^{-\frac{1}{4}}\xi < m_\mu \\
m_\pi^{-4}, & 90^{-\frac{1}{4}}\xi < m_\pi \\
T_c^{-4}, & 226^{-\frac{1}{4}}\xi < T_c \\
m_s^{-4}, & 268^{-\frac{1}{4}}\xi < m_s \\
m_c^{-4}, & 310^{-\frac{1}{4}}\xi < m_c \\
m_\tau^{-4}, & 324^{-\frac{1}{4}}\xi < m_\tau \\
m_b^{-4}, & 366^{-\frac{1}{4}}\xi < m_b \\
m_{W,Z}^{-4}, & 402^{-\frac{1}{4}}\xi < m_{W,Z} \\
m_H^{-4}, & 406^{-\frac{1}{4}}\xi < m_H \\
m_t^{-4}, & 448^{-\frac{1}{4}}\xi < m_t
\end{cases}
.
\tag{6.17}
$$

Hence, the temperature law will be written as

$$
T_r^{Dir}(t) = \left(\frac{90 H_0^2 \Omega_r^T(t_x)}{8\pi^3 G N^{Dir}(t)} \right)^{\frac{1}{4}} \frac{1}{Q(t)},
\tag{6.18}
$$

and we can plot it along with (6.5). In figure 6.12 we see that there is only a small
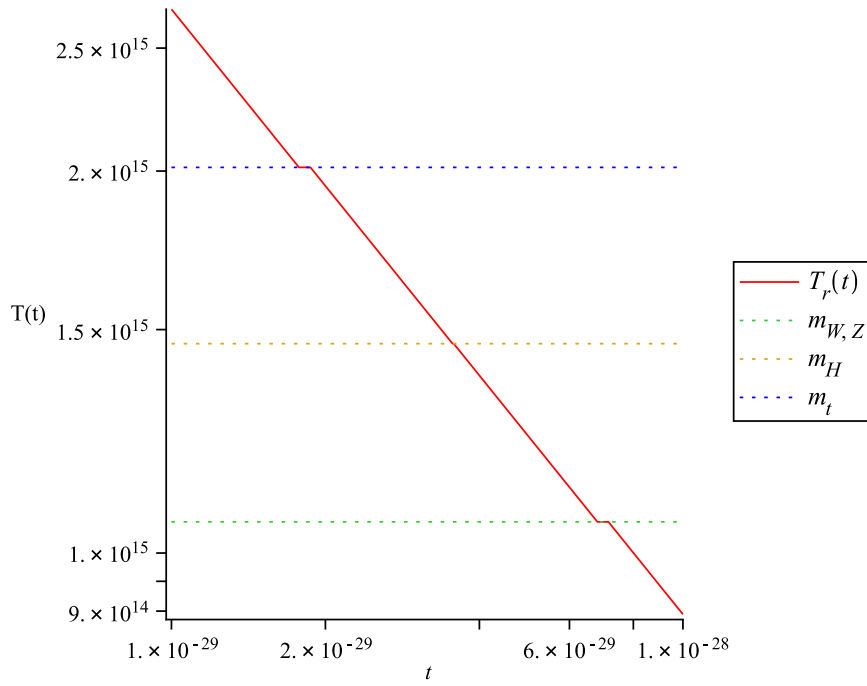
Figure 6.11: Radiation temperature, in logarithmic scale, with t in H_0^{-1} units and T in K, showing the threshold of annihilation of W and Z bosons, Higgs boson and top quark.
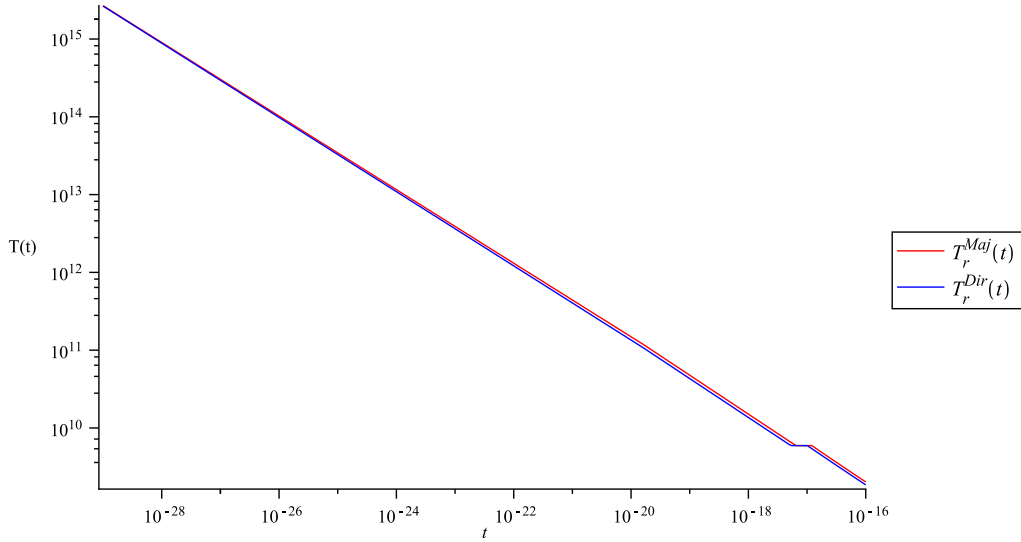
Figure 6.12: Radiation temperature considering neutrinos as Majorana fermions, $T_r^{Maj}(t)$, and Dirac fermions $T_r^{Dir}(t)$ as functions of time in logarithmic scale, with t in H_0^{-1} units and T in K.

difference between $T_r^{Maj}(t)$ and $T_r^{Dir}(t)$. For higher temperatures, the deviation between both curves is smaller than for lower temperatures. Neutrinos do not enter the last drop

in effective degrees of freedom, where the coefficients of $N_r^{Maj}(t)$ and $N_r^{Dir}(t)$ become the same and $\Omega_r^T(t_x) = \Omega_\gamma(t_0)$ also does not depend on the kind of neutrinos we consider. However, there is a difference between $Q^{Maj}(t)$ and $Q^{Dir}(t)$ as we have seen in figure 6.5, which results in the deviation between both curves one can observe for temperatures below m_e.

Since the difference is not too significant, for the sake of simplicity, from here on, when we talk about the temperature of radiation we are referring to the Majorana component.

6.3.2 Neutrino Temperature

It is at the last step of particle creation, when electrons separate from radiation, that the neutrino temperature component deviates from that of radiation, as seen in §5.4 and the expression (5.29), derived for the temperature law of neutrinos, holds after neutrinos decouple. Neutrinos differ from photons in temperature because they have decoupled shortly before electrons and positrons and do not "see" the change in effective degrees of freedom provoked by them. In this way, we will use the radiation temperature until $t = t_e$, the point at which we need to alter $N(t)$ to N_ν^{Maj} and $\Omega_r^T(t_x)$ to $\Omega_\nu^{Maj}(t_0)$. Thus, we can write for Majorana neutrinos

$$T_\nu^{Maj}(t) = \left(\frac{90 H_0^2 \Omega_\nu^{Maj}(t_0)}{8\pi^3 G N_\nu^{Maj}} \right)^{\frac{1}{4}} \frac{1}{Q(t)}, \quad t \geq t_e, \tag{6.19}$$

while before they share the radiation temperature, (6.5).

Now let us take neutrinos as Dirac particles and rewrite their temperature as

$$T_\nu^{Dir}(t) = \left(\frac{90 H_0^2 \Omega_\nu^{Dir}(t_0)}{8\pi^3 G N_\nu^{Dir}(t)} \right)^{\frac{1}{4}} \frac{1}{Q^{Dir}(t)}, \quad t \geq t_e^{Dir}, \tag{6.20}$$

where t_e^{Dir} corresponds to the time when the rest-mass of the electron is reached by the radiation temperature $T_r^{Dir}(t)$ when we consider Dirac neutrinos, which is different from t_e in the case of Majorana neutrinos as we can see in figure 6.12, and yields the result $t_e^{Dir} = 5.29 \times 10^{-18} \ H_0^{-1}$.

Plotting $T_r^{Maj}(t)$ and $T_\nu^{Maj}(t)$ given by (6.19), as it is done in figure 6.13, we can see the moment when neutrinos decoupled from radiation, around $t \simeq 10^{-17} H_0^{-1}$. We observe that having $\Omega_r(t_e)$ and $4N = 43$ in (6.5) is equivalent to having $\Omega_\nu^{Maj}(t_0)$ and $4N = 21$ in (6.19), because the temperature of radiation before m_e is reached coincides with the temperature of neutrino when they become a separate species, at $t = t_{T_{D\nu}}$.

We can also use figure 6.13 to investigate the difference between the Majorana and the Dirac neutrino temperatures by plotting $T_r^{Dir}(t)$ and $T_\nu^{Dir}(t)$ given by (6.20). We see the decoupling of Dirac neutrinos is analogous to the decoupling of Majorana ones and we can
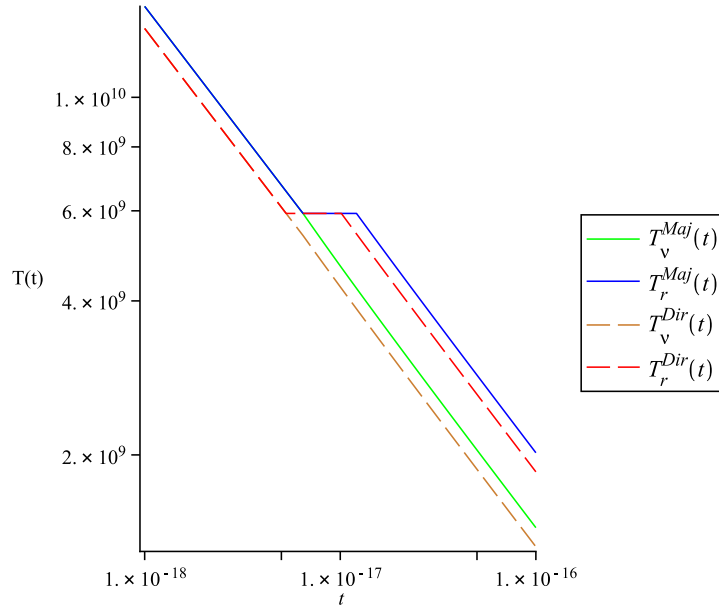
Figure 6.13: Radiation and neutrino temperatures $T_r^{Maj}(t)$, $T_r^{Dir}(t)$, $T_\nu^{Maj}(t)$ and $T_\nu^{Dir}(t)$ as functions of time in logarithmic scale, with t in H_0^{-1} units and T in K, showing the different behaviors due to Majorana and Dirac fermions.

clearly perceive the difference between $T_\nu^{Maj}(t)$ and $T_\nu^{Dir}(t)$. This was expected since we already observed in figure 6.12 the difference between the radiation temperature taking neutrinos to be Majorana or Dirac fermions. As compared to $T_\nu^{Maj}(t)$, $T_\nu^{Dir}(t)$ presents a different number of effective degrees of freedom, scale factor and $\Omega_\nu(t_0)$.

In figure 6.13, the Majorana and Dirac curves yield different temperature values, but regardless of the type of neutrinos considered, the present temperature is 2.725 K for radiation and 1.945 K for neutrinos. However, the value of the present time t_0 will be different in each case, because as we have seen in figure 6.5, $Q^{Maj}(t)$ and $Q^{Dir}(t)$ yield slightly different values and this difference will be reflected in a different value for the present moment t_0.

6.3.3   Matter Temperature

Matter, both baryonic and dark matter, decrease at a different rate after decoupling from the thermal bath, according to (5.48) and (5.58), respectively. The background temperature of matter is not observable presently, as happens with photons and is expected to happen with neutrinos, because instead of forming a homogeneous background, matter clustered, condensing into structures.

Dark Matter

We can begin by looking at the decoupling temperature of dark matter, as it happens prior to the baryonic matter separation from radiation. As examples of neutralino masses, we will choose $m_1 = 10$ GeV/c^2, $m_2 = 100$ GeV/c^2 and $m_3 = 1$ TeV/c^2, to understand how different dark matter particle masses affect the universe.

The chemical decoupling of dark matter, given by (5.55), occurred around $T_{cd}(m_1) \simeq 4.6 \times 10^{12}$ K, $T_{cd}(m_2) \simeq 4.6 \times 10^{13}$ K and $T_{cd}(m_3) \simeq 4.6 \times 10^{14}$ K for each mass considered. For the kinetic decoupling, that we estimate occurs at (5.58), we need to also choose the mass of sleptons. From literature [48], $m_{\tilde{L}} = 200$ GeV/c^2 may be a good estimation. Then, we will find that the kinetic decoupling of dark matter happened around $T_{kd}(m_1) \simeq 2.1 \times 10^{11}$ K, $T_{kd}(m_2) \simeq 3.2 \times 10^{11}$ K and $T_{kd}(m_3) \simeq 3.3 \times 10^{12}$ K. The different order of magnitude that the decoupling temperature for m_3 renders, compared to that of the particles with m_1 and m_2, may come from the fact that the slepton mass $m_{\tilde{L}}$ matches less a neutralino mass as high as m_3.

These temperatures for the chemical and kinetic decoupling are located in the particle annihilation range, as we can see from figure 6.8.

The kinetic decoupling represents the moment when dark matter becomes transparent to radiation and begins following its own temperature law. In (5.48), $T_{DM}(t_0) = T_{kd}(M_{\tilde{\chi}})Q_{kd}^2$, which enables us to write for dark matter a step function, that will be identical to (6.5) until neutralinos decouple kinetically and that follows (5.48) afterwards

$$
T_{DM}(t) = \begin{cases} \xi[4N_r(t)]^{-\frac{1}{4}}, & t < t_{kd}(M_{\tilde{\chi}}) \\ T_{kd}(M_{\tilde{\chi}})Q_{kd}^2 Q(t)^{-2}, & t \geq t_{kd}(M_{\tilde{\chi}}) \end{cases},
\tag{6.21}
$$

(taking the case where neutrinos are considered Majorana particles).

We can see how dark matter temperature behaves around the region of decoupling in figure 6.14, for the different masses chosen. Of course we should keep in mind that the real process was not instantaneous, as this treatment suggests.

Another interesting exercise is to obtain the present dark matter relic temperature, considering neutralinos. For the three masses we have taken, at t_0 its temperature will yield $T(m_1) \simeq 1.79 \times 10^{-11}$ K, $T(m_2) \simeq 1.16 \times 10^{-11}$ K and $T(m_3) \simeq 4.70 \times 10^{-13}$ K. These temperatures are extremely low and come from the fact that, although dark matter decoupled in our model in the range where other particles were decoupling from the plasma, they followed a temperature law that decreased their temperature with a factor $\propto Q(t)^{-2}$.

Baryonic Matter

Now let us focus on the baryonic component of matter, created around $T = T_c \simeq 2.3 \times 10^{12}$ K. It remained in thermal contact until decoupling; from that point on the baryonic matter
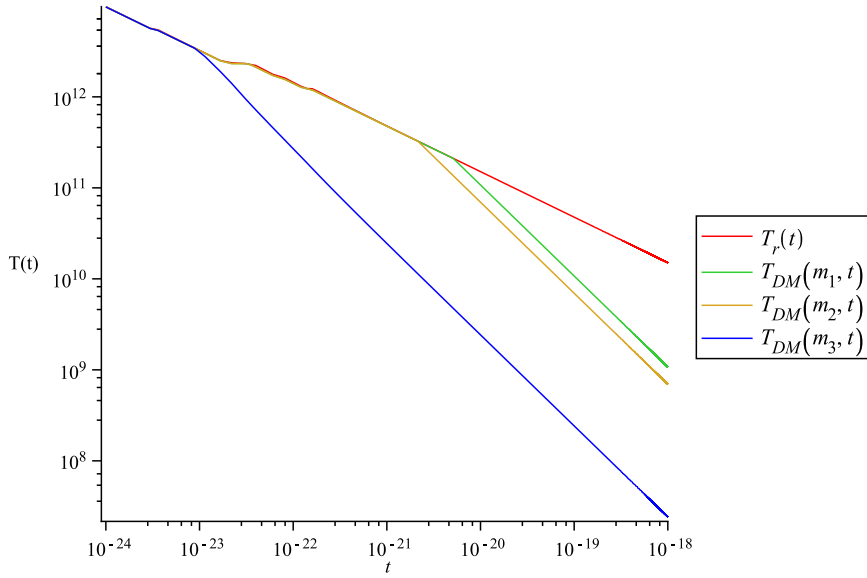
Figure 6.14: Representation of neutralinos decoupling kinetically from radiation by plotting $T_r(t)$ (taken as $T_r^{12}(t)$) and $T_{DM}(t)$ over time in logarithmic scale, with t in H_0^{-1} units and T in K.

temperature dropped faster than the radiation temperature, which means that it is lower than the radiation temperature today. From the dependences of (3.57) and (5.48) on the scale factor, we see that the matter temperature will grow faster than the radiation temperature when time runs backwards. Thus, both curves will intersect at some point and estimations indicate that this happens around the temperature $T_D \simeq 3000$ K [25]. From (5.47), when the radiation and baryonic matter temperatures intersect, we can write

$$\frac{T_r(t_0)}{Q_D} = \frac{T_D Q_D^2}{Q_D^2} \implies Q_D = \frac{T_r(t_0)}{T_D} \simeq 9.083 \times 10^{-4}. \tag{6.22}$$

Inserting this now back in (5.47), we obtain $T_{mat}(t_0) = T_D Q_D^2 = T_r^2(t_0)/T_D \simeq 2.475 \times 10^{-3}$ K. This is the present value of the temperature of matter, which is 3 orders of magnitude less than the present radiation temperature. In figure 6.15 we depict the region where it happens. This is the moment when baryons decouple from radiation, for $t_D \simeq 2.7 \times 10^{-5} H_0^{-1} \simeq 373$ thousand years at $T = 3000$ K.

Proceeding as in the case of dark matter, after determining the decoupling temperature of baryonic matter, we can use a step function to help us describe the baryonic matter temperature as follows

$$T_b(t) = \begin{cases} \xi[4N(t)]^{-\frac{1}{4}}, & t < t_D \\ T_{mat}(t_0)Q(t)^{-2}, & t \geq t_D \end{cases} \tag{6.23}$$
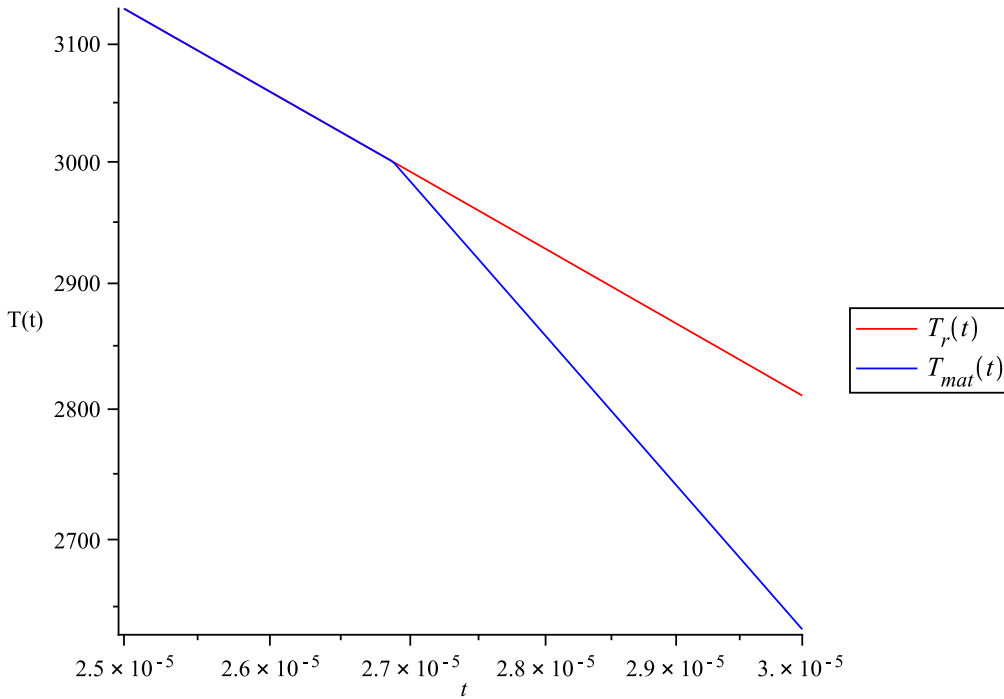
Figure 6.15: Representation of the matter temperature $T_{mat}(t)$ along with the radiation temperature $T_r(t)$ (taken as $T_r^{12}(t)$) over time in logarithmic scale, with t in H_0^{-1} units and T in K, emphasizing the intersection of the curves.

6.4 Density Parameter History $\Omega(t)$

The evolution of the universe in density terms is also worth studying as it changed from radiation-dominated to matter-dominated and into dark energy-dominated. The density parameter values of tables 5.3 and 5.2, along with the density expressions of section §3.3.4, allow our simulation to include the density of different entities.

6.4.1 Radiation density

The radiation density parameter includes photons and neutrinos and is given by

$$\Omega_r(t) = \frac{\Omega_r(t_x)}{Q(t)^4}, \tag{6.24}$$

where the values of $\Omega_r(t_x)$ are listed on table 5.2. In this section, we choose $\Omega_\nu(t_0) = \Omega_\nu^{Maj}(t_0)$. As we have seen, it is this $\Omega_r(t_x)$ that we use in the simulation, to integrate (6.13), either in the form of (6.7) or (6.14).

In figure 6.16 we plot the radiation density parameter obtained using (6.7) and $Q_2(t)$ for $\Omega_r^2(t)$, and (6.14) and $Q_{12}(t)$ for $\Omega_r^{12}(t)$, over the range of particle annihilation. One can not distinguish both curves, which reinforces the validity of using $Q_2(t)$. Analogously to

what happened in the radiation temperature case, the only annihilation threshold perceivable at this scale is the electron decoupling.
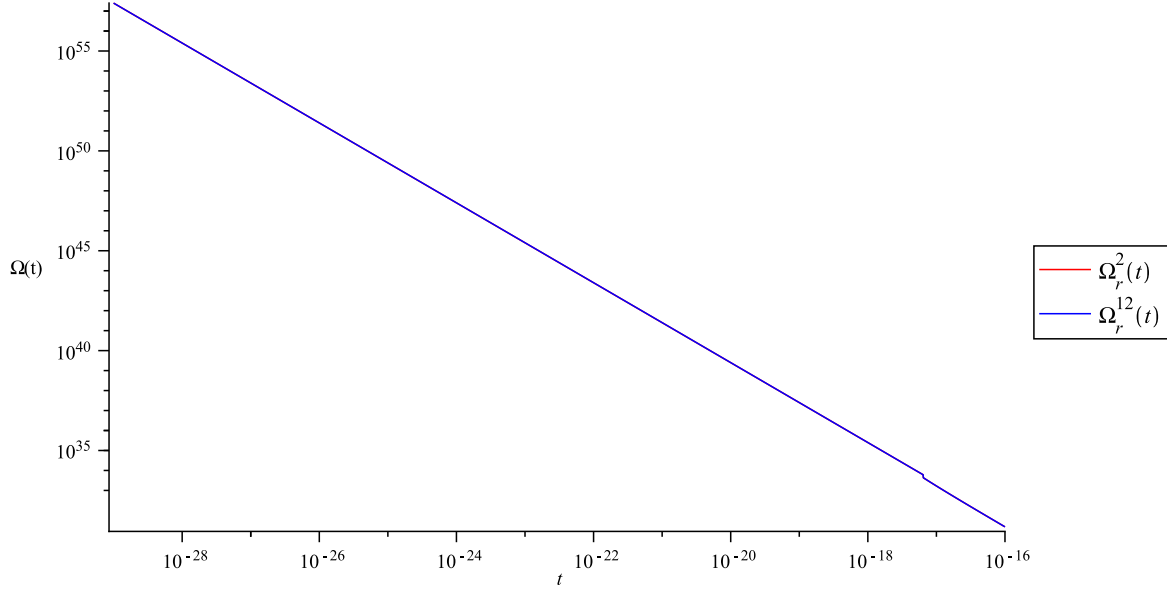
Figure 6.16: Radiation density parameter in the range of particle annihilation for a general universe, in logarithmic scale, with t in H_0^{-1} units, where $\Omega_r^2(t)$ represents the density parameter calculated with $\Omega_r(t_x)$ given by (6.7) and $Q_2(t)$, and $\Omega_r^{12}(t)$ represents the density parameter calculated with $\Omega_r(t_x)$ given by (6.14) and $Q_{12}(t)$.

Let us have a zoomed look, through figures 6.17, 6.18, 6.19 and 6.20. At the electron threshold there is no difference between $\Omega_r^2(t)$ and $\Omega_r^{12}(t)$ because both curves were constructed in the same way at this range. From figure 6.16 we were already expecting not to see a very significant deviation between the curves on the other thresholds.
In the transition where $N(t)$ performs the biggest jump, at T_c, we observe that the behaviour of $\Omega_r^{12}(t)$ is not so regular as the behaviour of $\Omega_r^2(t)$. In each threshold both densities agree but begin deviating as we go back in time, in the direction of increasing densities until the next particle threshold is reached. There, the scale factor and the density parameter constant entering $\Omega_r^{12}(t)$ perform a step, that results in $\Omega_r^{12}(t)$ coinciding with $\Omega_r^2(t)$ again. This happens because we obtained the time at which each threshold occurred according to $\Omega_r^2(t)$, so it is now natural that its behaviour is guiding the $\Omega_r^{12}(t)$ curve.
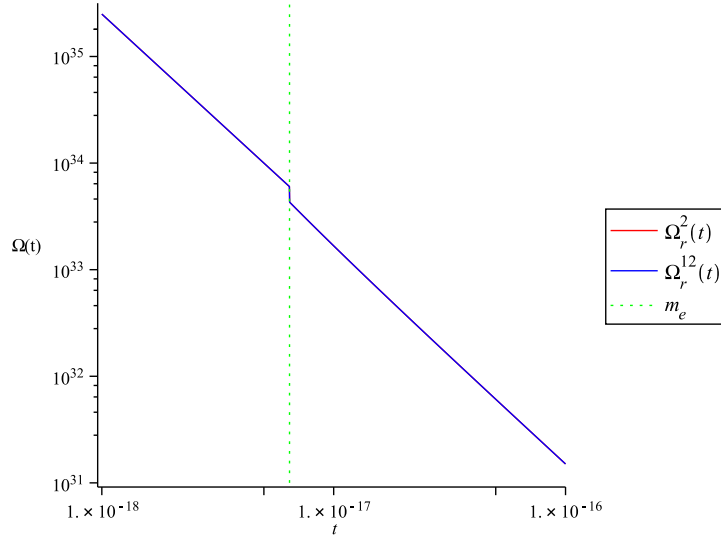
Figure 6.17: Radiation density parameter, where $\Omega_r^2(t)$ represents the density parameter calculated with $\Omega_r(t_x)$ given by (6.7) and $Q_2(t)$, and $\Omega_r^{12}(t)$ represents the density parameter calculated with $\Omega_r(t_x)$ given by (6.14) and $Q_{12}(t)$, in logarithmic scale, with t in H_0^{-1} units, showing the threshold of annihilation of electrons.
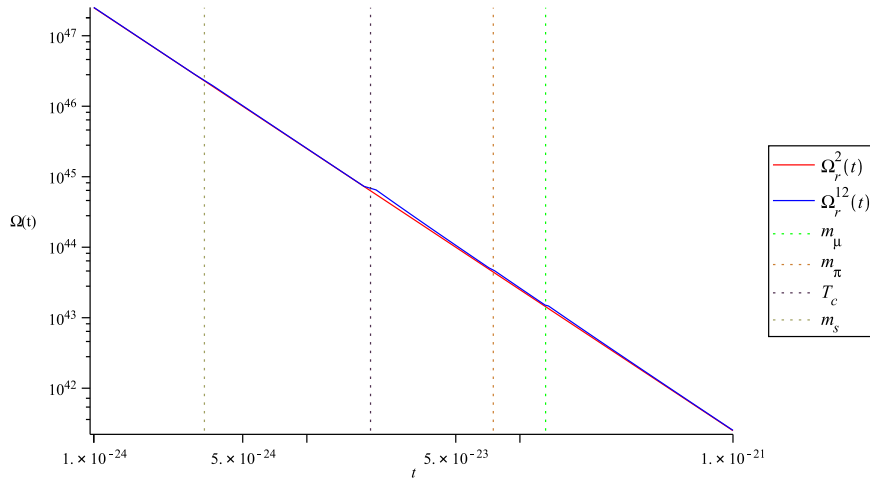
Figure 6.18: Radiation density parameter, where $\Omega_r^2(t)$ represents the density parameter calculated with $\Omega_r(t_x)$ given by (6.7) and $Q_2(t)$, and $\Omega_r^{12}(t)$ represents the density parameter calculated with $\Omega_r(t_x)$ given by (6.14) and $Q_{12}(t)$, in logarithmic scale, with t in H_0^{-1} units, showing the threshold of annihilation of μ, π, hadrons and strange quark.

6.4.2 Matter Density

Dark energy is constant in density over time, Ω_Λ, while matter density is divided into the dark matter and baryonic parts. We saw that the last one appears only after baryogenesis,
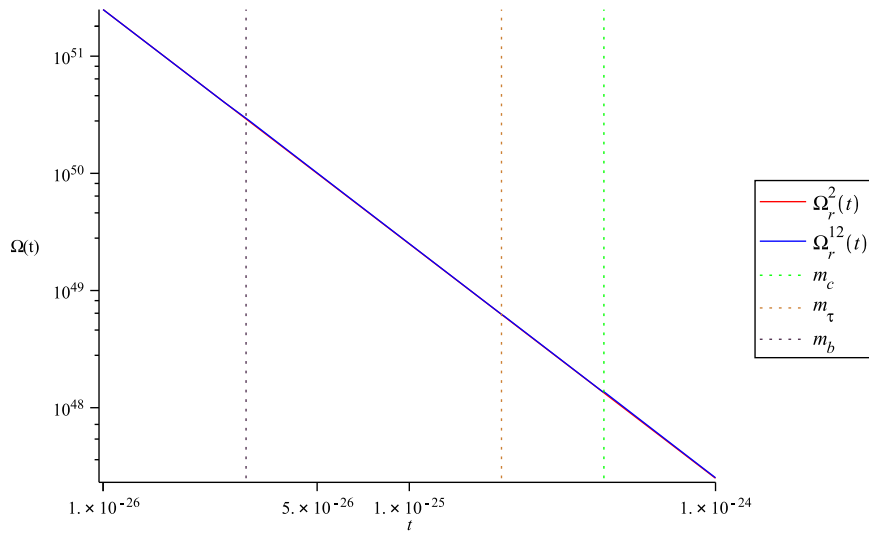
Figure 6.19: Radiation density parameter, where $\Omega_r^2(t)$ represents the density parameter calculated with $\Omega_r(t_x)$ given by (6.7) and $Q_2(t)$, and $\Omega_r^{12}(t)$ represents the density parameter calculated with $\Omega_r(t_x)$ given by (6.14) and $Q_{12}(t)$, in logarithmic scale, with t in H_0^{-1} units, showing the threshold of annihilation of charm quark, τ particle and bottom quark.
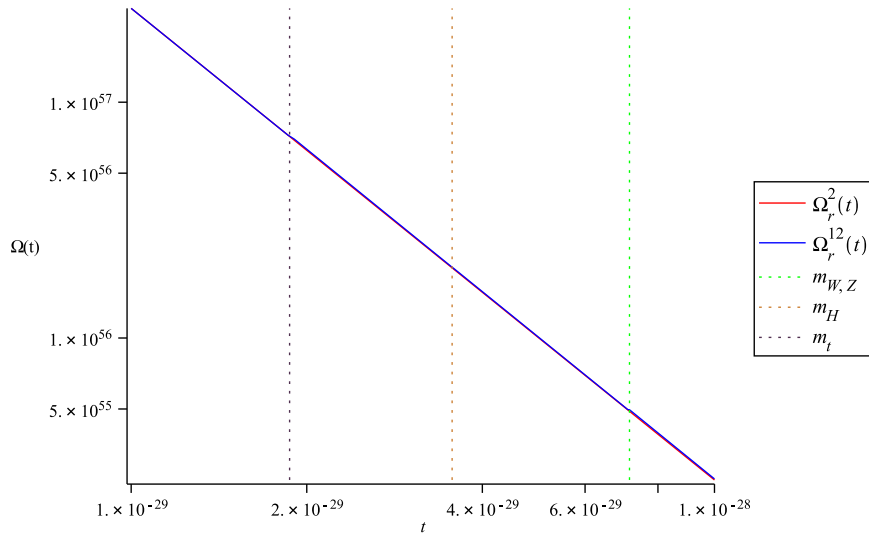
Figure 6.20: Radiation density parameter, where $\Omega_r^2(t)$ represents the density parameter calculated with $\Omega_r(t_x)$ given by (6.7) and $Q_2(t)$, and $\Omega_r^{12}(t)$ represents the density parameter calculated with $\Omega_r(t_x)$ given by (6.14) and $Q_{12}(t)$, in logarithmic scale, with t in H_0^{-1} units, showing the threshold of annihilation of W and Z bosons, Higgs boson and top quark.

when part of the radiation density is transferred to the new-born baryons, summing up to the dark matter density. This happens around the temperature T_c, which corresponds in the simulation to a time $t_{T_c} \simeq 1.99 \times 10^{-23} H_0^{-1}$. We can describe this process using again a step function

$$\Omega_{mat}(t) = \begin{cases} \Omega_{cdm}(t_0)Q(t)^{-3}, & t < t_{T_c} \\ [\Omega_{cdm}(t_0) + \Omega_b(t_0)] Q(t)^{-3}, & t \geq t_{T_c} \end{cases} \tag{6.25}$$

We are now able to plot an overview of the behaviour of the density contributions in a general universe, which is done in figure 6.21. In this broad range of densities, the step performed by $\Omega_{mat}(t)$ at T_c is too small to be perceived in the plot. It is possible to clearly see the matter-radiation equality and to observe the dark energy component, constant over time, gaining importance for later times. Choosing to plot the radiation density parameter as $\Omega_r^2(t)$ or $\Omega_r^{12}(t)$ is irrelevant, as we saw by looking at figure 6.17.
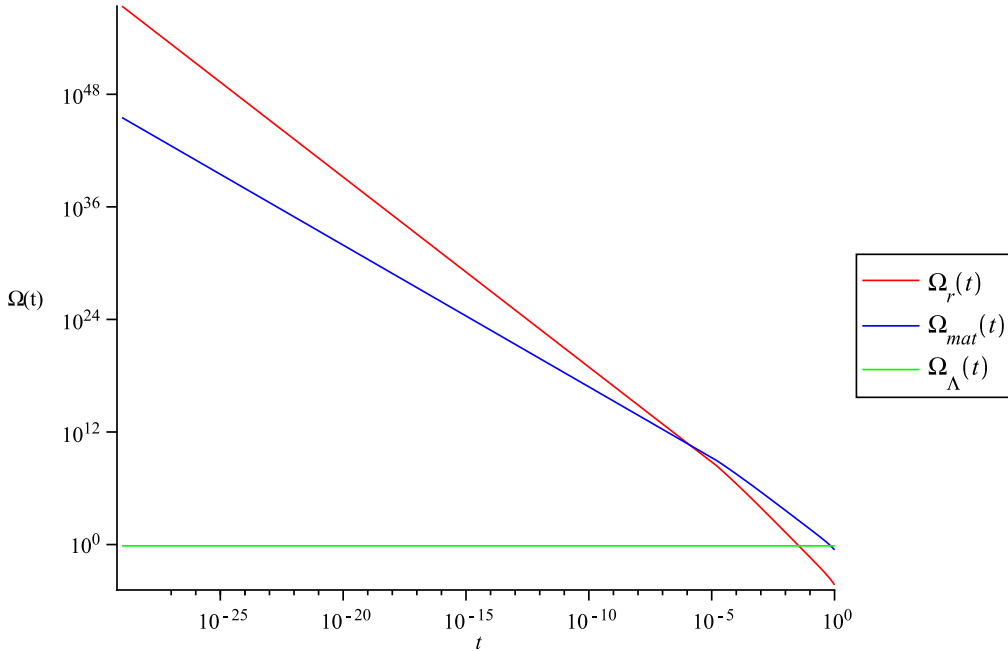
Figure 6.21: Representation of the density parameters (where the density parameter of radiation is taken as $\Omega_r^{12}(t)$) over time in logarithmic scale, with t in H_0^{-1} units, from the beginning of the particle thresholds to the present time.

Figure 6.22 shows the density parameter of matter with time for the QCD phase transition, to see the dimension of the change *produced* by the appearance of the baryonic matter component. We can confirm it represents only a small increase in the matter density.
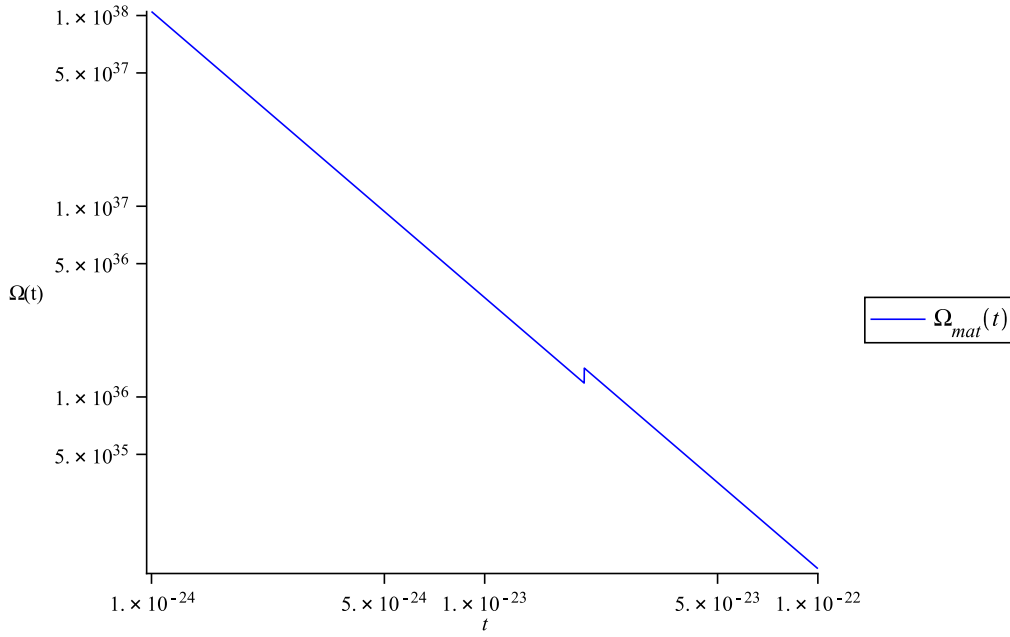
Figure 6.22: Representation of the density parameter of matter over time in logarithmic scale, with t in H_0^{-1} units, around the quark-hadron confinement transition.

6.4.3 Matter-Radiation and Dark Energy-Matter Equalities

The decrease of the matter density with expansion will be less accentuated than for the radiation density, leading to the matter-radiation equality. This is pictured in figure 6.23 and the intersection between the two components happens in the simulation at $t \simeq 1.6 \times 10^{-6} H_0^{-1} \simeq 22$ thousand years, when the universe becomes matter-dominated. We conclude the universe was already matter-dominated when baryonic matter decoupled from radiation.

The point when dark energy becomes the dominant component of the universe is depicted in figure 6.24, at $t = 0.69 H_0^{-1}$, which corresponds to 9.6 Gyrs.

6.5 Age of the Universe

A question worth considering is how old the universe is, since its age is model dependent. The time has been measured in Hubble time units and we defined the present moment t_0 as the time when $Q_0 = 1$. $t = 0$ corresponds to extrapolate to the time when $Q = 0$, in other words, to the Big Bang, but we only work with values of Q and t posterior to the end of inflation. Asking our program what value of t renders $Q_0 = 1$, we will find two answers, depending on whether we take neutrinos to be Majorana or Dirac particles.

We saw in figure 6.5 that the scale factor *changes* slightly according to the type of neutrinos
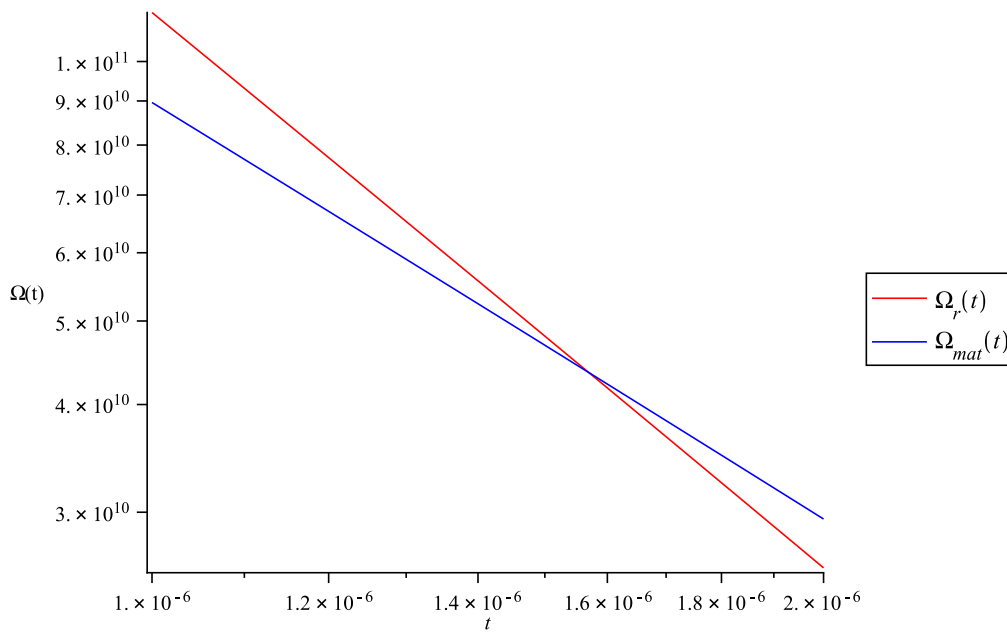
Figure 6.23: Representation of the density parameters of matter and radiation $(\Omega_r^{12}(t))$ over time in logarithmic scale, with t in H_0^{-1} units, around the matter-radiation equality.

considered. This is reflected now in the age of the universe. Then, we obtain $t_0 \simeq 0.9983$ H_0^{-1} for Majorana neutrinos, equivalent to 13.87 Gyrs and $t_0 \simeq 0.9981$ H_0^{-1} for Dirac neutrinos, equivalent to 13.86 Gyrs. This small difference comes from the fact that the value of the present density of radiation, which enters $\dot{Q}(t)$, depends on the type of neutrino we consider.

A universe with a dark energy component will be older than one comprised only of matter and radiation. This happens because the expansion rate is accelerating in a model with Λ [12].
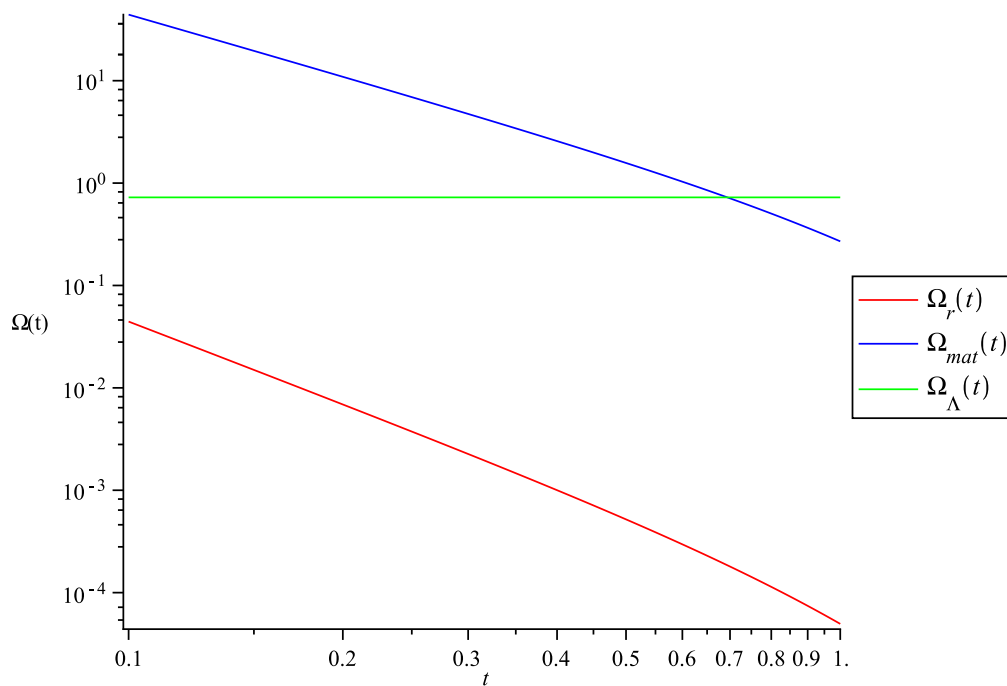
Figure 6.24: Representation of the density parameters (where the density parameter of radiation is taken as $\Omega_r^{12}(t)$) over time in logarithmic scale, with t in H_0^{-1} units, around the Λ-matter equality.

Chapter 7

Conclusion

In this work, the quantum effects on gravitation at the Planck scale are accounted by conformal fluctuations of the metric. We use a scalar field φ to model the fluctuations around the classical value of the metric. Macroscopically, these fluctuations result in a term equivalent to a cosmological constant in Einstein's equations. This term will be present in the equations of motion of the universe and we identify it with the dark energy component, responsible for the observed accelerated expansion of the universe.

Our goal is to model the evolution of a universe with such dark energy. We consider a perfect fluid universe and show that dark energy will be a constant term over time. We also want to account the dark matter component, thus, from the sea of particle candidates, we choose one where its decoupling has been quantitatively studied – neutralinos.

We then use standard particle physics, thermodynamics and statistics to write a program in *Maple* that enables us to follow the behaviour of the scale factor, temperature and density with time. We integrate numerically the equation of motion of our universe to obtain the scale factor with respect to time. We separate the expansion of the universe in time intervals according to the particle annihilation thresholds and integrate a set of two or twelve differential equations depending on the context. We realize the approach where we divide the expansion in two regions is accurate enough. Both are similar after electrons and positrons decouple from radiation, which makes the events that happen afterwards being totally independent of this choice. Although the universe seems to be approximately flat and its present observational value is small, we included the curvature term in our model, enabling it to accommodate any curvature value that turns out to be more precise. This way, we are able to track the most relevant events in thermal history, from the end of inflation to the present time, such as particle annihilation and dark matter, neutrino and baryonic matter decoupling.

Studying the density, it is possible to observe the matter-radiation equality and the dark energy-matter equality, thus seeing when the universe changed from radiation-dominated to matter-dominated and, more recently, to dark energy-dominated. We notice that we

live in a universe mainly comprised and dominated by constituents we have very little knowledge about. The fact that we plotted the quantities in logarithmic scale, where what matters most are order of magnitude changes, makes us have a different perspective on the time passing, compared to a linear scale.

For the radiation temperature, we obtain an expression that can be used to determine the temperature value at each moment and that we believe is a good approximation since the present background temperature is reproduced and it accounts for the entropy changes that happened in the early universe while particles dropped out of thermal equilibrium. There is no observable difference between the radiation temperature computed using a set of two differential equations and density constants or with twelve, accounting for all particle thresholds. But it is important to make the distinction between the region before electrons decouple and afterwards.

It would be more realistic to use a smooth function to model the decoupling of particle species from the thermal bath than as we have done, using step functions. The temperature of other components would also benefit from an improved function to make the transition in the region where they stop sharing the radiation temperature and begin following a different one.

We conclude that considering neutrinos as Majorana or Dirac fermions, which have a different number of degrees of freedom, affects the present density parameter of neutrinos, which has consequences for the scale factor of the universe. With regard to radiation, the temperature also depends on the type of neutrino considered, as well as the age of the universe.

Based on our analysis, it is not possible to deduce if neutrinos are Majorana or Dirac fermions. If $\Omega_\nu(t_0)$ could be observationally measured, we would be able to compare it with our predictions and, if the measurement was accurate enough, see if it was closer to the density parameter obtained for Majorana or for Dirac neutrinos. The difference between the age of the universe that both neutrino types render is too small compared to its present observational error margin.

Since we have no idea about the present temperature of dark matter, we can not comment much on these results. For now, we cannot probe whether the model we used, with neutralinos comprising all cold dark matter, is a good approximation to the observable universe or not. Having such a low present dark matter temperature (in the order of 10^{-11} K) can still be consistent with studies that point to a temperature in the order of 10^3 K [40]. We computed the average temperature in the universe and it is believed dark matter clustered into structures, which means matter-rich regions are expected to present much higher values than the temperature of empty regions.

The same can be argued for baryonic matter, where we obtained an overall present temperature of $T_{mat}(t_0) \simeq 2.475 \times 10^{-3}$ K. But the case of baryonic matter is substantially

different because we know the mass of neutrons and protons and we also have good estimations on their abundances. Predictions about the time of recombination point to an age of the universe of a few hundred thousand years [25]. We obtained $t_D \simeq 373$ thousand years for the decoupling between matter and radiation, which we take as evidence that the model we consider can make good predictions of the main events of standard cosmology. In the density parameter plots, as well as in the scale factor one, the logarithmic scale yields linear curves over time while the universe is radiation-dominated. After it becomes matter-dominated, the importance of the other components of the universe, whose density parameter enters the Friedmann equation, makes the curve bend in a way closer to a matter-dominated universe. The presence of Λ, as it is a constant term, does not show up in the behaviour of the curves, but it alters the present time t_0, consequently influencing the age of the universe. It will be the dominating entity in the future, as it already is presently. In the radiation density, we can notice the small effect that the particle annihilation originates, a result from the decrease in degrees of freedom that radiation suffers over time.

The age of the universe is greater for a model that includes dark energy (in a significant abundance) than for a matter or radiation-dominated model, because the expansion rate is accelerating [12]. It is also highly dependent on the Hubble constant. We obtained the values $t_0^{Maj} \simeq 13.87$ Gyrs and $t_0^{Dir} \simeq 13.86$ Gyrs, consistent with the error margins of recent measurements (13.77 ± 0.13 Gyrs [11]).

Despite approximating the chemical potentials to zero in §5.2.1 being quite reasonable, our simulation could improve by an approach where they are accounted. The simulation would also benefit from more precise estimations of the end of the inflation.

Summarizing this work, we realize how much we can predict from standard cosmology by looking at all the consistent information we can get on the history of the universe. The numerical analyses were performed in *Maple* [50]. We also realize that to write a complete thermal history version we need far more ingredients than we currently have at our disposal.

Hence we conclude that insights on the processes involved in the Planck scale universe or a successful GUT are crucial to understand the subsequent stages of the world we are in. Fortunately, we live in exciting times regarding scientific discoveries and there is no doubt that we, the result of such a complex and majestic process with almost 14 billion years, will try as hard as possible to understand our own evolution.

Appendix A

Maple Simulation

> *restart*

> *# Constants:*

> $gs := \left(\dfrac{4}{11}\right); eV := 1.60217646 \cdot 10^{-19}; k_B := 1.3806504 \cdot 10^{-23}; G := 6.674287 \cdot 10^{-11}; \hbar := 1.054571726 \cdot 10^{-34}; c$
> $:= 299792458; H_0 := \dfrac{70.4 \cdot 10^3}{3.08567758 \cdot 10^{22}};$

> $m_{Pl} := 1.2209 \cdot 10^{19} \cdot 10^9 \cdot eV; m_e := 0.510998928 \cdot 10^6 \cdot eV; m_{mu} := 105.65837 \cdot 10^6 \cdot eV; m_{pion} := 139.5701 \cdot 10^6 \cdot eV; Tc$
> $:= 200 \cdot 10^6 \cdot eV; m_s := 483 \cdot 10^6 \cdot eV; m_{charm} := 1.275 \cdot 10^9 \cdot eV; m_{tau} := 1.77682 \cdot 10^9 \cdot eV; m_b := 4.65 \cdot 10^9 \cdot eV; m_{W,Z}$
> $:= 91.1876 \cdot 10^9 \cdot eV; m_H := 126 \cdot 10^9 \cdot eV; m_{top} := 173.5 \cdot 10^9 \cdot eV; \#Particle\ masses$

> $\Omega_{Lambda} := 0.725; \Omega_k := -0.0111; \ \Omega_b := 0.0451; \Omega_{cdm} := 0.226; T_{mat} := \dfrac{T_{rad}^2}{3000}; T_{rad} := 2.725;$
> *#Presently known density parameters and temperature*

> $\Omega_{gamma} := evalf\left(\dfrac{\pi^2}{30}\left(\dfrac{8}{4}\right) \cdot \dfrac{\dfrac{(k_B \cdot T_{rad})^4}{\hbar^3 \cdot c^5}}{\dfrac{3 \cdot H_0^2}{8\,\pi\,G}} \right); \#Present\ density\ parameter\ of\ photons$

> $\Omega_{nu,\,Maj} := evalf\left(\dfrac{\pi^2}{30}\left(\dfrac{21}{4}\right) \cdot \dfrac{\dfrac{(k_B \cdot gs^{\frac{1}{3}} T_{rad})^4}{\hbar^3 \cdot c^5}}{\dfrac{3 \cdot H_0^2}{8\,\pi\,G}} \right); \#Present\ density\ parameter\ of\ Majorana\ neutrinos$

> $\Omega_{nu,\,Dir} := evalf\left(\dfrac{\pi^2}{30}\left(\dfrac{42}{4}\right) \cdot \dfrac{\dfrac{(k_B \cdot gs^{\frac{1}{3}} T_{rad})^4}{\hbar^3 \cdot c^5}}{\dfrac{3 \cdot H_0^2}{8\,\pi\,G}} \right); \#Present\ density\ parameter\ of\ Dirac\ neutrinos$

> $\Omega_{r,\,Maj} := evalf\left(\left(\dfrac{4}{11}\right)^{\frac{1}{3}} \cdot \Omega_{gamma} + \Omega_{\nu,\,Maj} \right); \#Density\ parameter\ of\ radiation\ before\ e^{\pm}\ annihilation,$
> *considering neutrinos as Majorana particles*

> $\Omega_{r,\,Dir} := evalf\left(\left(\dfrac{4}{11}\right)^{\frac{1}{3}} \cdot \Omega_{gamma} + \Omega_{\nu,\,Dir} \right); \#Density\ parameter\ of\ radiation\ before\ e^{\pm}\ annihilation,$
> *considering neutrinos as Dirac particles*

> $\Omega_{r0,\,Maj} := \Omega_\gamma + \Omega_{\nu,\,Maj}; \#Present\ density\ parameter\ of\ radiation,\ considering\ neutrinos\ as\ Majorana\ fermions$

> $\Omega_{r0,\,Dir} := \Omega_\gamma + \Omega_{\nu,\,Dir}; \#Present\ density\ parameter\ of\ radiation,\ considering\ neutrinos\ as\ Dirac\ fermions$

> $\Omega_{r2,\,Maj} := evalf\left(\left(\dfrac{43}{57} \cdot \dfrac{4}{11}\right)^{\frac{1}{3}} \cdot \Omega_{gamma} + \left(\dfrac{43}{57}\right)^{\frac{1}{3}} \cdot \Omega_{\nu,\,Maj} \right); \#Density\ parameter\ of\ radiation\ for\ m_\mu < T < m_\pi,$
> *considering neutrinos as Majorana fermions*

> $\Omega_{r2,\,Dir} := evalf\left(\left(\dfrac{64}{78} \cdot \dfrac{4}{11}\right)^{\frac{1}{3}} \cdot \Omega_{gamma} + \left(\dfrac{64}{78}\right)^{\frac{1}{3}} \cdot \Omega_{\nu,\,Dir} \right); \#Density\ parameter\ of\ radiation\ for\ m_\mu < T < m_\pi,$
> *considering neutrinos as Dirac fermions*

> $\Omega_{r3, Maj} := evalf\left(\left(\dfrac{43}{69}\cdot\dfrac{4}{11}\right)^{\frac{1}{3}}\cdot\Omega_{gamma} + \left(\dfrac{43}{69}\right)^{\frac{1}{3}}\cdot\Omega_{\nu, Maj}\right);$ *#Density parameter of radiation for* $m_\pi < T < T_c$, *considering neutrinos as Majorana fermions*

> $\Omega_{r3, Dir} := evalf\left(\left(\dfrac{64}{90}\cdot\dfrac{4}{11}\right)^{\frac{1}{3}}\cdot\Omega_{gamma} + \left(\dfrac{64}{90}\right)^{\frac{1}{3}}\Omega_{\nu, Dir}\right);$ *#Density parameter of radiation for* $m_\pi < T < T_c$, *considering neutrinos as* Dirac *fermions*

> $\Omega_{r4, Maj} := evalf\left(\left(\dfrac{43}{205}\cdot\dfrac{4}{11}\right)^{\frac{1}{3}}\cdot\Omega_{gamma} + \left(\dfrac{43}{205}\right)^{\frac{1}{3}}\Omega_{\nu, Maj}\right);$ *#Density parameter of radiation for* $T_c < T < m_s$, *considering neutrinos as Majorana fermions*

> $\Omega_{r4, Dir} := evalf\left(\left(\dfrac{64}{226}\cdot\dfrac{4}{11}\right)^{\frac{1}{3}}\cdot\Omega_{gamma} + \left(\dfrac{64}{226}\right)^{\frac{1}{3}}\Omega_{\nu, Dir}\right);$ *#Density parameter of radiation for* $T_c < T < m_s$, *considering neutrinos as Dirac fermions*

> $\Omega_{r5, Maj} := evalf\left(\left(\dfrac{43}{247}\cdot\dfrac{4}{11}\right)^{\frac{1}{3}}\cdot\Omega_{gamma} + \left(\dfrac{43}{247}\right)^{\frac{1}{3}}\Omega_{\nu, Maj}\right);$ *#Density parameter of radiation for* $m_s < T < m_c$, *considering neutrinos as Majorana fermions*

> $\Omega_{r5, Dir} := evalf\left(\left(\dfrac{64}{268}\cdot\dfrac{4}{11}\right)^{\frac{1}{3}}\cdot\Omega_{gamma} + \left(\dfrac{64}{268}\right)^{\frac{1}{3}}\Omega_{\nu, Dir}\right);$ *#Density parameter of radiation for* $m_s < T < m_c$, *considering neutrinos as Dirac fermions*

> $\Omega_{r6, Maj} := evalf\left(\left(\dfrac{43}{289}\cdot\dfrac{4}{11}\right)^{\frac{1}{3}}\cdot\Omega_{gamma} + \left(\dfrac{43}{289}\right)^{\frac{1}{3}}\Omega_{\nu, Maj}\right);$ *#Density parameter of radiation for* $m_c < T < m_\tau$, *considering neutrinos as Majorana fermions*

> $\Omega_{r6, Dir} := evalf\left(\left(\dfrac{64}{310}\cdot\dfrac{4}{11}\right)^{\frac{1}{3}}\cdot\Omega_{gamma} + \left(\dfrac{64}{310}\right)^{\frac{1}{3}}\Omega_{\nu, Dir}\right);$ *#Density parameter of radiation for* $m_c < T < m_\tau$, *considering neutrinos as Dirac fermions*

> $\Omega_{r7, Maj} := evalf\left(\left(\dfrac{43}{303}\cdot\dfrac{4}{11}\right)^{\frac{1}{3}}\cdot\Omega_{gamma} + \left(\dfrac{43}{303}\right)^{\frac{1}{3}}\Omega_{\nu, Maj}\right);$ *#Density parameter of radiation for* $m_\tau < T < m_b$, *considering neutrinos as Majorana fermions*

> $\Omega_{r7, Dir} := evalf\left(\left(\dfrac{64}{324}\cdot\dfrac{4}{11}\right)^{\frac{1}{3}}\cdot\Omega_{gamma} + \left(\dfrac{64}{324}\right)^{\frac{1}{3}}\Omega_{\nu, Dir}\right);$ *#Density parameter of radiation for* $m_\tau < T < m_b$, *considering neutrinos as Dirac fermions*

> $\Omega_{r8, Maj} := evalf\left(\left(\dfrac{43}{345}\cdot\dfrac{4}{11}\right)^{\frac{1}{3}}\cdot\Omega_{gamma} + \left(\dfrac{43}{345}\right)^{\frac{1}{3}}\Omega_{\nu, Maj}\right);$ *#Density parameter of radiation for* $m_b < T < m_{W, Z}$, *considering neutrinos as Majorana fermions*

> $\Omega_{r8, Dir} := evalf\left(\left(\dfrac{64}{366}\cdot\dfrac{4}{11}\right)^{\frac{1}{3}}\cdot\Omega_{gamma} + \left(\dfrac{64}{366}\right)^{\frac{1}{3}}\Omega_{\nu, Dir}\right);$ *#Density parameter of radiation for* $m_b < T < m_{W, Z}$, *considering neutrinos as Dirac fermions*

> $\Omega_{r9, Maj} := evalf\left(\left(\dfrac{43}{381}\cdot\dfrac{4}{11}\right)^{\frac{1}{3}}\cdot\Omega_{gamma} + \left(\dfrac{43}{381}\right)^{\frac{1}{3}}\Omega_{\nu, Maj}\right);$ *#Density parameter of radiation for* $m_{W, Z} < T$

$< m_{H'}$ considering neutrinos as Majorana fermions

> $\Omega_{r9,\,Dir} := evalf\left(\left(\dfrac{64}{402} \cdot \dfrac{4}{11}\right)^{\frac{1}{3}} \cdot \Omega_{gamma} + \left(\dfrac{64}{402}\right)^{\frac{1}{3}} \Omega_{\nu,\,Dir}\right);$ #Density parameter of radiation for $m_{W,\,Z} < T$
$< m_{H'}$ considering neutrinos as Dirac fermions

> $\Omega_{r10,\,Maj} := evalf\left(\left(\dfrac{43}{385} \cdot \dfrac{4}{11}\right)^{\frac{1}{3}} \cdot \Omega_{gamma} + \left(\dfrac{43}{385}\right)^{\frac{1}{3}} \Omega_{\nu,\,Maj}\right);$ #Density parameter of radiation for $m_H < T$
$< m_t$, considering neutrinos as Majorana fermions

> $\Omega_{r10,\,Dir} := evalf\left(\left(\dfrac{64}{406} \cdot \dfrac{4}{11}\right)^{\frac{1}{3}} \cdot \Omega_{gamma} + \left(\dfrac{64}{406}\right)^{\frac{1}{3}} \Omega_{\nu,\,Dir}\right);$ #Density parameter of radiation for $m_H < T < m_t$,
considering neutrinos as Dirac fermions

> $\Omega_{r11,\,Maj} := evalf\left(\left(\dfrac{43}{427} \cdot \dfrac{4}{11}\right)^{\frac{1}{3}} \cdot \Omega_{gamma} + \left(\dfrac{43}{427}\right)^{\frac{1}{3}} \Omega_{\nu,\,Maj}\right);$ #Density parameter of radiation for $m_t < T$,
considering neutrinos as Majorana fermions

> $\Omega_{r11,\,Dir} := evalf\left(\left(\dfrac{64}{448} \cdot \dfrac{4}{11}\right)^{\frac{1}{3}} \cdot \Omega_{gamma} + \left(\dfrac{64}{448}\right)^{\frac{1}{3}} \Omega_{\nu,\,Dir}\right);$ #Density parameter of radiation for $m_t < T$,
considering neutrinos as Dirac fermions

> $\Omega_m := \Omega_b + \Omega_{cdm};$ #Present density parameter of matter

> #Q(t) numerically computed, with initial conditions miming the end of inflation and a density parameter of radiation
valid before $e^{\pm}$ annihilation :

> $eq_Q(Om) := diff(Q(t), t) = \left(\dfrac{\Omega_m}{Q(t)} + \Omega_\Lambda \cdot Q(t)^2 + \dfrac{Om}{Q(t)^2} + \Omega_k\right)^{\frac{1}{2}};$

> $solution1 := dsolve\left(\left\{eq_Q\left(\Omega_{r,\,Maj}\right), Q(10^{-54}) = 10^{-27}\right\}, numeric, abserr = 1.\,10^{-30}, relerr = 10^{-13}, output = listprocedure, maxfun = 5000000\right);$

> $sol_{Q1} := rhs(solution1[2]);$

> #Radiation temperature

> $N_r(Q, Om, S) := piecewise\left(k_B \cdot \dfrac{\left(\dfrac{90 \cdot H_0^2 \cdot \hbar^3 \cdot c^5}{8 \cdot \pi^3 \cdot G \cdot \left(\dfrac{8}{4}\right) \cdot k_B^4} \cdot Om\right)^{\frac{1}{4}}}{Q} \le m_e, 8, \, m_e < k_B \cdot\right.$

$\cdot \dfrac{\left(\dfrac{90 \cdot H_0^2 \cdot \hbar^3 \cdot c^5}{8 \cdot \pi^3 \cdot G \cdot \left(\dfrac{43}{4}\right) \cdot k_B^4} \cdot Om\right)^{\frac{1}{4}}}{Q} \le m_\mu, 43, m_\mu < k_B \cdot \dfrac{\left(\dfrac{90 \cdot H_0^2 \cdot \hbar^3 \cdot c^5}{8 \cdot \pi^3 \cdot G \cdot \left(\dfrac{57}{4}\right) \cdot k_B^4} \cdot Om\right)^{\frac{1}{4}}}{Q} \le m_{pion}, 57, m_{pion} < k_B \cdot$

$\cdot \dfrac{\left(\dfrac{90 \cdot H_0^2 \cdot \hbar^3 \cdot c^5}{8 \cdot \pi^3 \cdot G \cdot \left(\dfrac{69}{4}\right) \cdot k_B^4} \cdot Om\right)^{\frac{1}{4}}}{Q} \le Tc, 69, Tc < k_B \cdot \dfrac{\left(\dfrac{90 \cdot H_0^2 \cdot \hbar^3 \cdot c^5}{8 \cdot \pi^3 \cdot G \cdot \left(\dfrac{205}{4}\right) \cdot k_B^4} \cdot Om\right)^{\frac{1}{4}}}{Q} \le m_s, 205, m_s < k_B$

$$\cdot \frac{\left(\dfrac{90 \cdot H_0^2 \cdot \hbar^3 \cdot c^5}{8 \cdot \pi^3 \cdot G \cdot \left(\dfrac{247}{4} \right) \cdot k_B^4} \cdot Om \right)^{\frac{1}{4}}}{Q} \leq m_{charm}, 247, m_{charm} < k_B \cdot \frac{\left(\dfrac{90 \cdot H_0^2 \cdot \hbar^3 \cdot c^5}{8 \cdot \pi^3 \cdot G \cdot \left(\dfrac{289}{4} \right) \cdot k_B^4} \cdot Om \right)^{\frac{1}{4}}}{Q} \leq m_\tau,$$

$$289, m_\tau < k_B \cdot \frac{\left(\dfrac{90 \cdot H_0^2 \cdot \hbar^3 \cdot c^5}{8 \cdot \pi^3 \cdot G \cdot \left(\dfrac{303}{4} \right) \cdot k_B^4} \cdot Om \right)^{\frac{1}{4}}}{Q} \leq m_b, 303, m_b < k_B \cdot \frac{\left(\dfrac{90 \cdot H_0^2 \cdot \hbar^3 \cdot c^5}{8 \cdot \pi^3 \cdot G \cdot \left(\dfrac{345}{4} \right) \cdot k_B^4} \cdot Om \right)^{\frac{1}{4}}}{Q}$$

$$\leq m_{W,Z}, 345, m_{W,Z} < k_B \cdot \frac{\left(\dfrac{90 \cdot H_0^2 \cdot \hbar^3 \cdot c^5}{8 \cdot \pi^3 \cdot G \cdot \left(\dfrac{381}{4} \right) \cdot k_B^4} \cdot Om \right)^{\frac{1}{4}}}{Q} \leq m_H, 381, m_H < k_B$$

$$\cdot \frac{\left(\dfrac{90 \cdot H_0^2 \cdot \hbar^3 \cdot c^5}{8 \cdot \pi^3 \cdot G \cdot \left(\dfrac{385}{4} \right) \cdot k_B^4} \cdot Om \right)^{\frac{1}{4}}}{Q} \leq m_{top}, 385, m_{top} < k_B \cdot \frac{\left(\dfrac{90 \cdot H_0^2 \cdot \hbar^3 \cdot c^5}{8 \cdot \pi^3 \cdot G \cdot \left(\dfrac{427}{4} \right) \cdot k_B^4} \cdot Om \right)^{\frac{1}{4}}}{Q}, 427, S \Bigg);$$

#effective number of degrees of freedom for radiation, considering neutrinos as Majorana fermions

$$> step_r(Q, Om) := \left(\frac{90 \cdot H_0^2 \cdot \hbar^3 \cdot c^5 \cdot 4}{8 \cdot \pi^3 \cdot G \cdot k_B^4} \cdot \frac{Om}{Q^4} \right) \cdot piecewise\left(k_B \cdot \frac{\left(\dfrac{90 \cdot H_0^2 \cdot \hbar^3 \cdot c^5}{8 \cdot \pi^3 \cdot G \cdot \left(\dfrac{43}{4} \right) \cdot k_B^4} \cdot Om \right)^{\frac{1}{4}}}{Q} < m_e, \left(\frac{k_B}{m_e} \right)^4, k_B \right.$$

$$\cdot \frac{\left(\dfrac{90 \cdot H_0^2 \cdot \hbar^3 \cdot c^5}{8 \cdot \pi^3 \cdot G \cdot \left(\dfrac{57}{4} \right) \cdot k_B^4} \cdot Om \right)^{\frac{1}{4}}}{Q} < m_{mu}, \left(\frac{k_B}{m_{mu}} \right)^4, k_B \cdot \frac{\left(\dfrac{90 \cdot H_0^2 \cdot \hbar^3 \cdot c^5}{8 \cdot \pi^3 \cdot G \cdot \left(\dfrac{69}{4} \right) \cdot k_B^4} \cdot Om \right)^{\frac{1}{4}}}{Q} < m_{pion},$$

$$\left(\frac{k_B}{m_{pion}} \right)^4, k_B \cdot \frac{\left(\dfrac{90 \cdot H_0^2 \cdot \hbar^3 \cdot c^5}{8 \cdot \pi^3 \cdot G \cdot \left(\dfrac{205}{4} \right) \cdot k_B^4} \cdot Om \right)^{\frac{1}{4}}}{Q} < Tc, \left(\frac{k_B}{Tc} \right)^4, k_B \cdot \frac{\left(\dfrac{90 \cdot H_0^2 \cdot \hbar^3 \cdot c^5}{8 \cdot \pi^3 \cdot G \cdot \left(\dfrac{247}{4} \right) \cdot k_B^4} \cdot Om \right)^{\frac{1}{4}}}{Q}$$

$$< m_s, \left(\frac{k_B}{m_s} \right)^4, k_B \cdot \frac{\left(\dfrac{90 \cdot H_0^2 \cdot \hbar^3 \cdot c^5}{8 \cdot \pi^3 \cdot G \cdot \left(\dfrac{289}{4} \right) \cdot k_B^4} \cdot Om \right)^{\frac{1}{4}}}{Q} < m_{charm}, \left(\frac{k_B}{m_{charm}} \right)^4, k_B$$

$$\cdot \frac{\left(\dfrac{90 \cdot H_0^2 \cdot \hbar^3 \cdot c^5}{8 \cdot \pi^3 \cdot G \cdot \left(\dfrac{303}{4} \right) \cdot k_B^4} \cdot Om \right)^{\frac{1}{4}}}{Q} < m_\tau, \left(\frac{k_B}{m_{tau}} \right)^4, k_B \cdot \frac{\left(\dfrac{90 \cdot H_0^2 \cdot \hbar^3 \cdot c^5}{8 \cdot \pi^3 \cdot G \cdot \left(\dfrac{345}{4} \right) \cdot k_B^4} \cdot Om \right)^{\frac{1}{4}}}{Q} < m_b, \left(\frac{k_B}{m_b} \right)^4,$$

$$k_B \cdot \frac{\left(\dfrac{90 \cdot H_0^2 \cdot \hbar^3 \cdot c^5}{8 \cdot \pi^3 \cdot G \cdot \left(\dfrac{381}{4} \right) \cdot k_B^4} \cdot Om \right)^{\frac{1}{4}}}{Q} < m_{W,Z}, \left(\frac{k_B}{m_{W,Z}} \right)^4, k_B \cdot \frac{\left(\dfrac{90 \cdot H_0^2 \cdot \hbar^3 \cdot c^5}{8 \cdot \pi^3 \cdot G \cdot \left(\dfrac{385}{4} \right) \cdot k_B^4} \cdot Om \right)^{\frac{1}{4}}}{Q} < m_H,$$

$$\left(\frac{k_B}{m_H} \right)^4, k_B \cdot \frac{\left(\dfrac{90 \cdot H_0^2 \cdot \hbar^3 \cdot c^5}{8 \cdot \pi^3 \cdot G \cdot \left(\dfrac{427}{4} \right) \cdot k_B^4} \cdot Om \right)^{\frac{1}{4}}}{Q} < m_{top}, \left(\frac{k_B}{m_{top}} \right)^4 \Bigg);$$

#Function that simulates the passage between the steps of radiation, considering neutrinos as Majorana fermions

> $Temp(g, Q, Om) := \left(\dfrac{90 \cdot H_0^2 \cdot \hbar^3 \cdot c^5}{8 \cdot \pi^3 \cdot G \cdot \left(\dfrac{g}{4} \right) \cdot k_B^4} \cdot Om \right)^{\frac{1}{4}} \cdot \dfrac{1}{Q}$; *#General form of the temperature of radiation with respect*

  ***to** N, Q and Ω*

> $T_{r1}(t) := Temp\left(N_r\left(sol_{Q1}(t), \Omega_{r,Maj}, step_r\left(sol_{Q1}(t), \Omega_{r,Maj} \right) \right), sol_{Q1}(t), \Omega_{r,Maj} \right)$
  #Radiation temperature over time for $sol_{Q1}(t)$, considering neutrinos as Majorana fermions

> $T_{r1,e}(t) := \left(\dfrac{90 \cdot H_0^2 \cdot \hbar^3 \cdot c^5}{8 \cdot \pi^3 \cdot G \cdot \left(\dfrac{8}{4} \right) \cdot k_B^4} \cdot \Omega_{r,Maj} \right)^{\frac{1}{4}} \cdot \dfrac{1}{sol_{Q1}(t)}$;

  #simulation of the radiation temperature with the effective degrees of freedom of photons, considering neutrinos as Majorana fermions

> $T_{r1,mu}(t) := \left(\dfrac{90 \cdot H_0^2 \cdot \hbar^3 \cdot c^5}{8 \cdot \pi^3 \cdot G \cdot \left(\dfrac{43}{4} \right) \cdot k_B^4} \cdot \Omega_{r,Maj} \right)^{\frac{1}{4}} \cdot \dfrac{1}{sol_{Q1}(t)}$;

  #simulation of the radiation temperature with the effective degrees of freedom of photons, electrons, positrons and neutrinos, considering neutrinos as Majorana fermions

> $plot\left(\left[T_{r1}(t), T_{r1,e}(t), T_{r1,mu}(t), \dfrac{m_e}{k_B}, \right], t = 10^{-16} .. 10^{-18}, labels = [\ t\ , "T(t)"], color = [red, blue, green, orange], \right.$

  $\left. linestyle = [solid, dot, dot, dot], axis = [mode = \log], legend = \left["T_r(t)", "T_r^e(t)", "T_r^\mu(t)", "m_e" \right] \right);$ *#fig.1*

> $\dfrac{m_e}{k_B}$; $evalf\left(T_{r1}\left(6.45 \cdot 10^{-18} \right) \right)$; *#Obtaining the time when the density parameter of radiation changes*

> $te := 6.45 \cdot 10^{-18}$ *#Defining the time when the electron threshold is reached*

> $\Omega_2(t) := piecewise\left(t < te, \Omega_{r,Maj}, \Omega_\gamma \right)$;

  #Density parameter of radiation divided into a part after and before $e^\pm$ annihilation, considering neutrinos as Majorana fermions

> *#Q(t) with a radiation density parameter appropriate for $t > t_e$, considering neutrinos as Majorana fermions*

> $solution0 := dsolve\left(\left\{ eq_Q\left(\Omega_{r0,Maj} \right), Q(te) = sol_{Q1}(te) \right\}, numeric, abserr = 1.\,10^{-30}, relerr = 10^{-13}, output \right.$
  $\left. = listprocedure, maxfun = 5000000 \right);$

> $sol_{Q0} := rhs(solution0[2])$;

> $sol_{Q0}(0.998309931339387)$; *#Obtaining the present time value*

> $t_0 := 0.998309931339387$ #Defining the present time value

> $q_2(t) := piecewise(t < te, sol_{Q1}(t), sol_{Q0}(t));$ #Scale factor divided into a part after and before $e^{\pm}$ annihilation, considering neutrinos as Majorana fermions

> $plot([q_2(t)], t = 10^{-50}..1, labels = [t, Q(t)], axis = [mode = \log], legend = "Q(t)")$ #fig. 2

> $plot([sol_{Q1}(t), q_2(t)], t = 10^{-18}..10^{-15}, labels = [t, Q(t)], axis = [mode = \log]);$ #fig.3

> $T_{r2}(t) := Temp(N_r(q_2(t), \Omega_2(t), step_r(q_2(t), \Omega_2(t))), q_2(t), \Omega_2(t));$
  #Radiation temperature over time for Q(t) and $\Omega_2(t)$ divided into 2 regions, considering neutrinos as Majorana fermions

> $plot([T_{r1}(t), T_{r2}(t)], t = 10^{-16}..10^{-18}, labels = [t, "T(t)"], color = [red, blue, green, orange], axis = [mode = \log]);$ #fig. 6

> $evalf(T_{r2}(t_0)); evalf(T_{r1}(t_0))$ #Difference between the 2 approaches on the present radiation temperature

> #Obtaining the time when annihilation of species occur and the baryonic component of matter originates, considering neutrinos as Majorana fermions

> $\dfrac{m_{mu}}{k_B}; evalf(T_{r2}(1.32 \cdot 10^{-22}));$

> $\dfrac{m_{pion}}{k_B}; evalf(T_{r2}(7.5 \cdot 10^{-23}));$

> $\dfrac{Tc}{k_B}; evalf(T_{r2}(1.99 \cdot 10^{-23}));$

> $\dfrac{m_s}{k_B}; evalf(T_{r2}(3.305 \cdot 10^{-24}));$

> $\dfrac{m_{charm}}{k_B}; evalf(T_{r2}(4.32 \cdot 10^{-25}));$

> $\dfrac{m_{tau}}{k_B}; evalf(T_{r2}(2 \cdot 10^{-25}));$

> $\dfrac{m_b}{k_B}; evalf(T_{r2}(2.93 \cdot 10^{-26}));$

> $\dfrac{m_{W,Z}}{k_B}; evalf(T_{r2}(7.15 \cdot 10^{-29}));$

> $\dfrac{m_H}{k_B}; evalf(T_{r2}(3.55 \cdot 10^{-29}));$

> $\dfrac{m_{top}}{k_B}; evalf(T_{r2}(1.869 \cdot 10^{-29}));$

> $tm := 1.32 \cdot 10^{-22}; tp := 7.5 \cdot 10^{-23}; tTc := 1.99 \cdot 10^{-23}; ts := 3.305 \cdot 10^{-24}; tc := 4.32 \cdot 10^{-25}; tta := 2 \cdot 10^{-25}; tb := 2.93 \cdot 10^{-26}; tWZ := 7.15 \cdot 10^{-29}; tH := 3.55 \cdot 10^{-29}; tto := 1.869 \cdot 10^{-29};$
  #Defining the time when each species threshold is reached

> #Defining Q(t) through a set of solutions of differential equations with the radiation density parameter appropriate to each time range, considering neutrinos as Majorana fermions :

> $solution11 := dsolve(\{eq_Q(\Omega_{r11, Maj}), Q(10^{-54}) = 10^{-27}\}, numeric, abserr = 1. \, 10^{-30}, relerr = 10^{-13}, output = listprocedure, maxfun = 5000000)$

> $sol_{Q11} := rhs(solution11[2]);$

> $solution10 := dsolve(\{eq_Q(\Omega_{r10, Maj}), Q(tto) = sol_{Q11}(tto)\}, numeric, abserr = 1. \, 10^{-30}, relerr = 10^{-13}, output$

```
                  = listprocedure, maxfun = 5000000 )
> sol_Q10 := rhs( solution10[ 2 ] );
> solution9 := dsolve( { eq_Q( Ω_{r9, Maj} ) , Q( tH ) = sol_Q10( tH ) }, numeric, abserr = 1. 10^{-30}, relerr = 10^{-13}, output
                  = listprocedure, maxfun = 5000000 )
> sol_Q9 := rhs( solution9[ 2 ] );
> solution8 := dsolve( { eq_Q( Ω_{r8, Maj} ) , Q( tWZ ) = sol_Q9( tWZ ) }, numeric, abserr = 1. 10^{-30}, relerr = 10^{-13}, output
                  = listprocedure, maxfun = 5000000 )
> sol_Q8 := rhs( solution8[ 2 ] );
> solution7 := dsolve( { eq_Q( Ω_{r7, Maj} ) , Q( tb ) = sol_Q8( tb ) }, numeric, abserr = 1. 10^{-30}, relerr = 10^{-13}, output
                  = listprocedure, maxfun = 5000000 )
> sol_Q7 := rhs( solution7[ 2 ] );
> solution6 := dsolve( { eq_Q( Ω_{r6, Maj} ) , Q( tta ) = sol_Q7( tta ) }, numeric, abserr = 1. 10^{-30}, relerr = 10^{-13}, output
                  = listprocedure, maxfun = 5000000 )
> sol_Q6 := rhs( solution6[ 2 ] );
> solution5 := dsolve( { eq_Q( Ω_{r5, Maj} ) , Q( tc ) = sol_Q6( tc ) }, numeric, abserr = 1. 10^{-30}, relerr = 10^{-13}, output
                  = listprocedure, maxfun = 5000000 )
> sol_Q5 := rhs( solution5[ 2 ] );
> solution4 := dsolve( { eq_Q( Ω_{r4, Maj} ) , Q( ts ) = sol_Q5( ts ) }, numeric, abserr = 1. 10^{-30}, relerr = 10^{-13}, output
                  = listprocedure, maxfun = 5000000 )
> sol_Q4 := rhs( solution4[ 2 ] );
> solution3 := dsolve( { eq_Q( Ω_{r3, Maj} ) , Q( tTc ) = sol_Q4( tTc ) }, numeric, abserr = 1. 10^{-30}, relerr = 10^{-13}, output
                  = listprocedure, maxfun = 5000000 )
> sol_Q3 := rhs( solution3[ 2 ] );
> solution2 := dsolve( { eq_Q( Ω_{r2, Maj} ) , Q( tp ) = sol_Q3( tp ) }, numeric, abserr = 1. 10^{-30}, relerr = 10^{-13}, output
                  = listprocedure, maxfun = 5000000 )
> sol_Q2 := rhs( solution2[ 2 ] );
> solution := dsolve( { eq_Q( Ω_{r, Maj} ) , Q( tm ) = sol_Q2( tm ) }, numeric, abserr = 1. 10^{-30}, relerr = 10^{-13}, output
                  = listprocedure, maxfun = 5000000 )
> sol_Q := rhs( solution[ 2 ] );
> q_{12}( t ) := piecewise( t ≤ tto, sol_Q11( t ), tto < t ≤ tH, sol_Q10( t ), tH < t ≤ tWZ, sol_Q9( t ), tWZ < t ≤ tb, sol_Q8( t ), tb < t
                  ≤ tta, sol_Q7( t ), tta < t ≤ tc, sol_Q6( t ), tc < t ≤ ts, sol_Q5( t ), ts < t ≤ tTc, sol_Q4( t ), tTc < t ≤ tp, sol_Q3( t ), tp < t
                  ≤ tm, sol_Q2( t ), tm < t ≤ te, sol_Q( t ), te < t, sol_Q0( t ) )
> plot( [ q_2( t ), q_{12}( t ) ], t = 10^{-29} ..10^{-16}, labels = [ t , Q( t ) ], axis = [ mode = log ] );#fig. 4
> Ω_{12}( t ) := piecewise( t ≤ tto, Ω_{r11, Maj}, tto < t ≤ tH, Ω_{r10, Maj}, tH < t ≤ tWZ, Ω_{r9, Maj}, tWZ < t ≤ tb, Ω_{r8, Maj}, tb < t
                  ≤ tta, Ω_{r7, Maj}, tta < t ≤ tc, Ω_{r6, Maj}, tc < t ≤ ts, Ω_{r5, Maj}, ts < t ≤ tTc, Ω_{r4, Maj}, tTc < t ≤ tp, Ω_{r3, Maj}, tp < t ≤ tm,
                  Ω_{r2, Maj}, tm < t ≤ te, Ω_{r, Maj}, te < t, Ω_{gamma} );
                  #Radiation density parameter according to the species present in each time range
> T_{r12}( t ) := Temp( N_r( q_{12}( t ), Ω_{12}( t ), step_r( q_{12}( t ), Ω_{12}( t ) ) ), q_{12}( t ), Ω_{12}( t ) );
                  #Radiation temperature divided into 12 ranges
> plot( [ T_{r2}( t ), T_{r12}( t ) ], t = 10^{-16} ..10^{-29}, labels = [ t , "T( t )" ], color = [ red, blue ], axis = [ mode = log ] );#fig. 7
```

> $evalf\left(T_{r2}\left(t_0\right)\right); evalf\left(T_{r12}\left(t_0\right)\right); evalf\left(T_{r2}\left(tto\right)\right); evalf\left(T_{r12}\left(tto\right)\right)$

> $plot\left(\left[T_{r2}(t), \dfrac{m_e}{k_B}, \dfrac{m_{mu}}{k_B}, \dfrac{m_{pion}}{k_B}, \dfrac{Tc}{k_B}, \dfrac{m_s}{k_B}, \dfrac{m_{charm}}{k_B}, \dfrac{m_{tau}}{k_B}, \dfrac{m_b}{k_B}, \dfrac{m_{W,Z}}{k_B}, \dfrac{m_H}{k_B}, \dfrac{m_{top}}{k_B}\right], t = 10^{-16}..10^{-29}, labels\right.$

$\left.= \left[t, "T(t)"\right], linestyle = \left[solid, dot, dot, dot, dot, dot, dash, dash, dash, dash, dash, dash\right], axis = \left[mode = \log\right]\right);$

$\#fig.\ 8$

> $plot\left(\left[T_{r2}(t), \dfrac{m_{mu}}{k_B}, \dfrac{m_{pion}}{k_B}, \dfrac{Tc}{k_B}, \dfrac{m_s}{k_B}\right], t = 10^{-24}..10^{-21}, labels = \left[t, "T(t)"\right], linestyle = \left[solid, dot, dot, dot, dot\right],\right.$

$\left. axis = \left[mode = \log\right], numpoints = 20000\right); \#fig.\ 9$

> $plot\left(\left[T_{r2}(t), \dfrac{m_{charm}}{k_B}, \dfrac{m_{tau}}{k_B}, \dfrac{m_b}{k_B}\right], t = 10^{-24}..10^{-26}, labels = \left[t, "T(t)"\right], linestyle = \left[solid, dot, dot, dot\right], axis\right.$

$\left. = \left[mode = \log\right], numpoints = 20000\right); \#fig.\ 10$

> $plot\left(\left[T_{r2}(t), \dfrac{m_{W,Z}}{k_B}, \dfrac{m_H}{k_B}, \dfrac{m_{top}}{k_B}\right], t = 10^{-28}..10^{-29}, labels = \left[t, "T(t)"\right], linestyle = \left[solid, dot, dot, dot\right], axis\right.$

$\left. = \left[mode = \log\right], numpoints = 2000\right); \#fig.\ 11$

> $\#Maj.\ Neutrino\ Temperature:$

> $\Omega_{nu,\,Maj2}(t) := piecewise\left(t < te, \Omega_{r,\,Maj}, t \geq te, \Omega_{nu,\,Maj}\right);$
$\#Density\ parameter\ of\ Majorana\ neutrinos\ divided\ into\ a\ part\ after\ and\ before\ e^{\pm}\ annihilation$

> $N_{nu,\,Maj2}(Q, Om) := piecewise\left(k_B \cdot \dfrac{\left(\dfrac{90 \cdot H_0^2 \cdot \hbar^3 \cdot c^5}{8 \cdot \pi^3 \cdot G \cdot \left(\dfrac{21}{4}\right) \cdot k_B^4} \cdot Om\right)^{\frac{1}{4}}}{Q} < m_e, 21, N_r\left(Q, Om, step_{nu}(Q, Om)\right)\right);$
$\#effective\ number\ of\ degrees\ of\ freedom\ for\ Majorana\ neutrinos$

> $T_{nu,\,Maj2}(t) := Temp\left(N_{nu,\,Maj2}\left(q_2(t), \Omega_{nu,\,Maj2}(t)\right), q_2(t), \Omega_{nu,\,Maj2}(t)\right);$
$\#Maj.\ neutrino\ temperature\ over\ time\ for\ Q(t)\ and\ \Omega_2(t)\ divided\ into\ 2\ regions$

> $plot\left(\left[T_{nu,\,Maj2}(t), T_{r2}(t)\right], t = 10^{-16}..10^{-18}, labels = \left[t, "T(t)"\right], color = \left[red, blue\right], axis = \left[mode = \log\right]\right);$
$\#fig.\ 13$

> $evalf\left(T_{nu,\,Maj2}\left(t_0\right)\right); \#Confirming\ the\ present\ temperature\ of\ Maj.\ neutrinos$

> $\#Dirac\ Neutrinos:$

> $\Omega_{Dir2}(t) := piecewise\left(t < te, \Omega_{r,\,Dir}, \Omega_\gamma\right);$
$\#Density\ parameter\ of\ radiation\ divided\ into\ a\ part\ after\ and\ before\ e^{\pm}\ annihilation,$
$considering\ neutrinos\ as\ \mathrm{Dirac}\ fermions$

> $solutionD1 := dsolve\left(\left\{eq_Q\left(\Omega_{r,\,Dir}\right), Q\left(10^{-54}\right) = 10^{-27}\right\}, numeric, abserr = 1.\,10^{-30}, relerr = 10^{-13}, output\right.$
$\left. = listprocedure, maxfun = 5000000\right);$

> $sol_{QD1} := rhs(solutionD1[2]);$

> $solutionD0 := dsolve\left(\left\{eq_Q\left(\Omega_{r0,\,Dir}\right), Q(te) = sol_{QD1}(te)\right\}, numeric, abserr = 1.\,10^{-30}, relerr = 10^{-13}, output\right.$
$\left. = listprocedure, maxfun = 5000000\right);$

> $sol_{QD0} := rhs(solutionD0[2]);$

> $q_{D2}(t) := piecewise\left(t < te, sol_{QD1}(t), sol_{QD0}(t)\right); \#Scale\ factor\ divided\ into\ a\ part\ after\ and\ before\ e^{\pm}\ annihilation,$
$considering\ neutrinos\ as\ \mathrm{Dirac}\ fermions$

> $plot\left(\left[q_2(t), q_{D2}(t)\right], t = 10^{-29}..10^{-16}, labels = [t, Q(t)], axis = [mode = \log]\right); \#fig. 5$

> #Radiation temperature:

> $N_{r,Dir}(Q, Om, S) := piecewise\left(k_B \cdot \dfrac{\left(\dfrac{90 \cdot H_0^2 \cdot \hbar^3 \cdot c^5}{8 \cdot \pi^3 \cdot G \cdot \left(\dfrac{8}{4}\right) \cdot k_B^4} \cdot Om\right)^{\frac{1}{4}}}{Q} \leq m_e, 8, \, m_e < k_B \right.$

$\cdot \dfrac{\left(\dfrac{90 \cdot H_0^2 \cdot \hbar^3 \cdot c^5}{8 \cdot \pi^3 \cdot G \cdot \left(\dfrac{64}{4}\right) \cdot k_B^4} \cdot Om\right)^{\frac{1}{4}}}{Q} \leq m_\mu, 64, m_\mu < k_B \cdot \dfrac{\left(\dfrac{90 \cdot H_0^2 \cdot \hbar^3 \cdot c^5}{8 \cdot \pi^3 \cdot G \cdot \left(\dfrac{78}{4}\right) \cdot k_B^4} \cdot Om\right)^{\frac{1}{4}}}{Q} \leq m_{pion}, 78, m_{pion} < k_B$

$\cdot \dfrac{\left(\dfrac{90 \cdot H_0^2 \cdot \hbar^3 \cdot c^5}{8 \cdot \pi^3 \cdot G \cdot \left(\dfrac{90}{4}\right) \cdot k_B^4} \cdot Om\right)^{\frac{1}{4}}}{Q} \leq Tc, 90, Tc < k_B \cdot \dfrac{\left(\dfrac{90 \cdot H_0^2 \cdot \hbar^3 \cdot c^5}{8 \cdot \pi^3 \cdot G \cdot \left(\dfrac{226}{4}\right) \cdot k_B^4} \cdot Om\right)^{\frac{1}{4}}}{Q} \leq m_s, 226, m_s < k_B$

$\cdot \dfrac{\left(\dfrac{90 \cdot H_0^2 \cdot \hbar^3 \cdot c^5}{8 \cdot \pi^3 \cdot G \cdot \left(\dfrac{268}{4}\right) \cdot k_B^4} \cdot Om\right)^{\frac{1}{4}}}{Q} \leq m_{charm}, 268, m_{charm} < k_B \cdot \dfrac{\left(\dfrac{90 \cdot H_0^2 \cdot \hbar^3 \cdot c^5}{8 \cdot \pi^3 \cdot G \cdot \left(\dfrac{310}{4}\right) \cdot k_B^4} \cdot Om\right)^{\frac{1}{4}}}{Q} \leq m_\tau,$

$310, m_\tau < k_B \cdot \dfrac{\left(\dfrac{90 \cdot H_0^2 \cdot \hbar^3 \cdot c^5}{8 \cdot \pi^3 \cdot G \cdot \left(\dfrac{324}{4}\right) \cdot k_B^4} \cdot Om\right)^{\frac{1}{4}}}{Q} \leq m_b, 324, m_b < k_B \cdot \dfrac{\left(\dfrac{90 \cdot H_0^2 \cdot \hbar^3 \cdot c^5}{8 \cdot \pi^3 \cdot G \cdot \left(\dfrac{366}{4}\right) \cdot k_B^4} \cdot Om\right)^{\frac{1}{4}}}{Q}$

$\leq m_{W,Z}, 366, m_{W,Z} < k_B \cdot \dfrac{\left(\dfrac{90 \cdot H_0^2 \cdot \hbar^3 \cdot c^5}{8 \cdot \pi^3 \cdot G \cdot \left(\dfrac{402}{4}\right) \cdot k_B^4} \cdot Om\right)^{\frac{1}{4}}}{Q} \leq m_H, 402, m_H < k_B$

$\cdot \dfrac{\left(\dfrac{90 \cdot H_0^2 \cdot \hbar^3 \cdot c^5}{8 \cdot \pi^3 \cdot G \cdot \left(\dfrac{406}{4}\right) \cdot k_B^4} \cdot Om\right)^{\frac{1}{4}}}{Q} \leq m_{top}, 406, m_{top} < k_B \cdot \dfrac{\left(\dfrac{90 \cdot H_0^2 \cdot \hbar^3 \cdot c^5}{8 \cdot \pi^3 \cdot G \cdot \left(\dfrac{448}{4}\right) \cdot k_B^4} \cdot Om\right)^{\frac{1}{4}}}{Q}, 448, S\right);$

#effective number of degrees of freedom for radiation, considering neutrinos as Dirac fermions

> $step_{r,Dir}(Q, Om) := \left(\dfrac{90 \cdot H_0^2 \cdot \hbar^3 \cdot c^5 \cdot 4}{8 \cdot \pi^3 \cdot G \cdot k_B^4} \cdot \dfrac{Om}{Q^4}\right) \cdot piecewise\left(k_B \cdot \dfrac{\left(\dfrac{90 \cdot H_0^2 \cdot \hbar^3 \cdot c^5}{8 \cdot \pi^3 \cdot G \cdot \left(\dfrac{64}{4}\right) \cdot k_B^4} \cdot Om\right)^{\frac{1}{4}}}{Q} < m_e, \left(\dfrac{k_B}{m_e}\right)^4, k_B\right.$

$$\cdot \frac{\left(\dfrac{90 \cdot H_0^2 \cdot \hbar^3 \cdot c^5}{8 \cdot \pi^3 \cdot G \cdot \left(\dfrac{78}{4} \right) \cdot k_B^4} \cdot Om \right)^{\frac{1}{4}}}{Q} < m_{\text{mu}}, \left(\frac{k_B}{m_{\text{mu}}} \right)^4, k_B \cdot \frac{\left(\dfrac{90 \cdot H_0^2 \cdot \hbar^3 \cdot c^5}{8 \cdot \pi^3 \cdot G \cdot \left(\dfrac{90}{4} \right) \cdot k_B^4} \cdot Om \right)^{\frac{1}{4}}}{Q} < m_{pion},$$

$$\left(\frac{k_B}{m_{pion}} \right)^4, k_B \cdot \frac{\left(\dfrac{90 \cdot H_0^2 \cdot \hbar^3 \cdot c^5}{8 \cdot \pi^3 \cdot G \cdot \left(\dfrac{226}{4} \right) \cdot k_B^4} \cdot Om \right)^{\frac{1}{4}}}{Q} < Tc, \left(\frac{k_B}{Tc} \right)^4, k_B \cdot \frac{\left(\dfrac{90 \cdot H_0^2 \cdot \hbar^3 \cdot c^5}{8 \cdot \pi^3 \cdot G \cdot \left(\dfrac{268}{4} \right) \cdot k_B^4} \cdot Om \right)^{\frac{1}{4}}}{Q}$$

$$< m_s, \left(\frac{k_B}{m_s} \right)^4, k_B \cdot \frac{\left(\dfrac{90 \cdot H_0^2 \cdot \hbar^3 \cdot c^5}{8 \cdot \pi^3 \cdot G \cdot \left(\dfrac{310}{4} \right) \cdot k_B^4} \cdot Om \right)^{\frac{1}{4}}}{Q} < m_{charm}, \left(\frac{k_B}{m_{charm}} \right)^4, k_B$$

$$\cdot \frac{\left(\dfrac{90 \cdot H_0^2 \cdot \hbar^3 \cdot c^5}{8 \cdot \pi^3 \cdot G \cdot \left(\dfrac{324}{4} \right) \cdot k_B^4} \cdot Om \right)^{\frac{1}{4}}}{Q} < m_{\tau}, \left(\frac{k_B}{m_{\text{tau}}} \right)^4, k_B \cdot \frac{\left(\dfrac{90 \cdot H_0^2 \cdot \hbar^3 \cdot c^5}{8 \cdot \pi^3 \cdot G \cdot \left(\dfrac{366}{4} \right) \cdot k_B^4} \cdot Om \right)^{\frac{1}{4}}}{Q} < m_b, \left(\frac{k_B}{m_b} \right)^4,$$

$$k_B \cdot \frac{\left(\dfrac{90 \cdot H_0^2 \cdot \hbar^3 \cdot c^5}{8 \cdot \pi^3 \cdot G \cdot \left(\dfrac{402}{4} \right) \cdot k_B^4} \cdot Om \right)^{\frac{1}{4}}}{Q} < m_{W, Z}, \left(\frac{k_B}{m_{W, Z}} \right)^4, k_B \cdot \frac{\left(\dfrac{90 \cdot H_0^2 \cdot \hbar^3 \cdot c^5}{8 \cdot \pi^3 \cdot G \cdot \left(\dfrac{406}{4} \right) \cdot k_B^4} \cdot Om \right)^{\frac{1}{4}}}{Q} < m_H,$$

$$\left(\frac{k_B}{m_H} \right)^4, k_B \cdot \frac{\left(\dfrac{90 \cdot H_0^2 \cdot \hbar^3 \cdot c^5}{8 \cdot \pi^3 \cdot G \cdot \left(\dfrac{448}{4} \right) \cdot k_B^4} \cdot Om \right)^{\frac{1}{4}}}{Q} < m_{top}, \left(\frac{k_B}{m_{top}} \right)^4 \Bigg);$$

#Function to simulate the passage between the steps of radiation, considering neutrinos as Dirac fermions

$>\quad T_{r, Dir2}(t) := Temp\left(N_{r, Dir}\left(q_{D2}(t), \Omega_{Dir2}(t), step_{r, Dir}\left(q_{D2}(t), \Omega_{Dir2}(t) \right) \right), q_{D2}(t), \Omega_{Dir2}(t) \right);$

#Radiation temperature over time for Q(t) and $\Omega_2(t)$ divided into 2 regions,
considering neutrinos as Dirac fermions

$>\quad plot\left(\left[T_{r2}(t), T_{r, Dir2}(t) \right], t = 10^{-16} .. 10^{-29}, labels = [\, t\, , "T(t)"\,], color = [\, red, blue\,], axis = [\, mode = \log\,] \right); \#fig.\ 12$

$>\quad \dfrac{m_e}{k_B}; evalf\left(T_{r, Dir2}(5.29 \cdot 10^{-18}) \right);$

#Obtaining the time when the density parameter of radiation changes in the Dirac case

$>\quad tDe := 5.29 \cdot 10^{-18}; \#Defining\ the\ time\ when\ the\ electron\ threshold\ is\ reached\ in\ the\ Dirac\ case$

$>\quad$ *#Neutrino Temperature:*

$>\quad \Omega_{\text{nu}, Dir2}(t) := piecewise\left(t < tDe, \Omega_{r, Dir}, t \geq tDe, \Omega_{\text{nu}, Dir} \right);$

#Density parameter of Dirac neutrinos divided into a part after and before $e^{\pm}$ annihilation

> $N_{nu, Dir2}(Q, Om) := piecewise\left(k_B \cdot \dfrac{\left(\dfrac{90 \cdot H_0^2 \cdot \hbar^3 \cdot c^5}{8 \cdot \pi^3 \cdot G \cdot \left(\dfrac{42}{4}\right) \cdot k_B^4} \cdot Om\right)^{\frac{1}{4}}}{Q} \le m_e, 42, N_{r, Dir}(Q, Om, step_{r, Dir}(Q, Om))\right);$
   #effective number of degrees of freedom for Dirac neutrinos

> $T_{nu, Dir2}(t) := Temp\left(N_{nu, Dir2}(q_{D2}(t), \Omega_{nu, Dir2}(t)), q_{D2}(t), \Omega_{nu, Dir2}(t)\right);$ #Dirac neutrino temperature over time
   for $Q(t)$ and $\Omega_2(t)$ divided into 2 regions

> $plot\left(\left[T_{nu, Maj2}(t), T_{r2}(t), T_{nu, Dir2}(t), T_{r, Dir2}(t)\right], t = 10^{-16} ..10^{-18}, labels = [t, "T(t)"], color = [green, blue,$
   $gold, red], linestyle = [solid, solid, dash, dash], axis = [mode = \log]\right);$ #fig. 13

> $q_{D2}(0.998131295538045);$ #Obtaining the present time value

> $t_{D0} := 0.998131295538045;$ #Defining the present time value

> $evalf\left(T_{nu, Dir2}(t_{D0})\right); evalf\left(T_{r, Dir2}(t_{D0})\right);$ #Confirming the present temperature of radiation and neutrinos,
   considering them as Dirac fermions

> $T_m(t) := \dfrac{T_{mat}}{q_2(t)^2};$ #Matter temperature over time (Maj. case)

> #$\Omega(t)$ expressions, considering Maj. neutrinos :

> $\Omega_{r2}(t) := \dfrac{\Omega_2(t)}{q_2(t)^4};$ #radiation contribution divided into 2 regimes

> $\Omega_{r12}(t) := \dfrac{\Omega_{12}(t)}{q_{12}(t)^4};$ #radiation contribution divided into 12 regimes

> $\Omega_{mat}(t) := \dfrac{\Omega_m}{q_2(t)^3};$ #matter contribution

> $\Omega_{DM}(t) := \dfrac{\Omega_{cdm}}{q_2(t)^3};$ #cold dark matter contribution

> $\Omega_M(t) := piecewise\left(tTc < t, \Omega_{mat}(t), \Omega_{DM}(t)\right)$
   #total matter contribution over time, including the baryonic part after T_c

> #Dark matter temperature:
> #WIMPs, from 10 GeV to 1 TeV
> $m_1 := 10 \cdot 10^9 \cdot eV$
> $m_2 := 100 \cdot 10^9 \cdot eV$
> $m_3 := 1000 \cdot 10^9 \cdot eV$
> $m_L := 200 \cdot 10^9 \cdot eV$

> $T_{cd}(M) := \dfrac{M}{k_B \cdot 25};$ #Chemical decoupling of DM

> $T_{kd}(M) := \dfrac{1}{k_B}\left(\dfrac{1.2 \cdot 10^{-2} \cdot m_{Pl}}{M \cdot \left(m_L^2 - M^2\right)^2}\right)^{-\frac{1}{4}};$ #Kinetic decoupling of DM

> $T_{dDM}(M, tkd, t) := \dfrac{T_{kd}(M) \cdot q_{12}(tkd)^2}{q_{12}(t)^2};$ #Temperature of the decoupled dark matter

> $T_{DM}(M, tkd, t) := piecewise\left(t < tkd, T_{r12}(t), tkd \le t, T_{dDM}(M, tkd, t)\right)$ #Dark matter temperature over time

> $T_{cd}(m_1); T_{cd}(m_2); T_{cd}(m_3);$ #Obtaining the dark matter chemical decoupling moment

> $T_{kd}(m_1); T_{kd}(m_2); T_{kd}(m_3);$ #Obtaining the dark matter kinetic decoupling moment

> $evalf(T_{r2}(5.10905 \cdot 10^{-21})); evalf(T_{r2}(2.14878 \cdot 10^{-21})); evalf(T_{r2}(9.7252 \cdot 10^{-24}));$
    #Obtaining the decoupling time of dark matter

> $sol_Q(5.10905 \cdot 10^{-21}); sol_Q(2.14878 \cdot 10^{-21}); sol_Q(9.7252 \cdot 10^{-24})$
    #Obtaining the decoupling scale factor of dark matter

> $tm1 := 5.10905 \cdot 10^{-21}; tm2 := 2.14878 \cdot 10^{-21}; tm3 := 9.7252 \cdot 10^{-24};$ #Defining the decoupling time for each mass

> $T_{DM}(m_1, tm1, t_0); T_{DM}(m_2, tm2, t_0); T_{DM}(m_3, tm3, t_0);$ #Present time temperature of dark matter

> $plot([T_{r12}(t), T_{DM}(m_1, tm1, t), T_{DM}(m_2, tm2, t), T_{DM}(m_3, tm3, t)], t = 10^{-24}..10^{-18}, axis = [mode = \log], labels$
    $= [t, "T(t)"], numpoints = 50000);$ #fig. 14

> $plot([T_{r12}(t), T_m(t)], t = 2.5 \cdot 10^{-5}..3 \cdot 10^{-5}, color = [red, blue], labels = [t, "T(t)"], axis = [mode = \log]);$

> $t_D := fsolve(T_{r12}(t) = T_m(t), t = 2 \cdot 10^{-5}..3 \cdot 10^{-5});$
    #Determining the intersection point of radiation and baryonic matter temperature

> $sol_Q(t_D);$ #Confirming the scale factor at the time when baryonic matter temperature decoupled

> $evalf(T_{r12}(t_D));$ #Temperature at which baryonic matter decoupled

> $T_{bm}(t) := piecewise(t < t_D, T_{r12}(t), T_m(t));$ #Temperature law of baryonic matter over time

> $plot([T_{r12}(t), T_{bm}(t)], t = 2.5 \cdot 10^{-5}..3 \cdot 10^{-5}, color = [red, blue], labels = [t, "T(t)"], axis = [mode = \log]);$
    #fig. 15

> #Density plots

> $plot([\Omega_{r2}(t), \Omega_{r12}(t)], t = 10^{-16}..10^{-29}, labels = [t, "\Omega(t)"], color = [red, blue], axis = [mode = \log],$
    $numpoints = 2000);$ #fig. 16

> $with(plots):$

> $OmA := plot([\Omega_{r2}(t), \Omega_{r12}(t)], t = 10^{-16}..10^{-18}, labels = [t, "\Omega(t)"], axis = [mode = \log], color = [red, blue])$

> $OmB := implicitplot(t = te, t = 10^{-16}..10^{-18}, \Omega = 10^{31}..10^{35.5}, color = green, linestyle = dot)$

> $display(OmA, OmB)$ #fig. 17

> $OmC := plot([\Omega_{r2}(t), \Omega_{r12}(t)], t = 10^{-24}..10^{-21}, labels = [t, "\Omega(t)"], axis = [mode = \log], color = [red, blue])$

> $OmD := implicitplot([t = tm, t = tp, t = tTc, t = ts], t = 10^{-24}..10^{-21}, \Omega = 2.5 \cdot 10^{41}..2.5 \cdot 10^{47}, color = [green, gold,$
    $violet, khaki], linestyle = dot)$

> $display(OmC, OmD);$ #fig. 18

> $OmE := plot([\Omega_{r2}(t), \Omega_{r12}(t)], t = 10^{-24}..10^{-26}, labels = [t, "\Omega(t)"], axis = [mode = \log], color = [red, blue])$

> $OmF := implicitplot([t = tc, t = tta, t = tb], t = 10^{-24}..10^{-26}, \Omega = 2.5 \cdot 10^{47}..2.5 \cdot 10^{51}, color = [green, gold, violet],$
    $linestyle = dot)$

> $display(OmE, OmF);$ #fig. 19

> $OmG := plot([\Omega_{r2}(t), \Omega_{r12}(t)], t = 10^{-28}..10^{-29}, labels = [t, "\Omega(t)"], axis = [mode = \log], color = [red, blue])$

> $OmH := implicitplot([t = tWZ, t = tH, t = tto], t = 10^{-28}..10^{-29}, \Omega = 2.5 \cdot 10^{55}..2.5 \cdot 10^{57}, color = [green, gold, violet],$
    $linestyle = dot)$

> $display(OmG, OmH);$ #fig. 20

> $plot([\Omega_{r12}(t), \Omega_M(t), \Omega_\Lambda], t = 10^{-29}..1, labels = [t, "\Omega(t)"], axis = [mode = \log], color = [red, blue, green],$
    $numpoints = 2000);$ #fig. 21

> $plot(\Omega_M(t), t = 10^{-24}..10^{-22}, labels = [t, "\Omega(t)"], axis = [mode = \log], color = [blue]);$ #fig. 22

> $plot([\Omega_{r12}(t), \Omega_M(t)], t = 10^{-6}..2 \cdot 10^{-6}, labels = [t, "\Omega(t)"], axis = [mode = \log], color = [red, blue]);$ #fig. 23

> $plot([\Omega_{r12}(t), \Omega_M(t), \Omega_\Lambda], t = 10^{-1}..1, labels = [t, "\Omega(t)"], axis = [mode = \log], color = [red, blue, green],$
    $numpoints = 2000);$ #fig. 24

> $Matrad := fsolve\left(\Omega_{r12}(t) = \Omega_M(t),\ t = 10^{-6}\ ..2 \cdot 10^{-6}\right)$
  #*Determining the intersection point of radiation and matter densities*

> $Lambdamat := fsolve\left(\Omega_M(t) = \Omega_\Lambda,\ t = 0.1\ ..1\right)$
  #*Determining the intersection point of matter and dark energy densities*

> #*Converting times from H_0^{-1} into years*

> $Hub := \dfrac{\left(\dfrac{1}{H_0}\right)}{60 \cdot 60 \cdot 24 \cdot 365.25}$ #*Hubble constant in years*

> $evalf(Matrad \cdot Hub);$ #*Matter-radiation equality in years*

> $evalf(Lambdamat \cdot Hub);$ #*Dark energy-matter equality in years*

> $evalf\left(t_D \cdot Hub\right);$ #*Decoupling of matter from radiation*

> $evalf\left(t_0 \cdot Hub\right);$ #*Present time in years for Maj. neutrinos*

> $evalf\left(t_{D0} \cdot Hub\right);$ #*Present time in years for Dir. neutrinos*

Bibliography

[1] H. Vega and N. Sanchez. Model independent analysis of dark matter points to a particle mass at the keV scale. *Mon. Not. R. Astron. Soc.*, 404(2):885–894, 2010.

[2] C. Destri *et al.* Quantum WDM fermions and gravitation determine the observed galaxy structures. *arXiv:1301.1864v3*, 2013.

[3] A. Boyarsky *et al.* The role of sterile neutrinos in cosmology and astrophysics. *Ann. Rev. Nucl. Part. Sci.*, 59:191–214, 2009.

[4] J. Ellis and K. Olive. Supersymmetric Dark Matter Candidates. *From 'Particle Dark Matter: Observations, Models and Searches'*, Chapter 8(ISBN 9780521763684):142–163, 2010.

[5] S. Perlmutter *et al.* Measurements of Ω and Λ from 42 High-Redshift Supernovae. *The Astrophys. J.*, 517:565–586, 1999.

[6] A. Riess *et al.* Observational Evidence from Supernovae for an Accelerating Universe and a Cosmological Constant. *The Astronomical Journal*, 116:1009–1038, 1998.

[7] J. Frieman *et al.* Dark Energy and the Accelerating Universe. *Ann. Rev. Astron. Astrophys.*, 46, 2008.

[8] J. Narlikar and T. Padmanabhan. *Gravity, Gauge Theories and Quantum Cosmology*. D. Reidel Publishing Company, 1986.

[9] A. Blin. Planck Scale Variations of the Metric Tensor Leading to a Cosmological Constant. *African J. of Mathematical Physics*, 3(1), 2006.

[10] E. Linder. The Dynamics of Quintessence, The Quintessence of Dynamics. *Gen. Rel. Grav.*, 40:329–356, 2007.

[11] E. Komatsu *et al.* Seven-Year Wilkinson Microwave Anisotropy Probe (WMAP) Observations: Cosmological Interpretation. *Astrophys. J. Supp*, 192(18), 2011.

[12] E. Kolb and M. Turner. *The Early Universe.* Addison-Wesley Publishing Company, Redwood City, California, 1989.

[13] M. Turner. The New Cosmology. *Int. J. Mod. Phys. A*, 17:3446–3458, 2002.

[14] A. Einstein. *Relativity, The Special and General Theory.* CreateSpace Independent Publishing Platform, 1920 Edition.

[15] R. d'Inverno. *Introducing Einstein's Relativity.* Clarendon Press, Oxford, 1992.

[16] B. Schutz. *A First Course in General Relativity.* Cambridge University Press, 2009.

[17] S. Weinberg. *Gravitation and Cosmology: Principles and Applications of the general theory of relativity.* John Wiley & Sons, Inc, 1972.

[18] R. Wald. *General Relativity.* The University of Chicago Press, 1984.

[19] J. Peacock. *Cosmological Physics.* Cambridge University Press, 1999.

[20] C.B. Netterfield *et al.* A measurement by BOOMERANG of multiple peaks in the angular power spectrum of the cosmic microwave background. *Astrophys. J.*, 571:604–614, 2002.

[21] J. Beringer *et al* (Particle Data Group). Particle Physics Booklet. Extracted from the *Review of Particle Physics.*

[22] S. Watson. An exposition on inflationary cosmology. *arXiv:astro-ph/0005003*, April 2000.

[23] A. Linde. Inflationary cosmology. *Lect. Notes Phys.*, 738:1–54, 2008.

[24] G. Felder. The expanding universe. *http://www.felderbooks.com/papers/cosmo.html*, 2000.

[25] J. Beringer *et al* (Particle Data Group). Review of Particle Physics. *Phys. Review D*, 86(010001), 2012.

[26] M. Turner. Dark Energy and the New Cosmology. *arXiv:astro-ph/0108103*, 2001.

[27] S. Weinberg. The Cosmological Constant Problem. *Rev. Mod. Phys.*, 61(1), 1989.

[28] S. Weinberg. The Cosmological Constant Problems. *arXiv:astro-ph/0005265, Talk given at Dark Matter 2000, Marina del Rey, CA*, February 2000.

[29] A. Blin. Fluctuations of the metric tensor: on fermion propagators and on the cosmological constant. *Int. J. Math. Phys.*, 2(4):61–66, 2012.

[30] D. Fixsen. The Temperature of the Cosmic Microwave Background. *The Astrophysical Journal*, 707, 2009.

[31] G.Feinberg S.Dodelson. Neutrino–two-photon vertex. *Phys. Rev. D*, 43(3):913–920, 1991.

[32] J. Dugdale. *Entropy and its Physical Meaning*. Taylor & Francis, 1996.

[33] J. Cline. Baryogenesis. *arXiv:hep-ph/0609145*, 2006.

[34] C. Miller. Cosmic hide and seek: the search for the missing mass. *http://www.eclipse.net/ cmmiller/DM/*, 1995.

[35] K. Freese *et al*. Limits on Stellar Objects as the Dark Matter of Our Halo: Nonbaryonic Dark Matter Seems to be Required. *Proceedings of the 19th Texas Symposium on Relativistic Astrophysics and Cosmology*, 1999.

[36] M. Hindmarsh and O. Philipsen. WIMP Dark Matter and the QCD Equation of State. *Phys.Rev. D*, 71 087302, 2005.

[37] A. Belikov *et al*. CoGeNT, DAMA, and Light Neutralino Dark Matter. *FERMILAB-PUB-10-316-A*, 2010.

[38] C. Destri *et al*. Fermionic warm dark matter produces galaxy cores in the observed scales because of quantum mechanics. *New Astronomy*, 22(39), 2013.

[39] A. Geringer-Sameth and S. Koushiappas. Exclusion of canonical WIMPs by the joint analysis of Milky Way dwarfs with data from the Fermi Gamma-ray Space Telescope. *Phys. Rev. Lett.*, 107(24), 2011.

[40] M. Wilkinson *et al*. The Internal Kinematics of Dwarf Spheroidal Galaxies. *EAS Publications Series*, 20, 2006.

[41] Z. Ahmed *et al*. Combined Limits on WIMPs from the CDMS and EDELWEISS Experiments. *Phys. Rev. D*, 84 011102, 2011.

[42] B. Kavanagh and A. Green. Improved determination of the WIMP mass from direct detection data. *Phys. Rev. D*, 86 065027, 2012.

[43] K. Abazajian *et al*. Limits on the Radiative Decay of Sterile Neutrino Dark Matter from the Unresolved Cosmic and Soft X-ray Backgrounds. *Phys. Rev. D*, 75 063511, 2007.

[44] S. Weinberg. A New Light Boson? *Phys. Rev. Lett.*, 40(4), 1978.

[45] P. Sikivie. Experimental Tests of the ”Invisible” Axion. *Phys. Rev. Lett.*, 51(16):1415–1417, 1983.

[46] ALEPH Collaboration R. Barate *et al.* Absolute mass lower limit for the lightest neutralino of the MSSM from e^+e^- data at $\sqrt{s}$ up to 209 GeV . *Phys. Lett. B*, 583(3–4):247–263, 2007.

[47] R. Gilmore. Mass limits on neutralino dark matter. *Phys. Rev. D*, 76 043520, 2007.

[48] S. Hofmann *et al.* Damping scales of neutralino cold dark matter. *Phys. Rev. D*, 64(083507), 2001.

[49] T. Bringmann and S. Hofmann. Thermal decoupling of WIMPs from first principles. *Journal of Cosmology and Astroparticle Physics*, 04(16), 2007.

[50] Maplesoft. *Maple User Manual.* Waterloo Maple Inc., 2011.